R O S E T T A

FLIGHT REPORTS of RPC–MAG

RO–IGEP–TR–0014

Issue: 3 Revision: 0

January 25, 2010

Report of the

First Earth Swing by (EAR1)

Time period: March 01 - 07, 2005

Andrea Diedrich
Karl-Heinz Glassmeier
Ingo Richter

Institut für Geophysik und extraterrestrische Physik
Technische Universität Braunschweig
Mendelssohnstraße 3, 38106 Braunschweig
Germany

Contents

1 Introduction

ROSETTA's first Earth Swing by (EAR1) happened in the time period March 01 – 07, 2005. RPC-MAG was switched on in the time between 2005-03-01T00:00:00 and 2005-03-08T00:00:00. The instrument performance was excellent. There were no problems.

This document gives a brief description of the executed activities and show the obtained data. Housekeeping data (Temperature of the OB & IB sensor, Filter Stages A & B, Filter configuration register, Reference voltage, negative and positive 5V supply voltage, and the coarse HK sampled magnetic field data of the OB sensor) are presented as well as magnetic field science data of the OB and IB sensor in the activated modes. Magnetic field data are plotted in s/c coordinates and ECLIPJ2000 coordinates if not otherwise stated. They are calibrated according to the results of the ground calibration and the results of the inflight temperature model 002 using the flight data from March 2004 until September 2004. Sensitivity, Misalignment, and Temperature effects are taken into account. The s/c residual field is not subtracted.

The spectra of the magnetic field data measured by the OB sensor are plotted as well in section 7. This time there is no influence of ROSETTAs reaction wheels (refer to section 8) as the instrument was only operated in normal mode SID2.

The data quality and a comparison between OB and IB sensor will be presented in chapter 4.

Additionally to the RPC–MAG instrument the LANDER Magnetometer ROMAP was switched on from 2005-03-01T01:00:00 until 2005-03-07T23:30:00. A comparison with RPCMAG will be shown in section 11.

The activation of the LANDER was associated with the test of some heaters onboard the LANDER. Unfortunately this caused magnetic disturbances presented in section 9.

The close Earth Swing by was a unique chance to check and improve the calibration of the instrument and to compare the measured field with a theoretical model of the earth. These investigations will be presented in chapter 5.

Also the comparison of our magnetic field data with data measured by different spacecrafts (e.g WIND) can give information about the data quality. A comparison to the WIND data can be found in section 6.

A temperature profile for the whole Earth Swing by is shown in section 10.

2 The Swing by Geometry

This section gives an overview about the trajectory during the Swing by. ROSETTA approached through the tail within 4 days (March 1 until March 4), had its closest approach on March 4 at 22:09, and left through magnetopause and bow shock. It performed the closest Swing-By manoeuver ever flown by an interplanetary spacecraft. The minimum distance to earth was 1961 km.

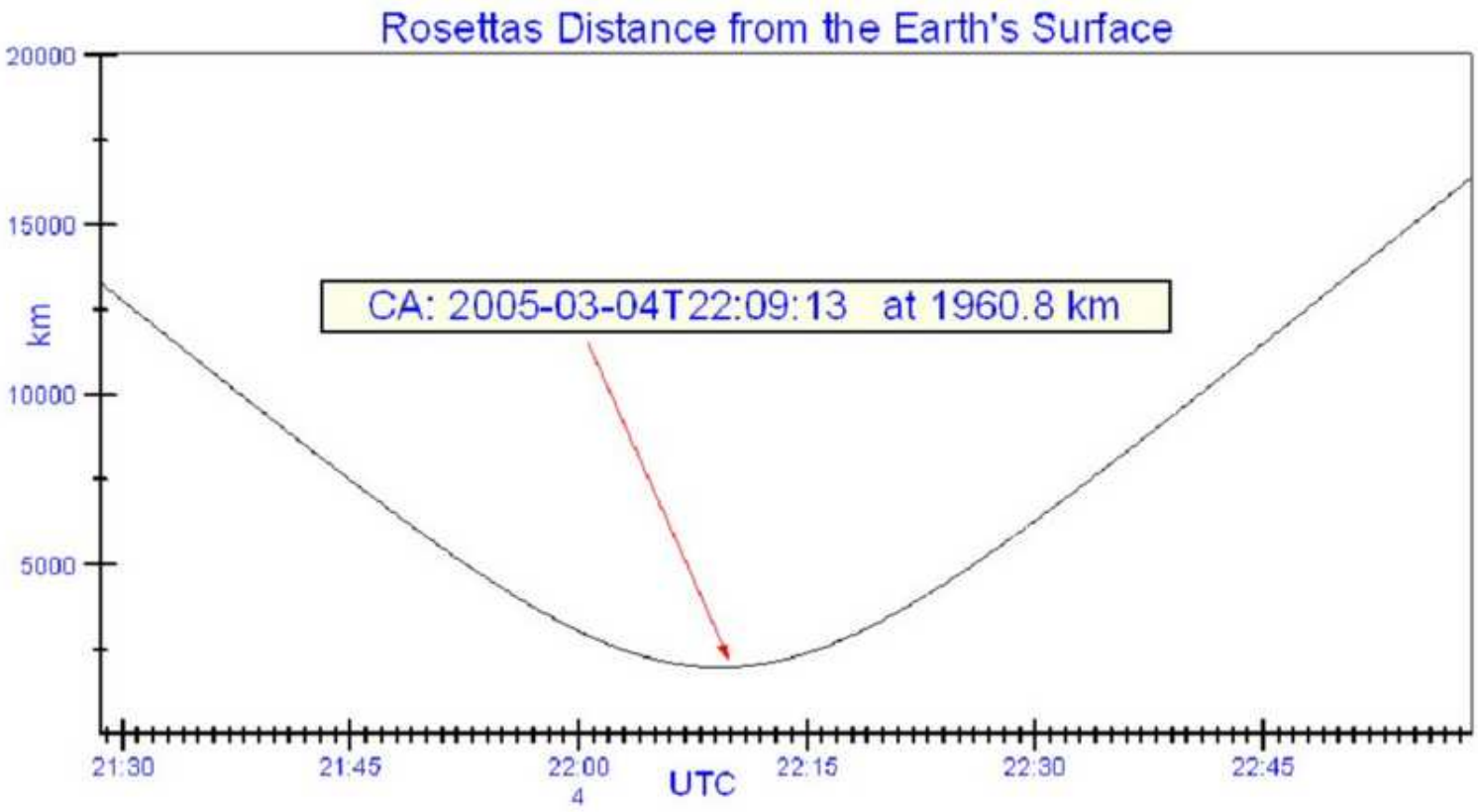

Figure 1: ROSETTA'S Distance to the EARTH'S Surface

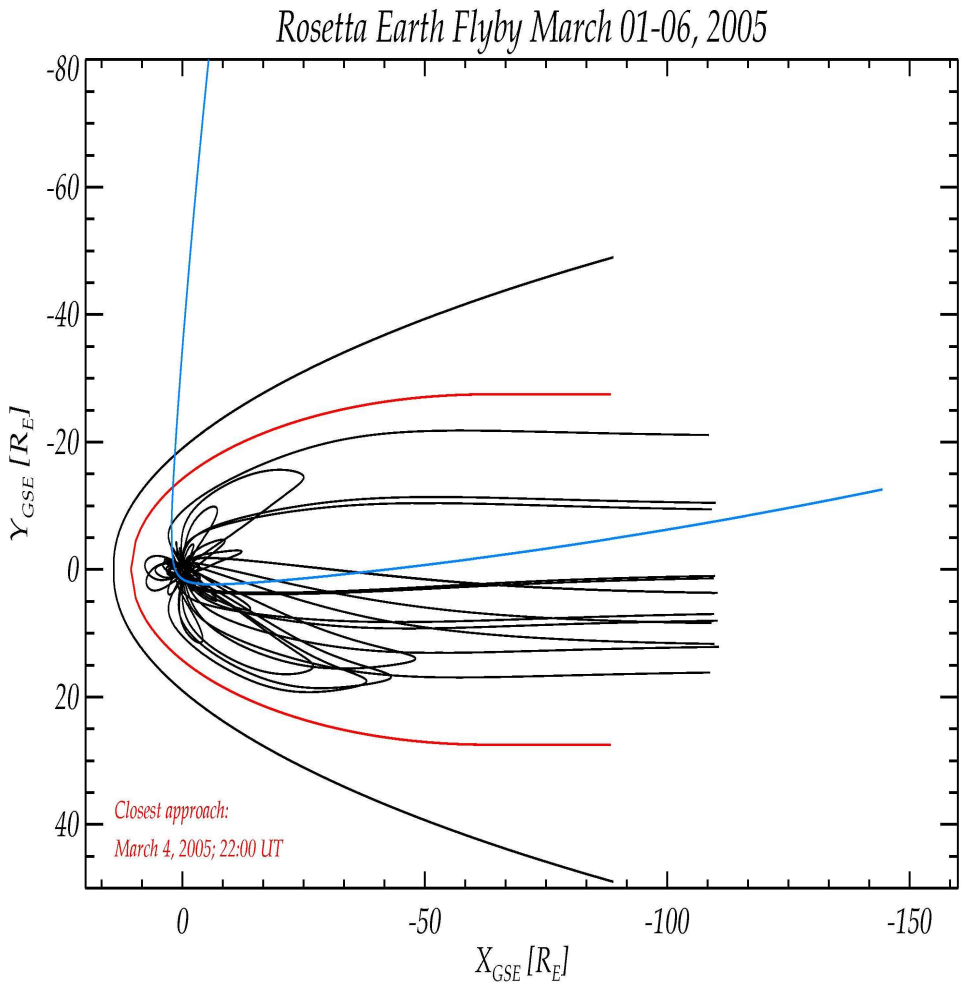

Figure 2: ROSETTA'S Swing by Trajectory in GSE coordinates: XY–Plane

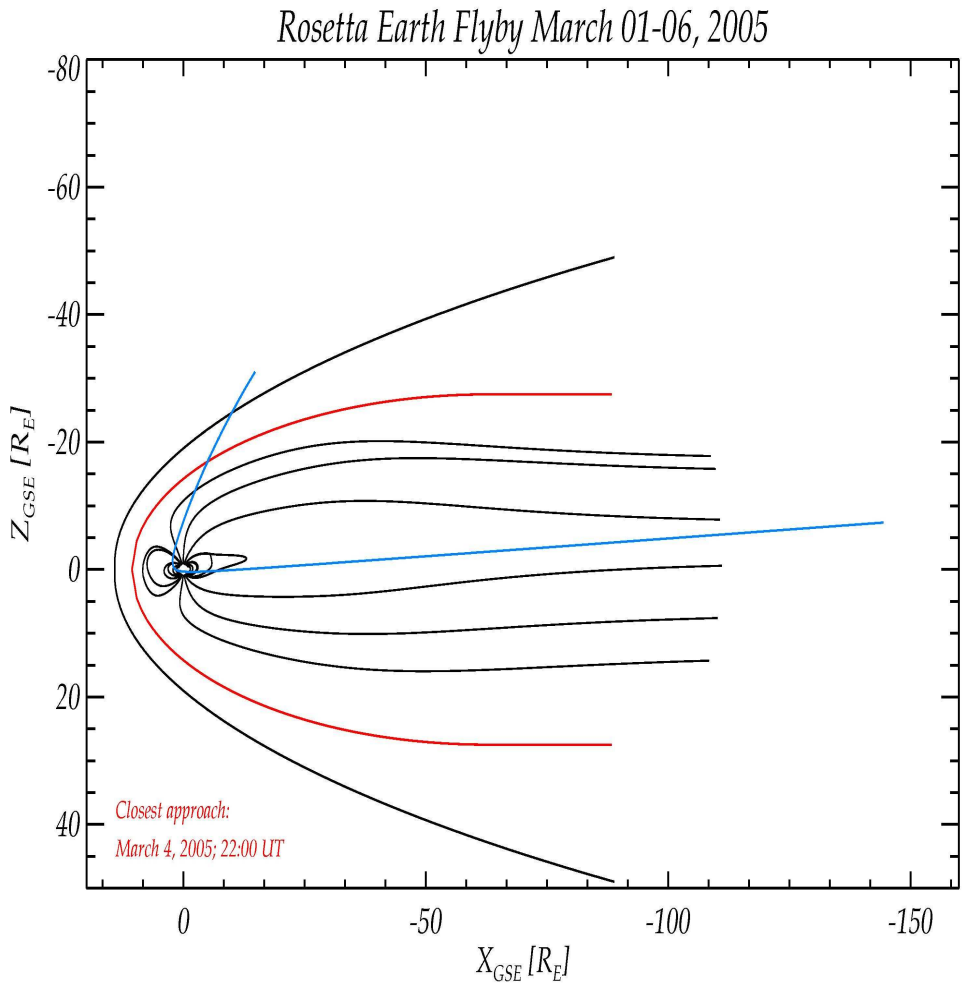

Figure 3: ROSETTA'S Swing by Trajectory in GSE coordinates: XZ–Plane

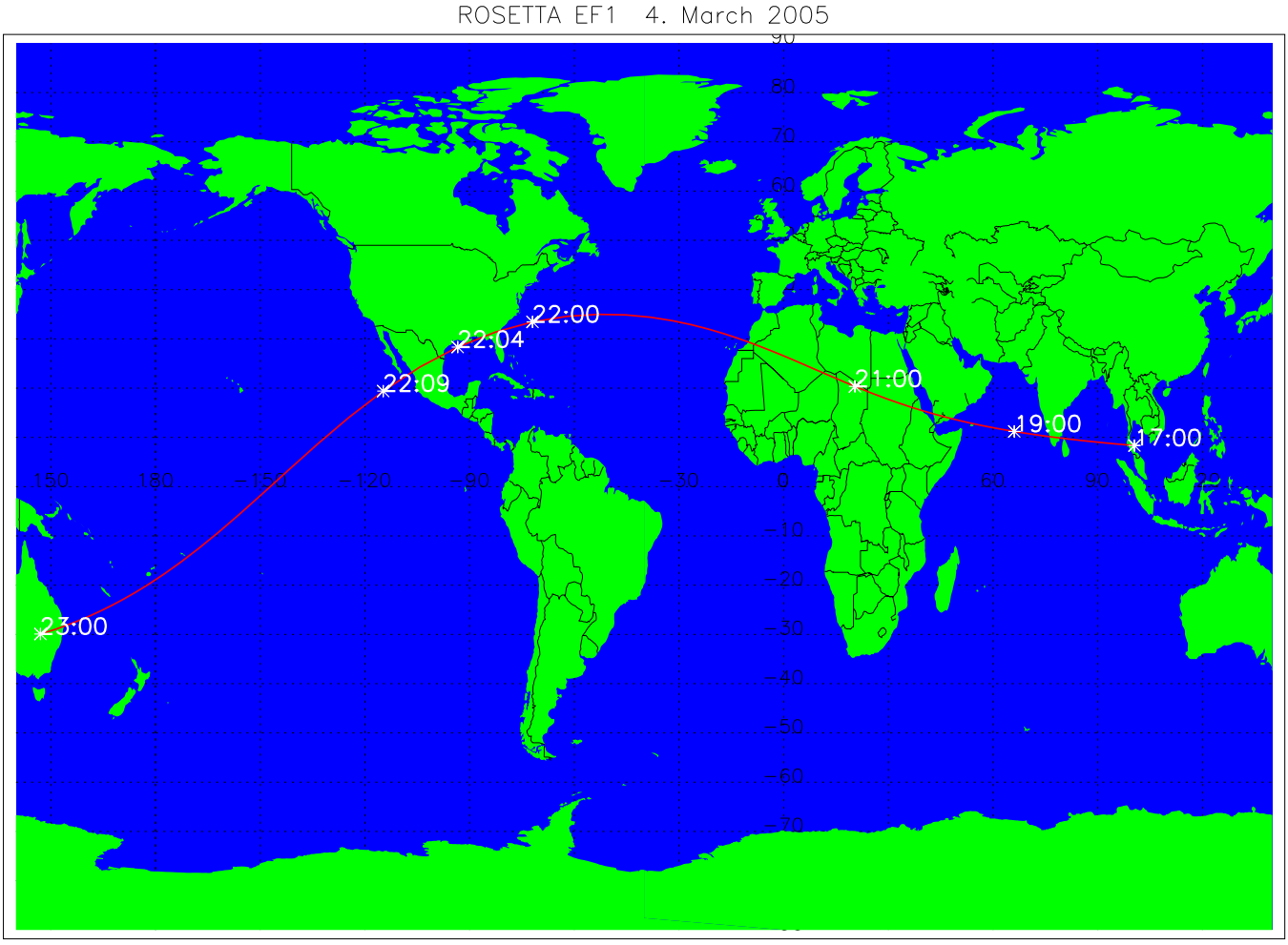

Figure 4: ROSETTA'S Ground Track during the Swing by

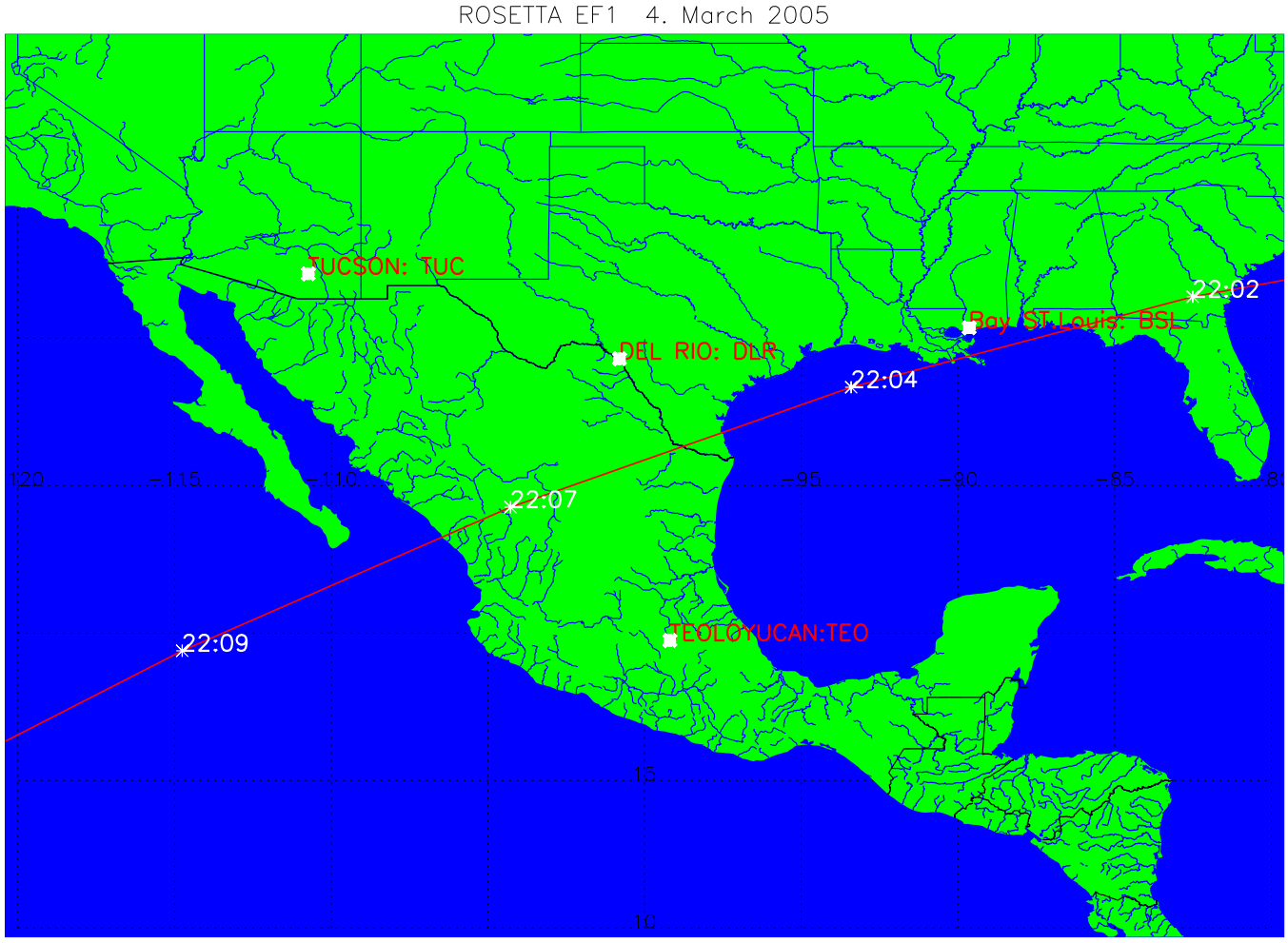

Figure 5: ROSETTA'S Ground Track during the Swing by (Zoomed)

3 Activities and data plots of EAR1

This chapter presents all relevant data /data types measured by RPCMAG day by day:

- Housekeeping data (HK).
- Magnetic field of the OB sensor, sampled with 16 bit in the HK stream.
- Calibrated LEVEL_B data (s/c coordinates) of the IB and OB sensor with the original sampling frequency.
- Calibrated LEVEL_C data (ECLIPJ2000 coordinates) of the IB and OB sensor with the original sampling frequency.
- Calibrated LEVEL_J data (PCA applied, correlated and uncorrelated part) of the IB and OB sensor. Data averaged to 1 s means.

3.1 March 01, 2005:

3.1.1 Actions

MAG was switched on immediately after PIU and set to HK mode at 00:02. The normal mode SID 2 was set at 00:14. All commands passed smoothly and the instrument followed in the expected way.

3.2 Plots of Calibrated Data

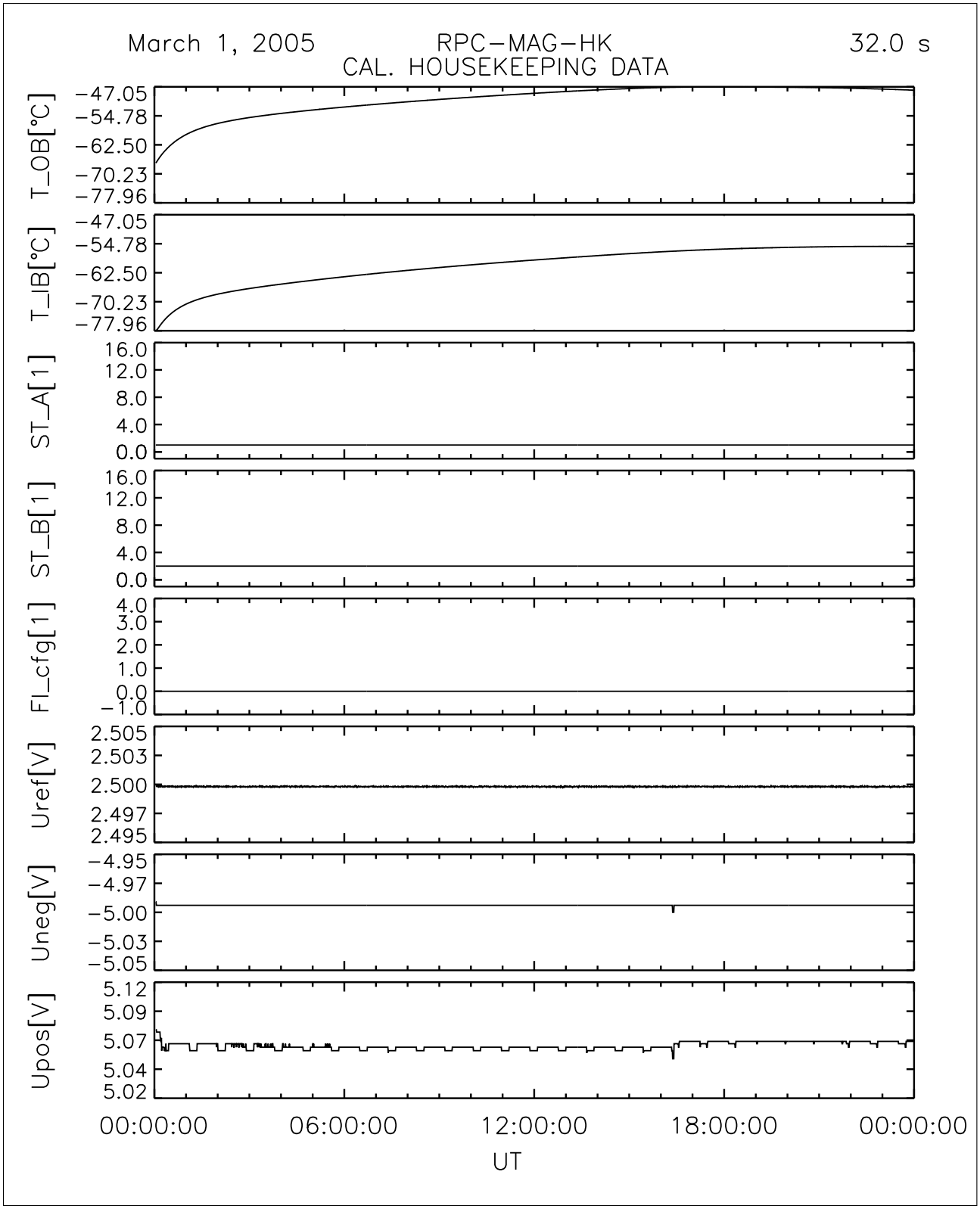

Figure 6: File: RPCMAG050301T0002_CLA_HK_P0000_2400

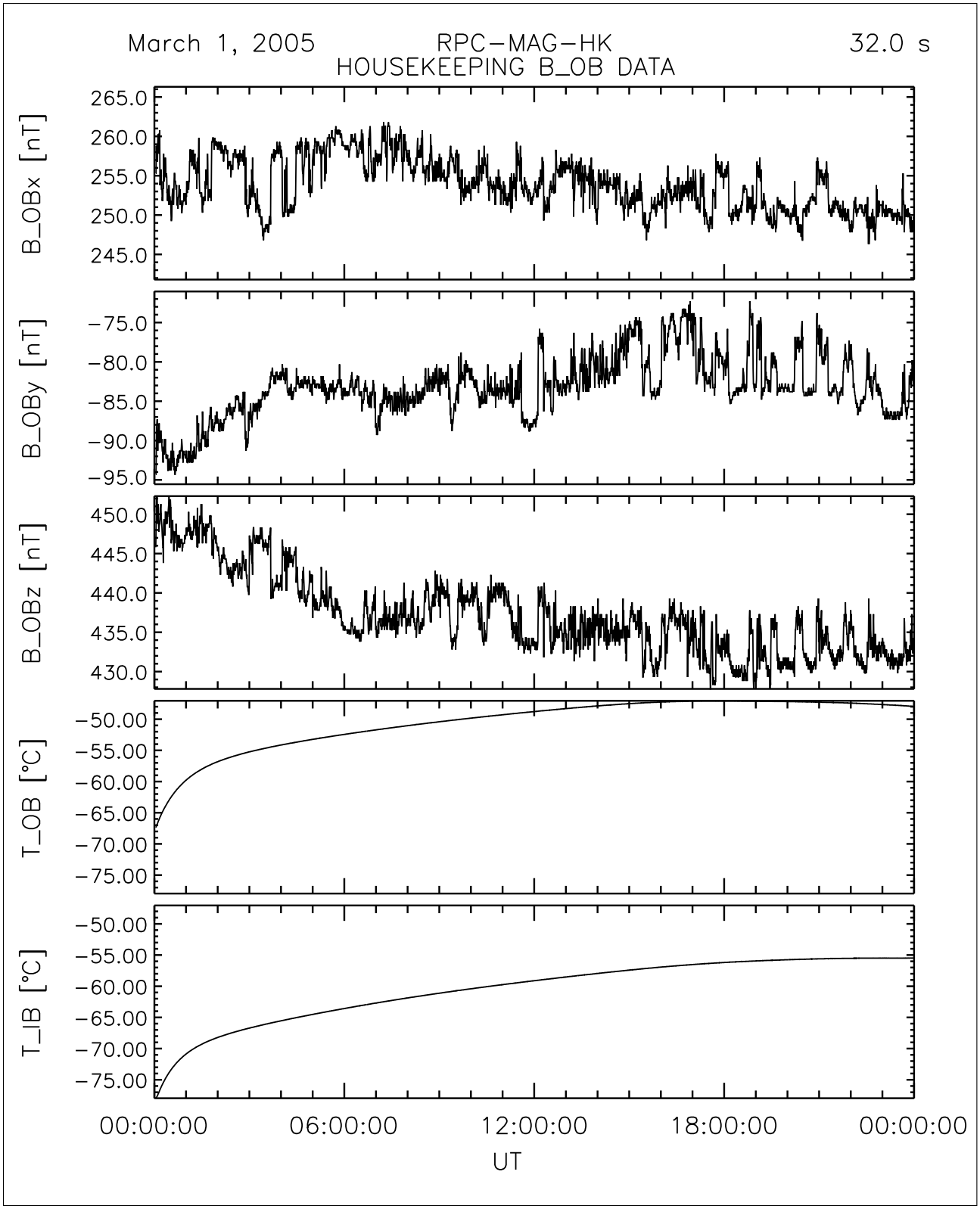

Figure 7: File: RPCMAG050301T0002_CLA_HK_B_P0000_2400

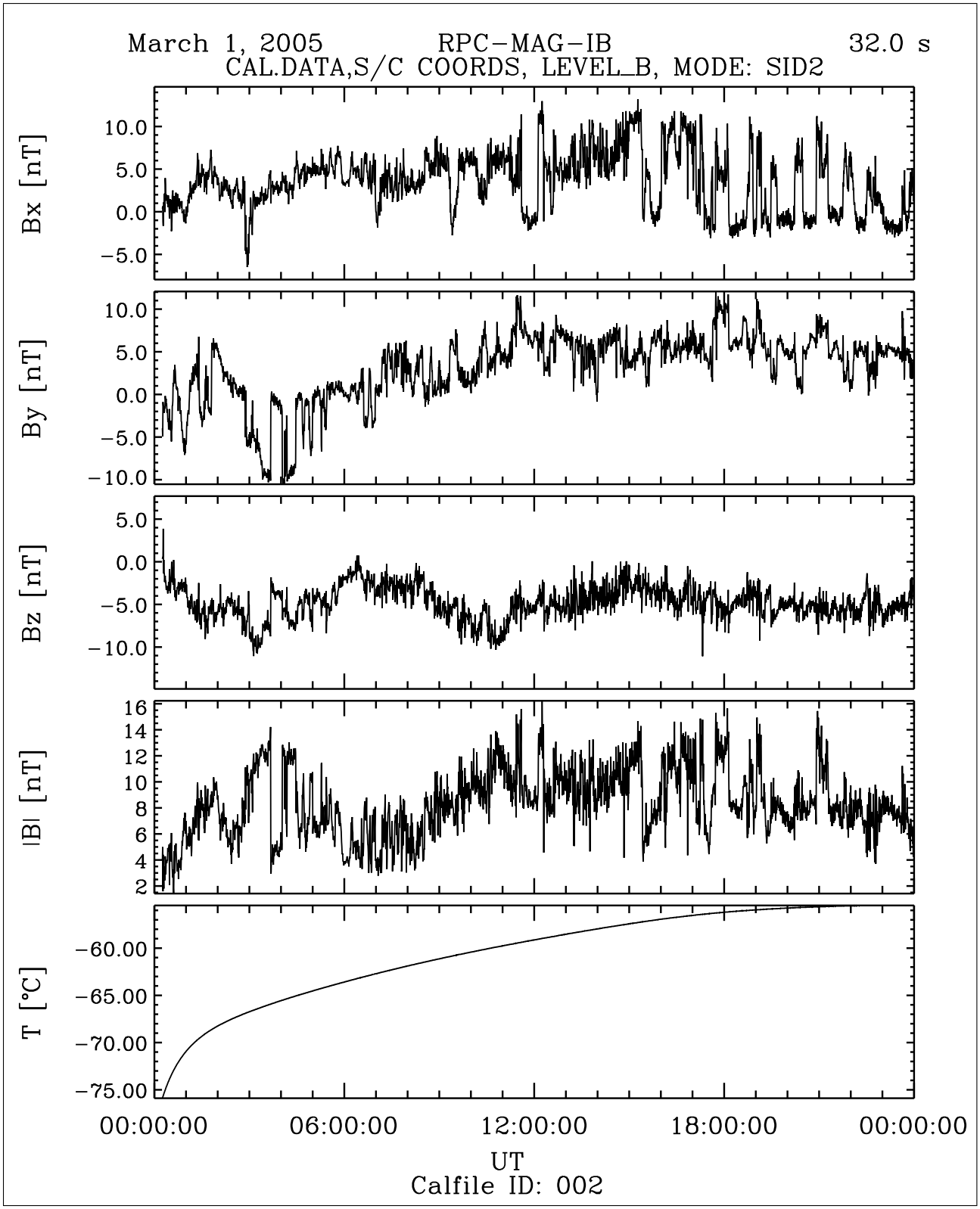

Figure 8: File: RPCMAG050301T0014_CLB_IB_M2_T0000_2400_002

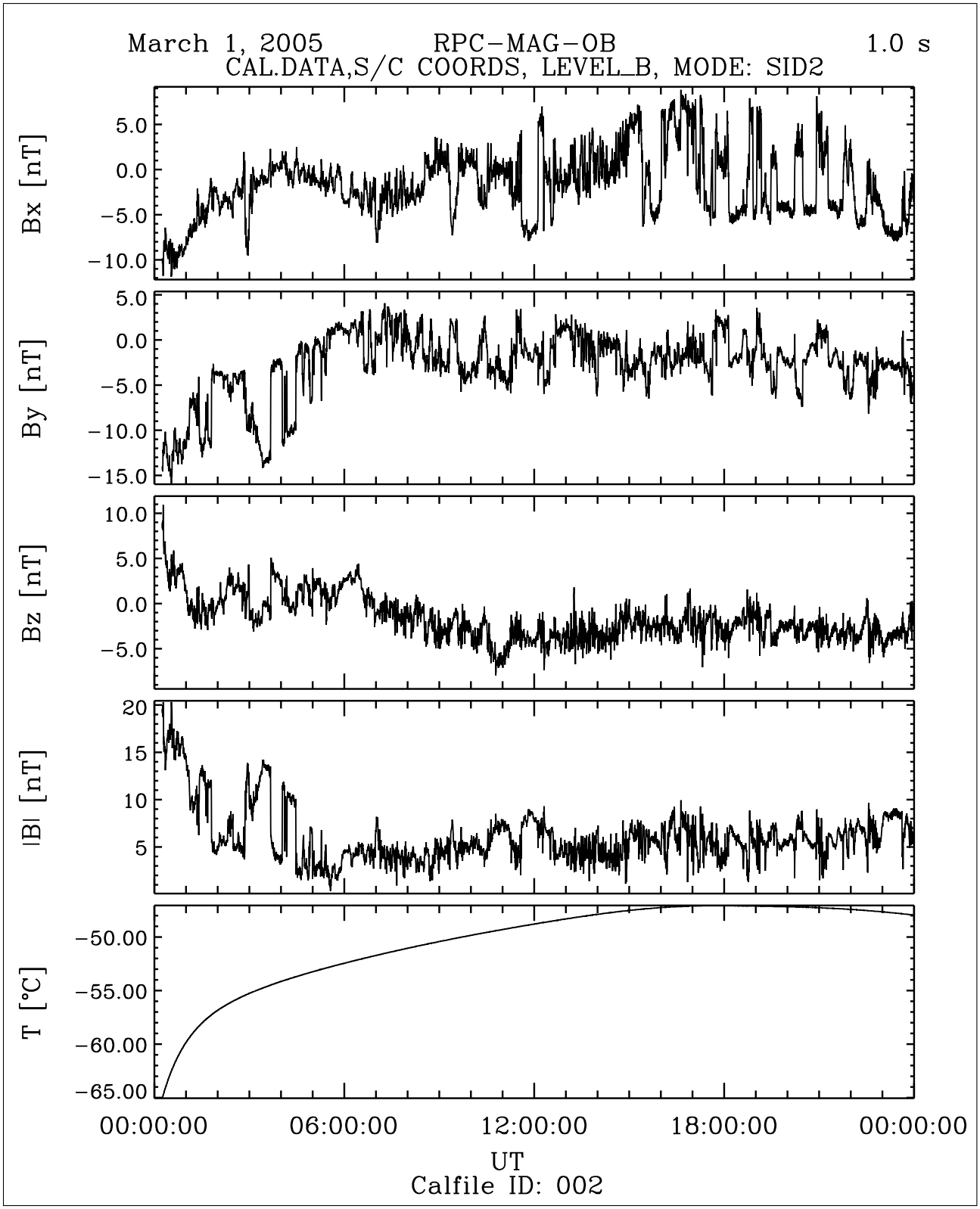

Figure 9: File: RPCMAG050301T0014_CLB_OB_M2_T0000_2400_002

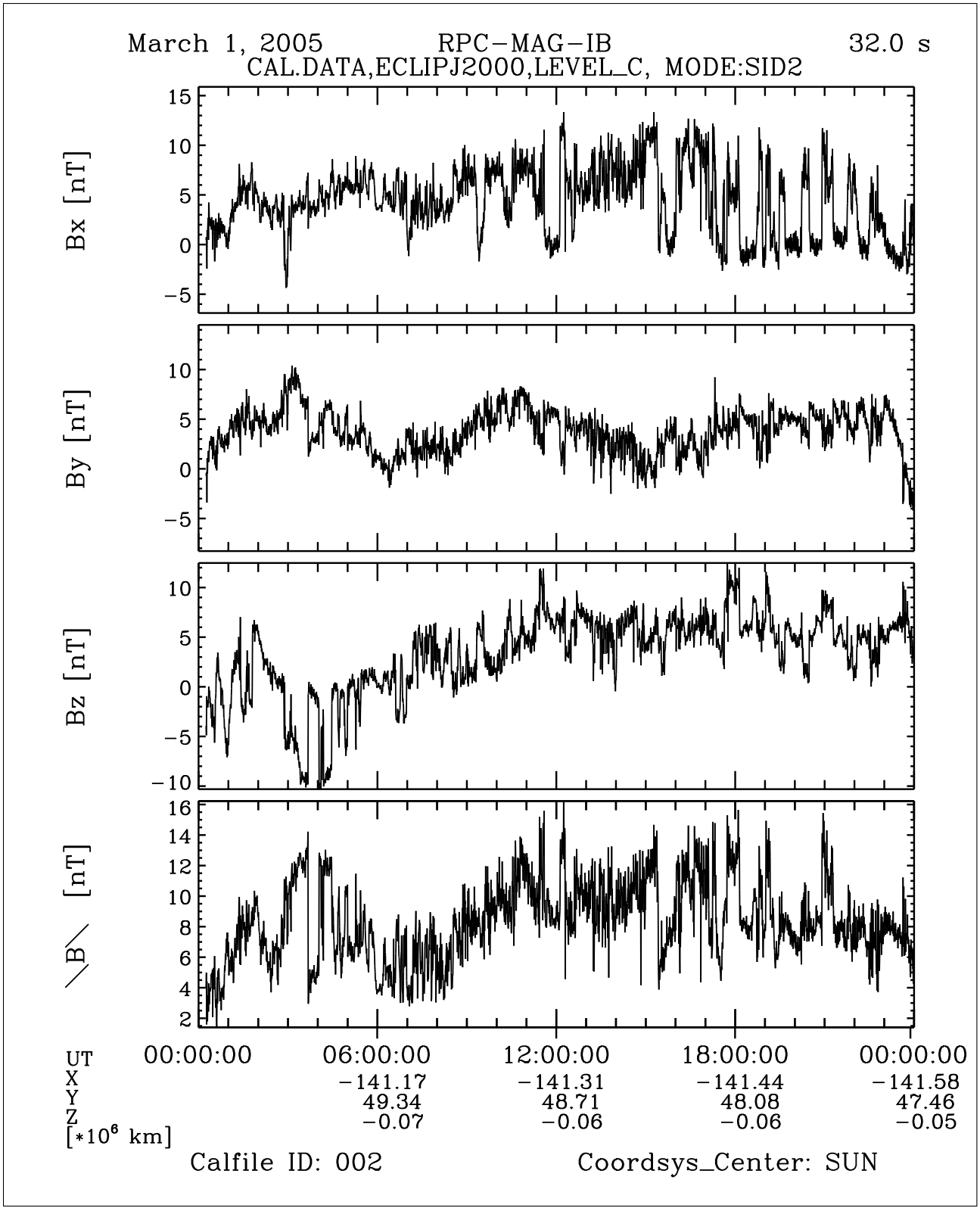

Figure 10: File: RPCMAG050301T0014_CLC_IB_M2_T0000_2400_002

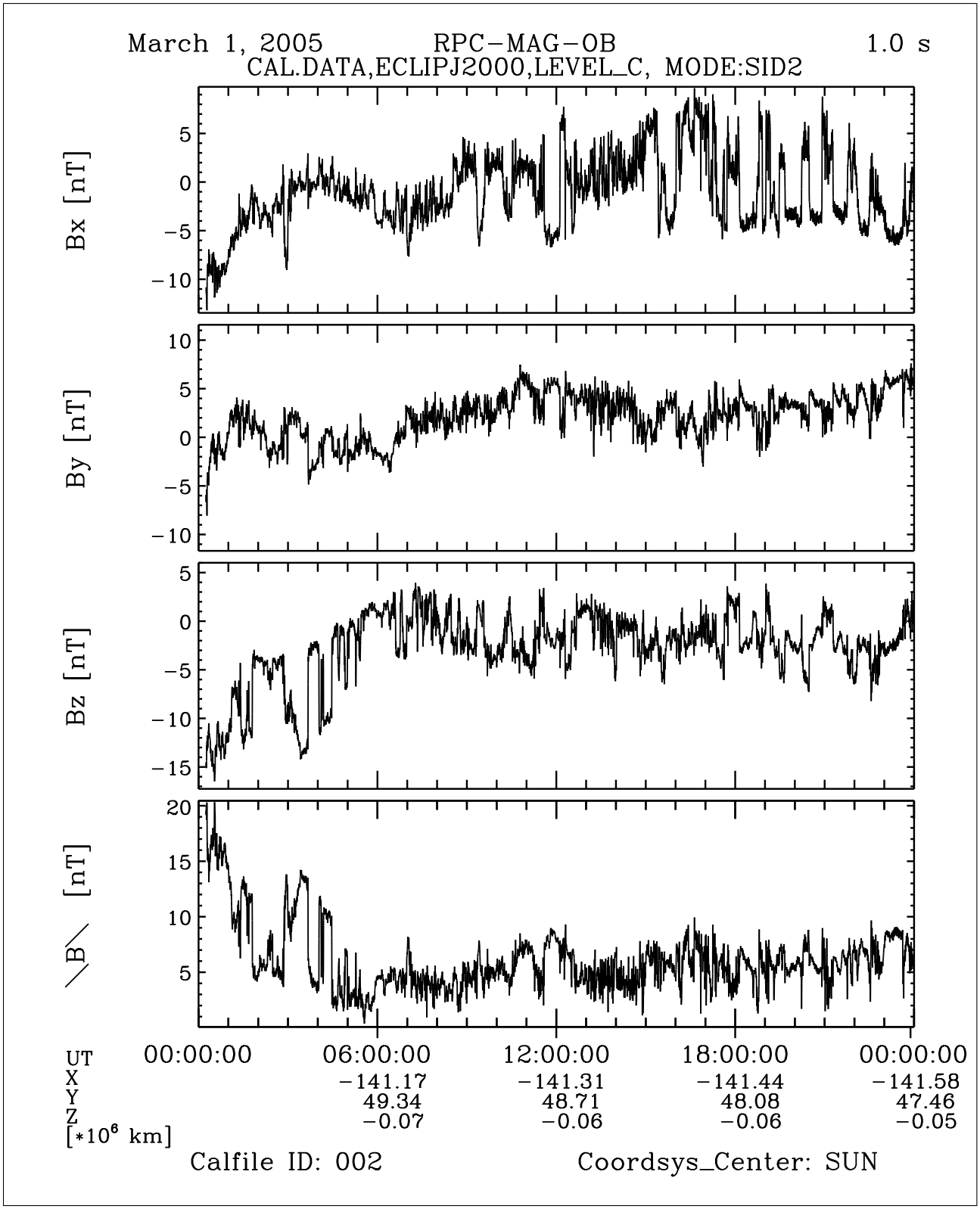

Figure 11: File: RPCMAG050301T0014_CLC_OB_M2_T0000_2400_002

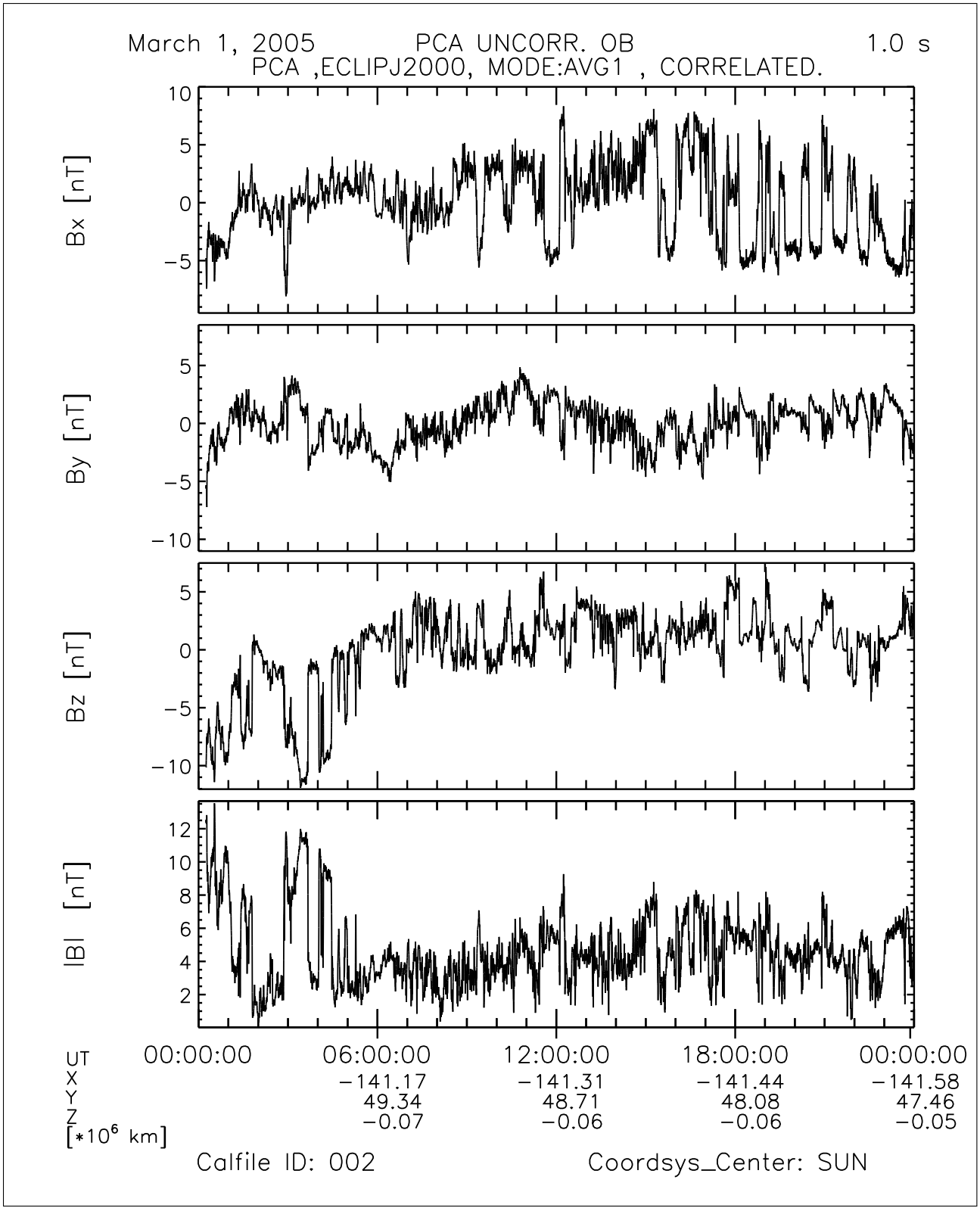

Figure 12: File: RPCMAG050301_CLJ_A1_C_T0000_2400_002

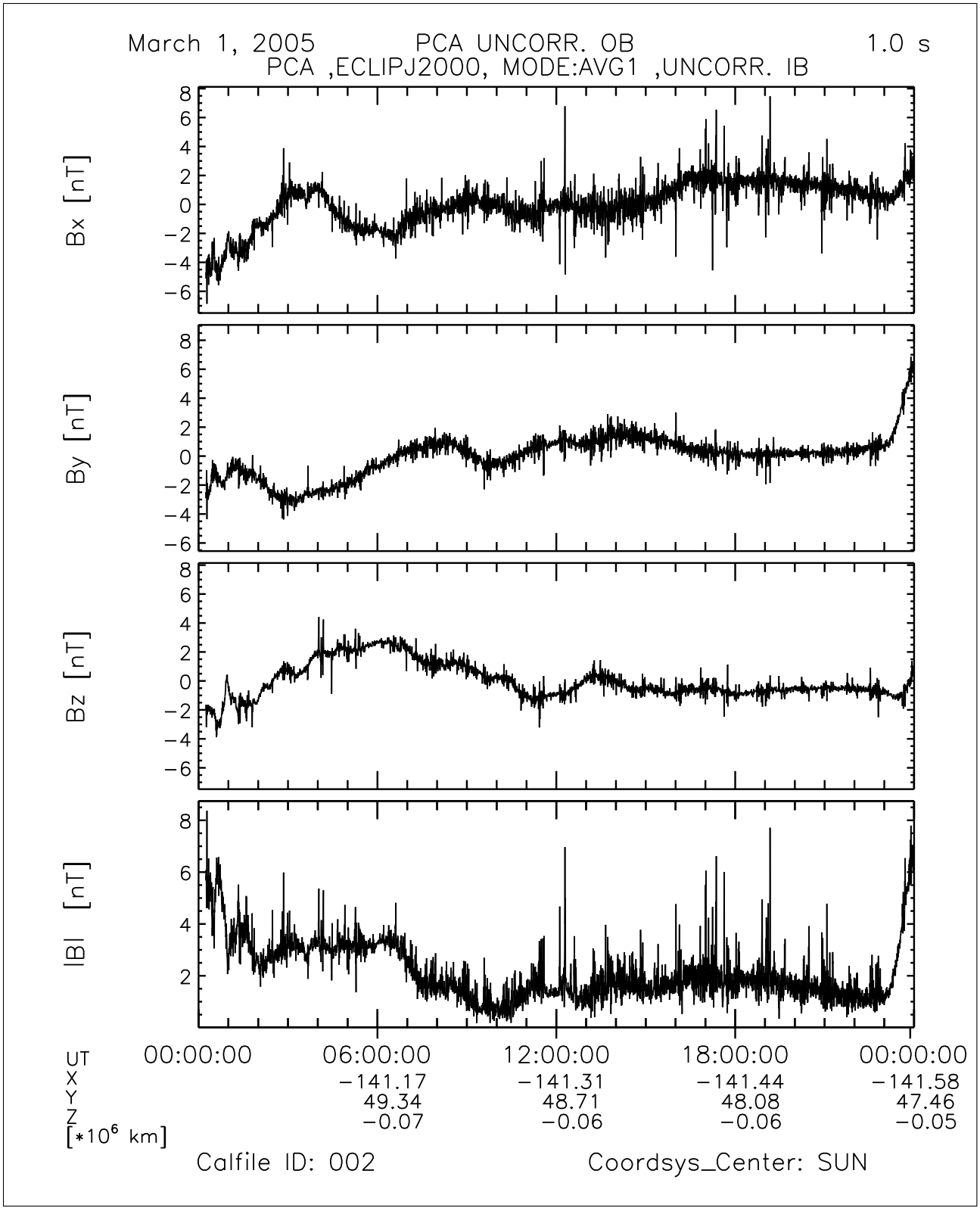

Figure 13: File: RPCMAG050301_CLJ_IB_A1_U_T0000_2400_002

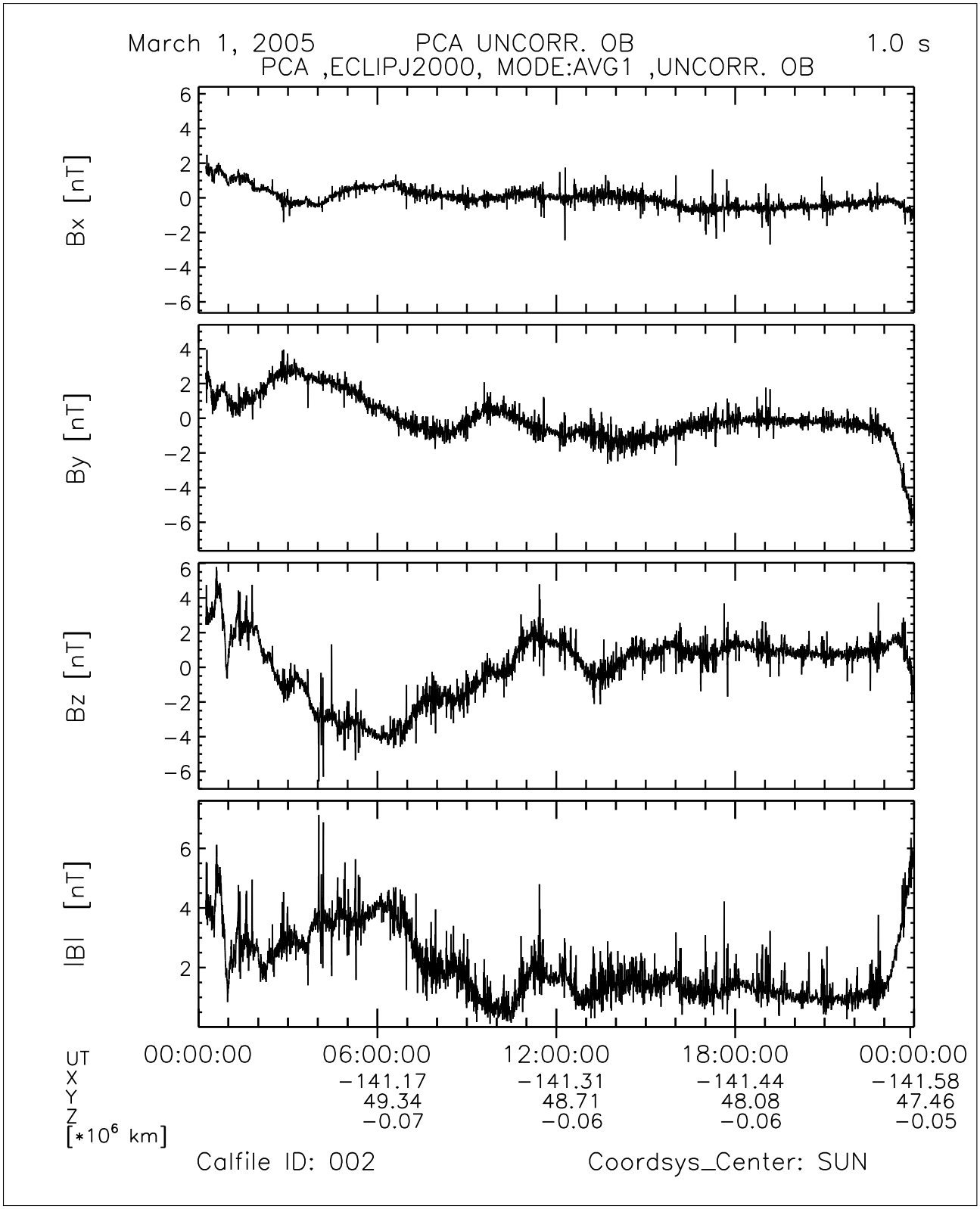

Figure 14: File: RPCMAG050301_CLJ_OB_A1_U_T0000_2400_002

3.3 March 02, 2005:

3.3.1 Actions

MAG stayed in SID 2. No problems occurred.

3.3.2 Plots of Calibrated Data

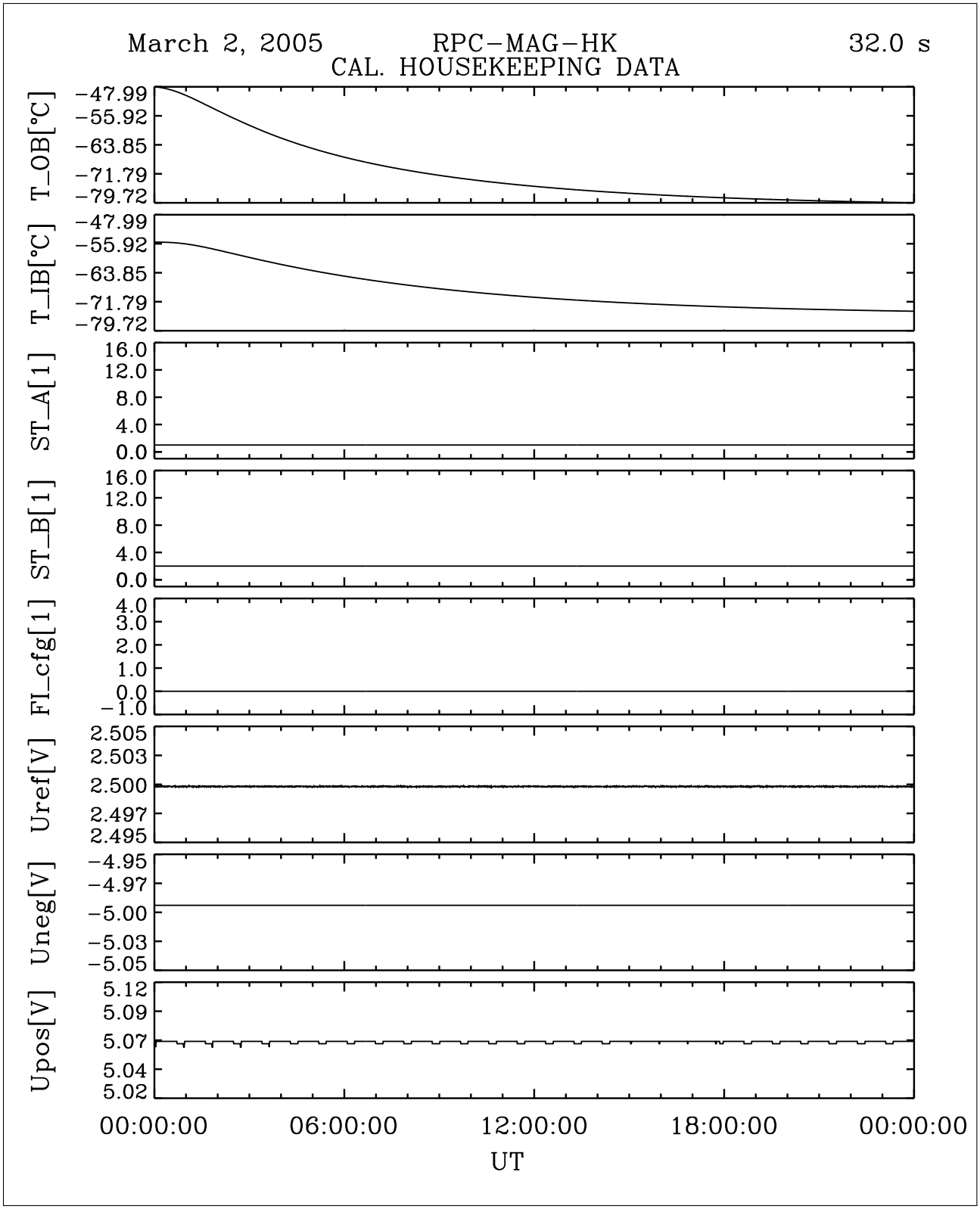

Figure 15: File: RPCMAG050302T0000_CLA_HK_P0000_2400

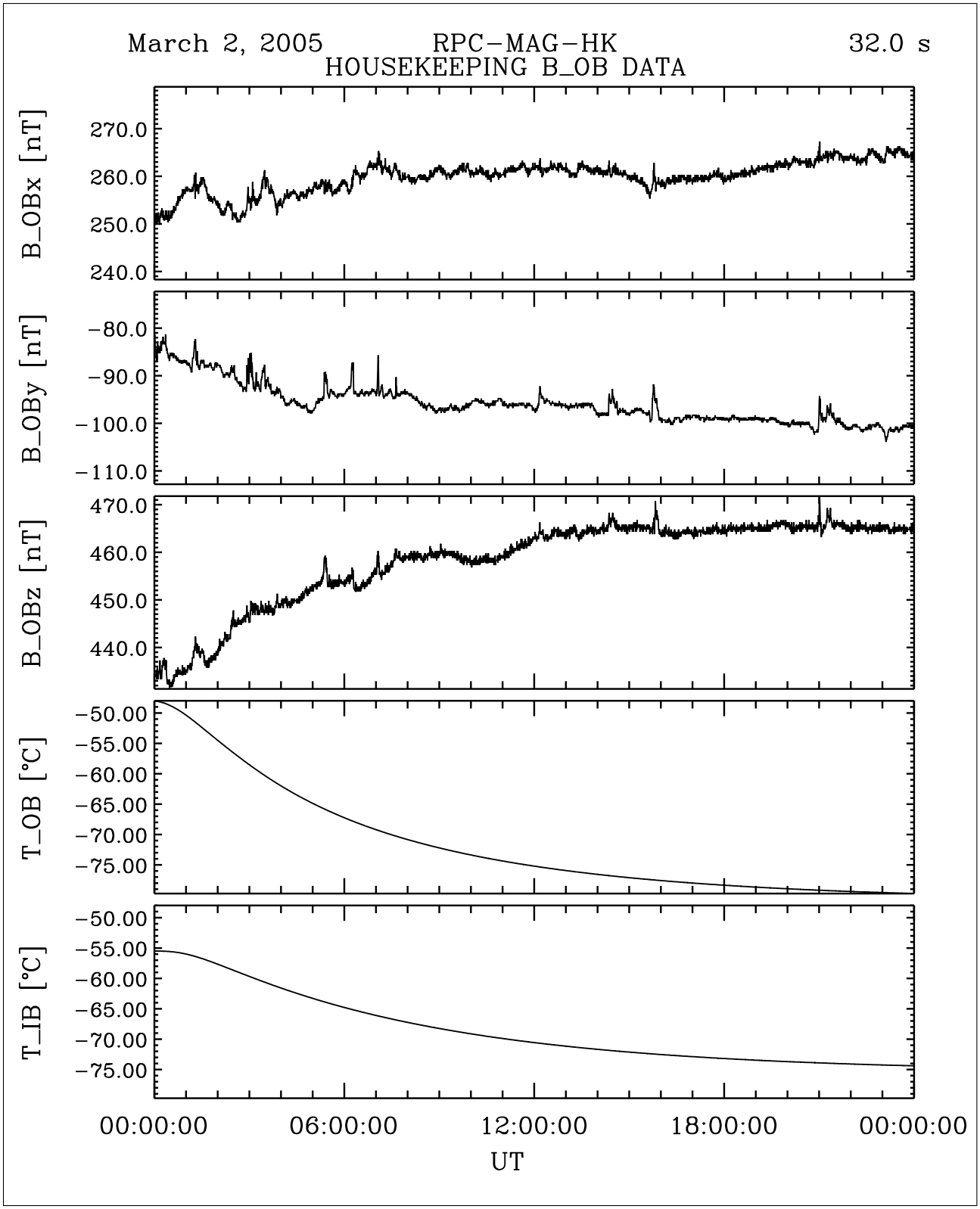

Figure 16: File: RPCMAG050302T0000_CLA_HK_B_P0000_2400

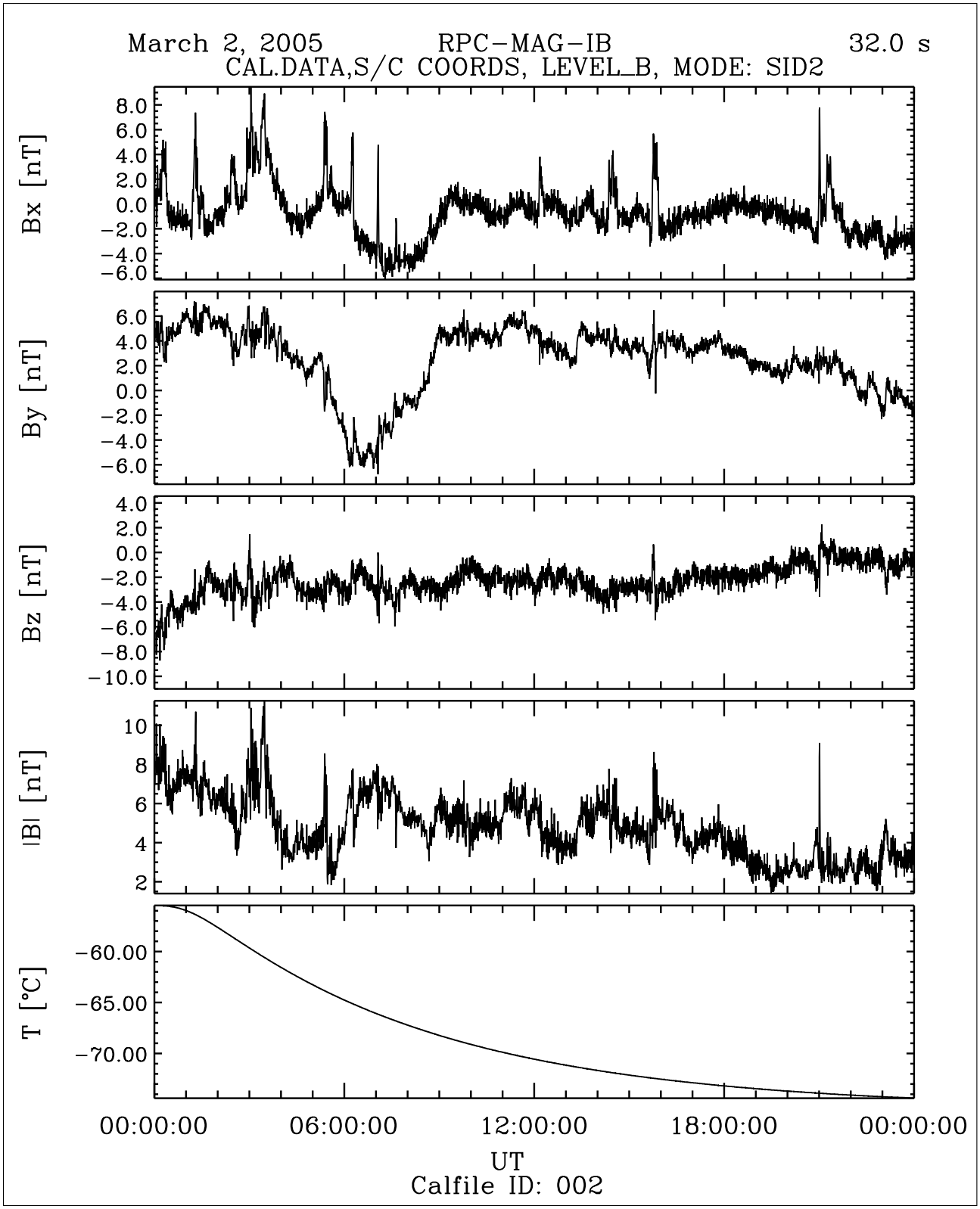

Figure 17: File: RPCMAG050302T0000_CLB_IB_M2_T0000_2400_002

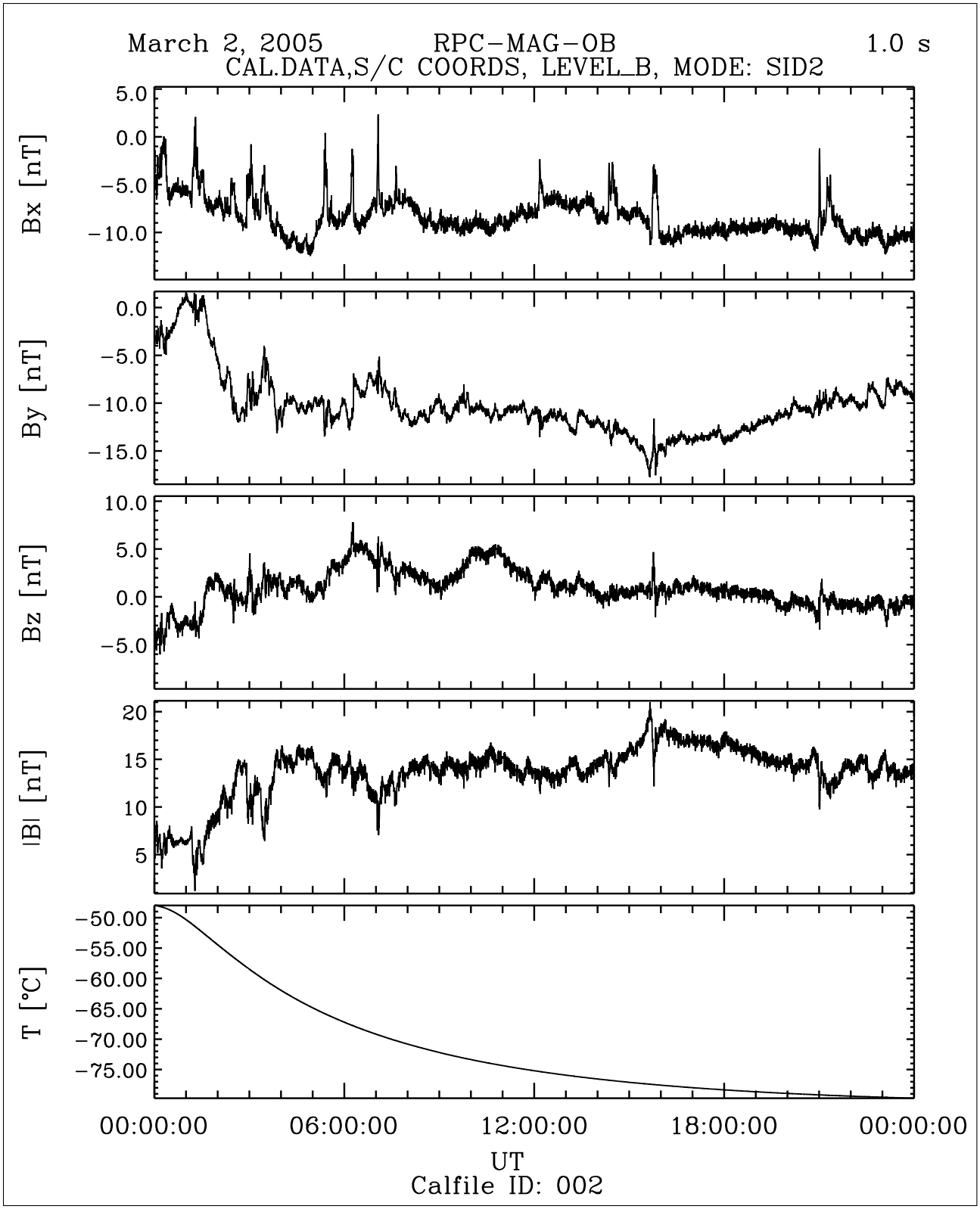

Figure 18: File: RPCMAG050302T0000_CLB_OB_M2_T0000_2400_002

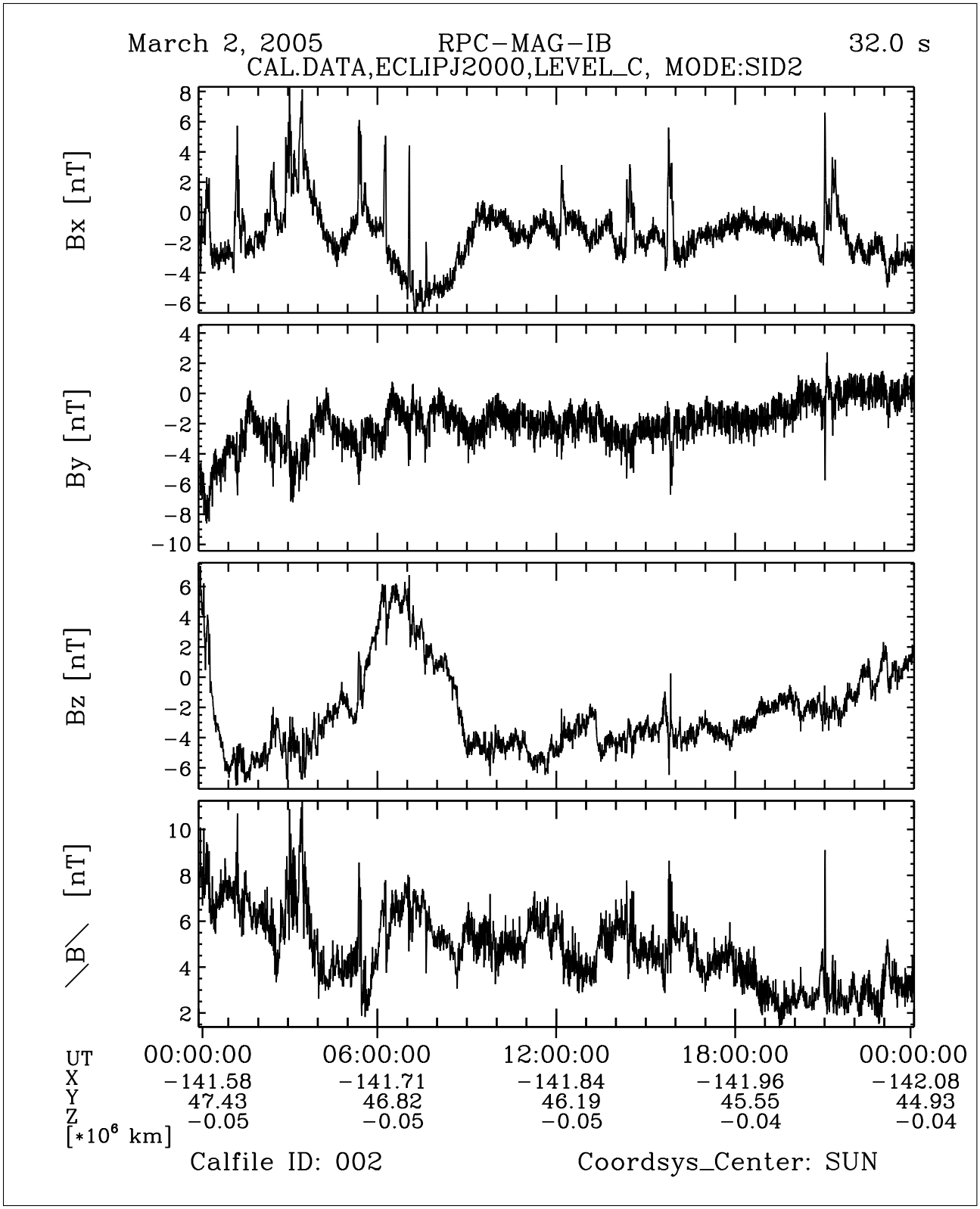

Figure 19: File: RPCMAG050302T0000_CLC_IB_M2_T0000_2400_002

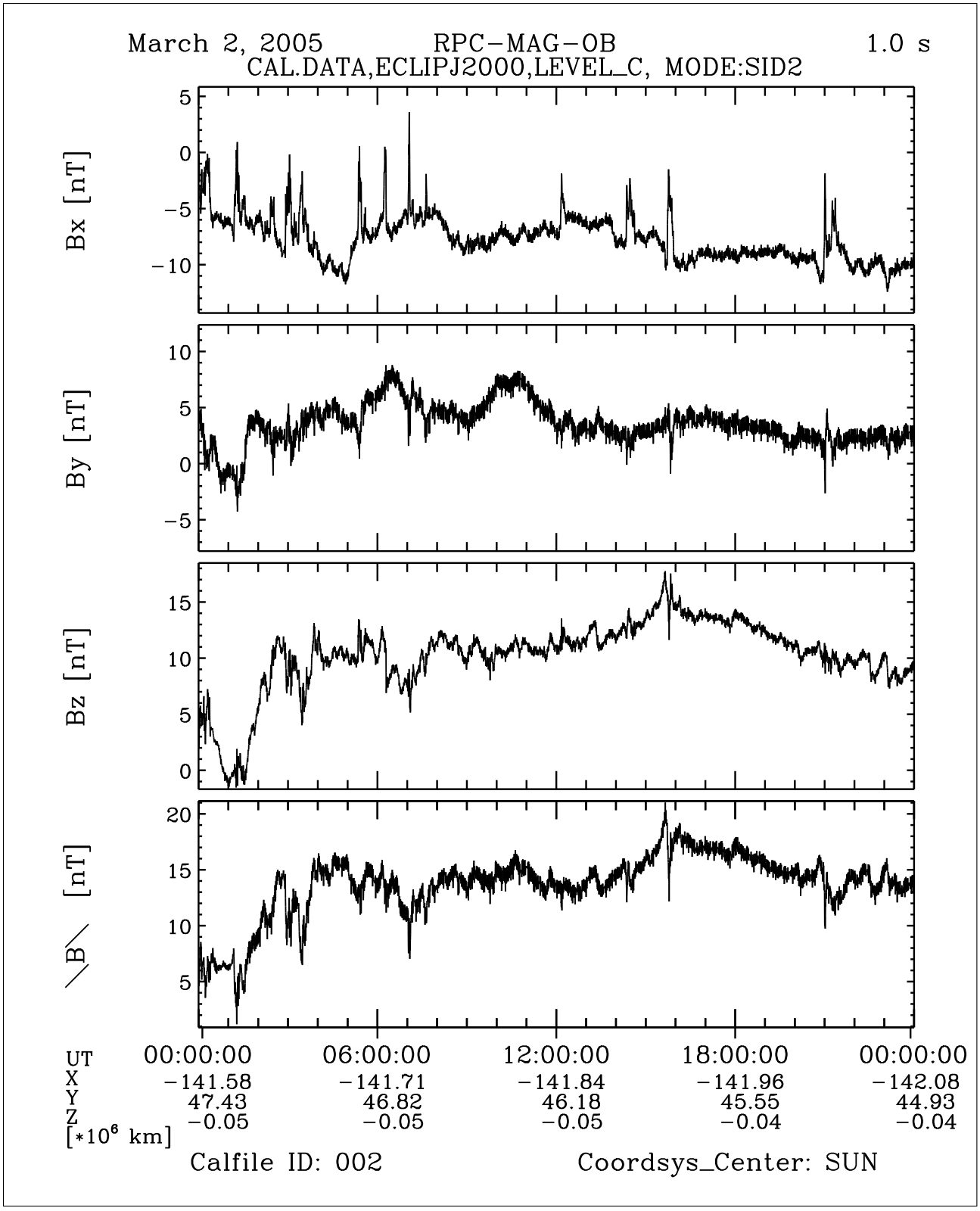

Figure 20: File: RPCMAG050302T0000_CLC_OB_M2_T0000_2400_002

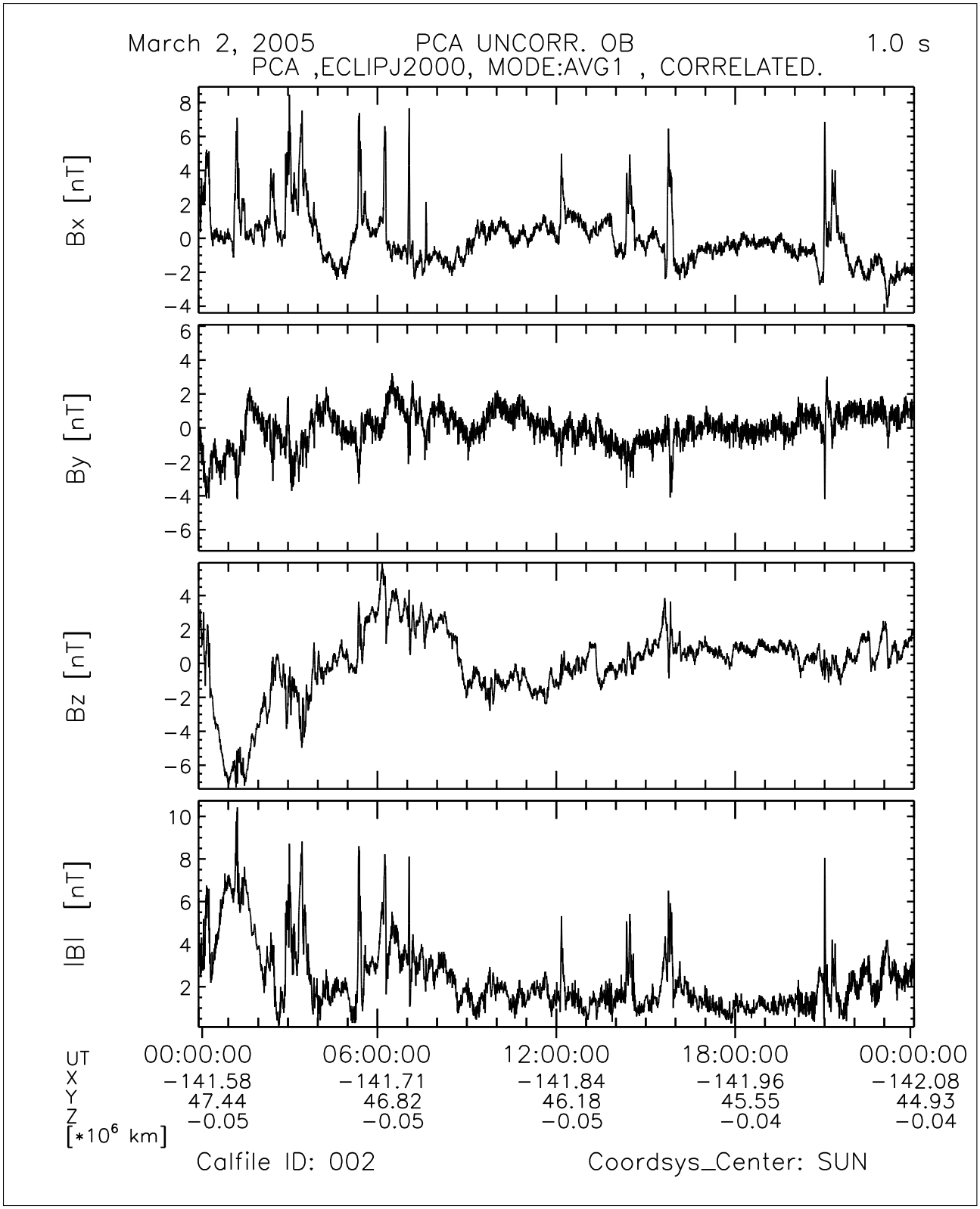

Figure 21: File: RPCMAG050302_CLJ_A1_C_T0000_2400_002

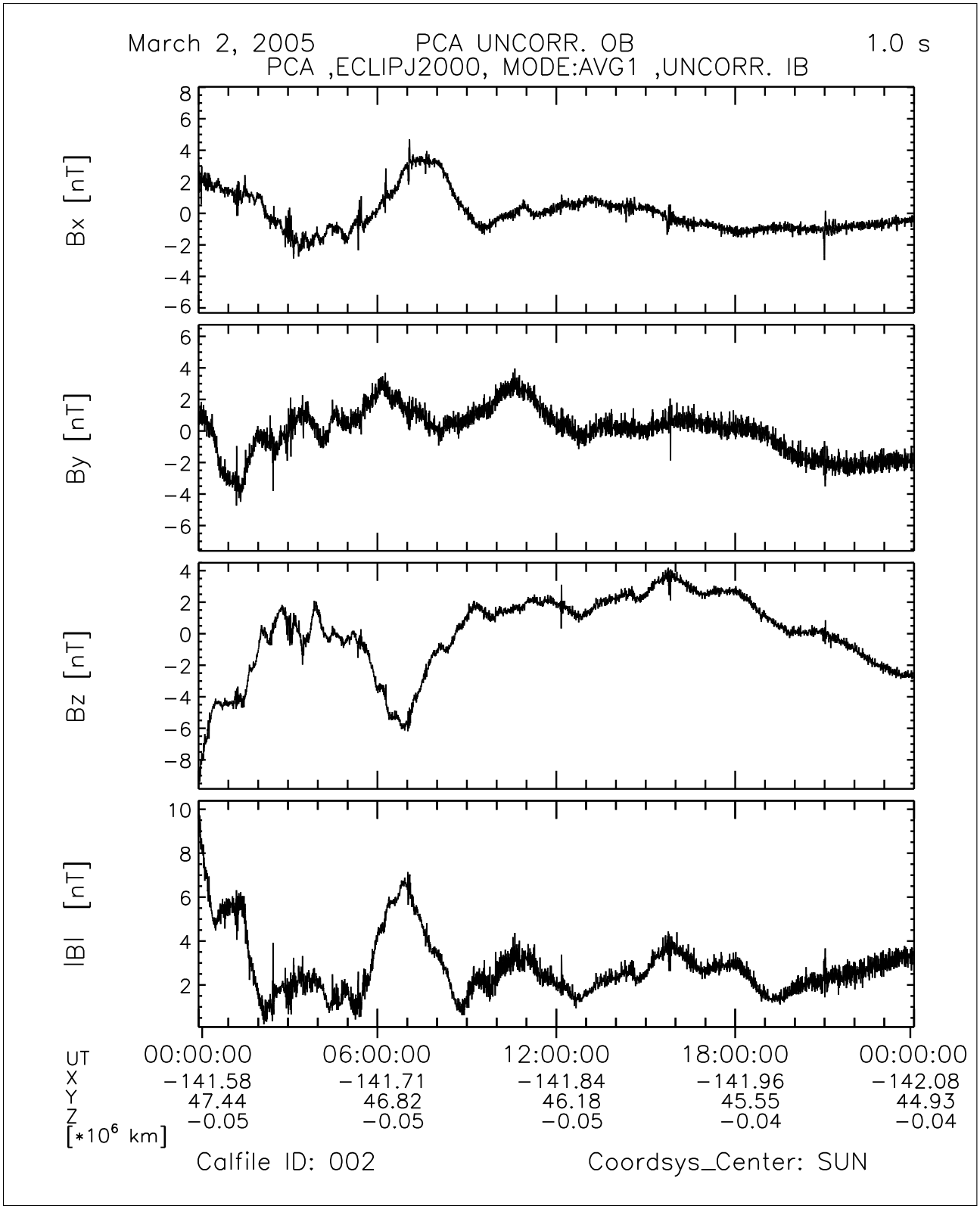

Figure 22: File: RPCMAG050302_CLJ_IB_A1_U_T0000_2400_002

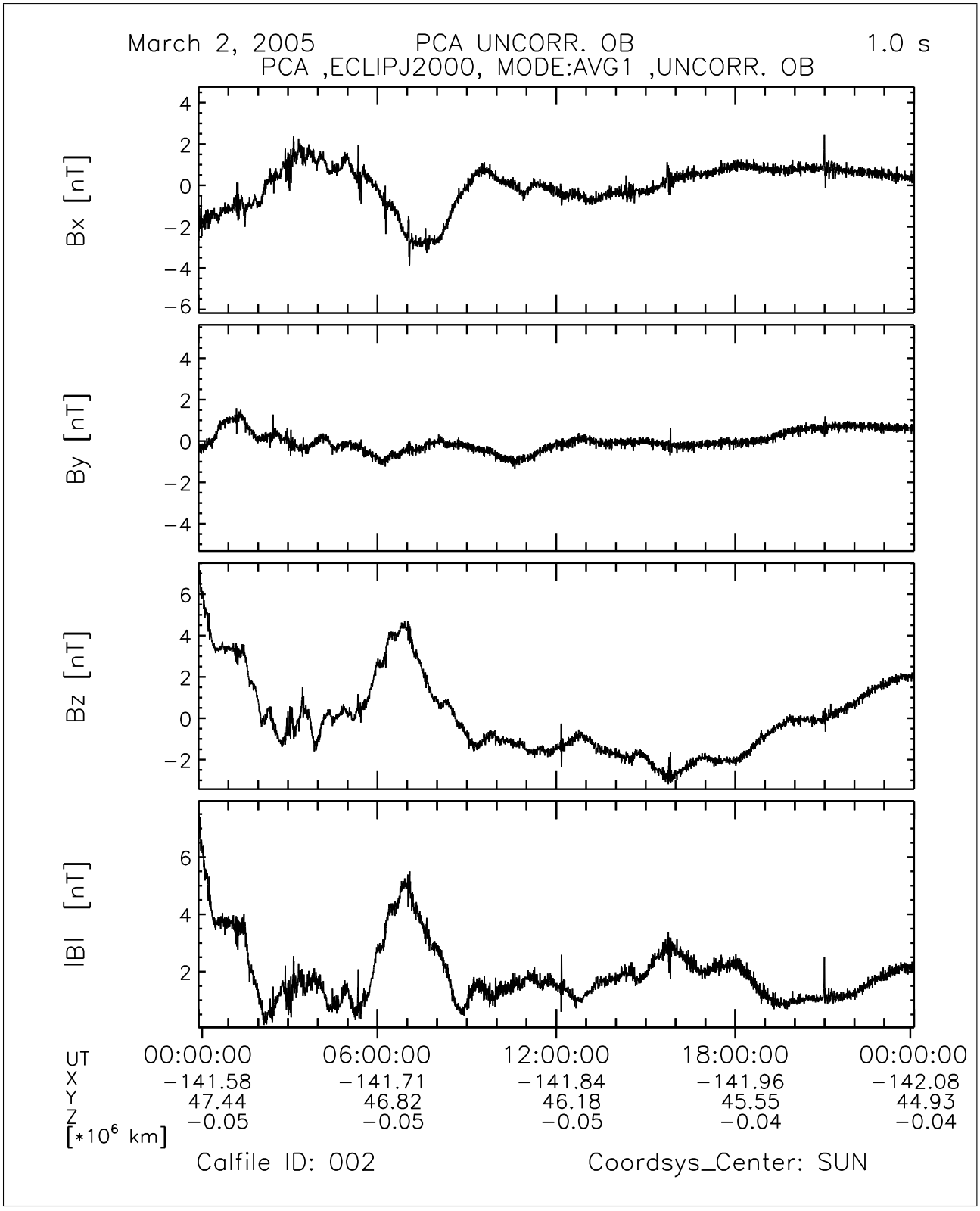

Figure 23: File: RPCMAG050302_CLJ_OB_A1_U_T0000_2400_002

3.4 March 03, 2005:

3.4.1 Actions

MAG stayed in SID 2. No problems occurred. Since today orbit data are available in Earth-centered coordinates.
ORER will be used instead of ORHR orbit files.

3.4.2 Plots of Calibrated Data

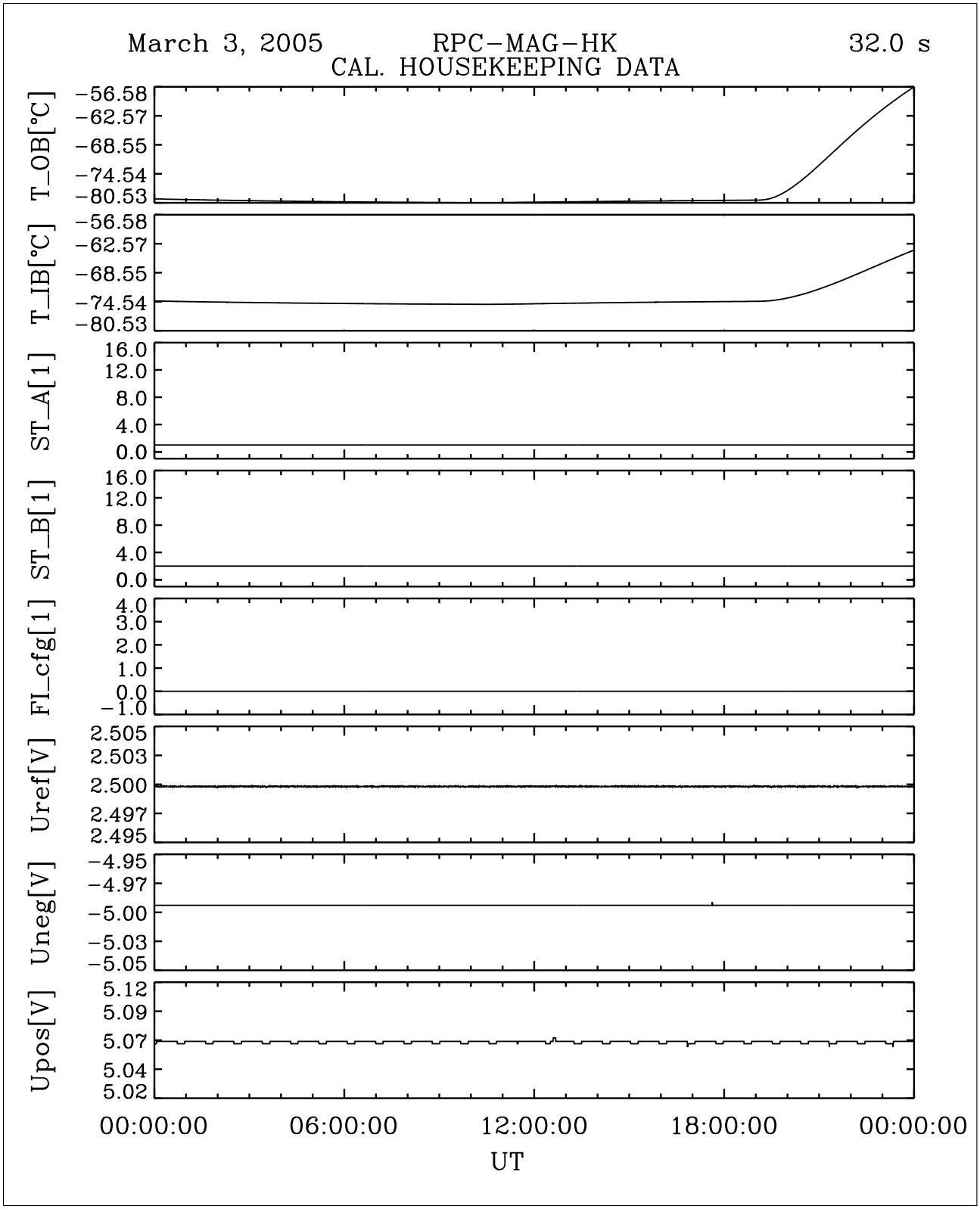

Figure 24: File: RPCMAG050303T0000_CLA_HK_P0000_2400

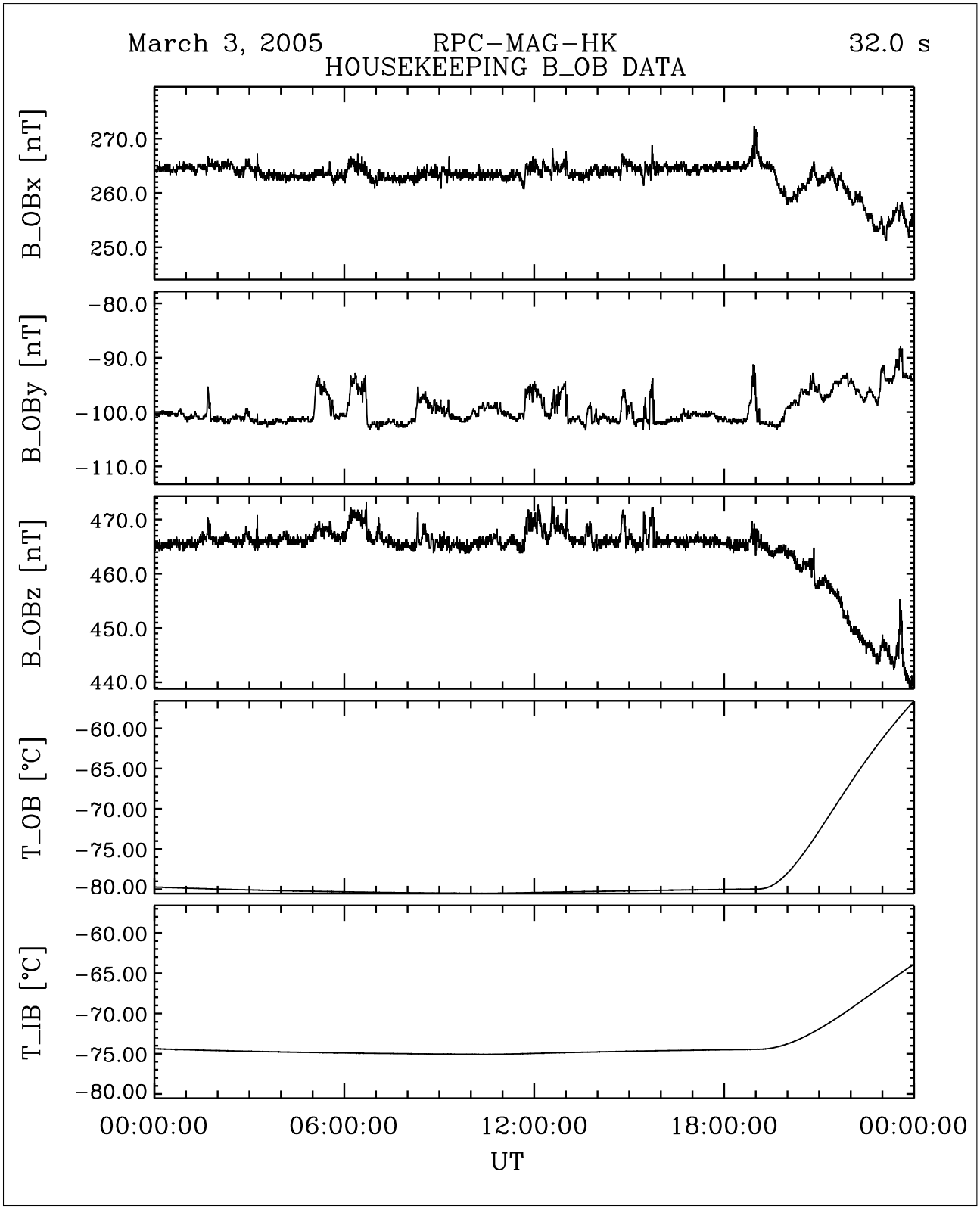

Figure 25: File: RPCMAG050303T0000_CLA_HK_B_P0000_2400

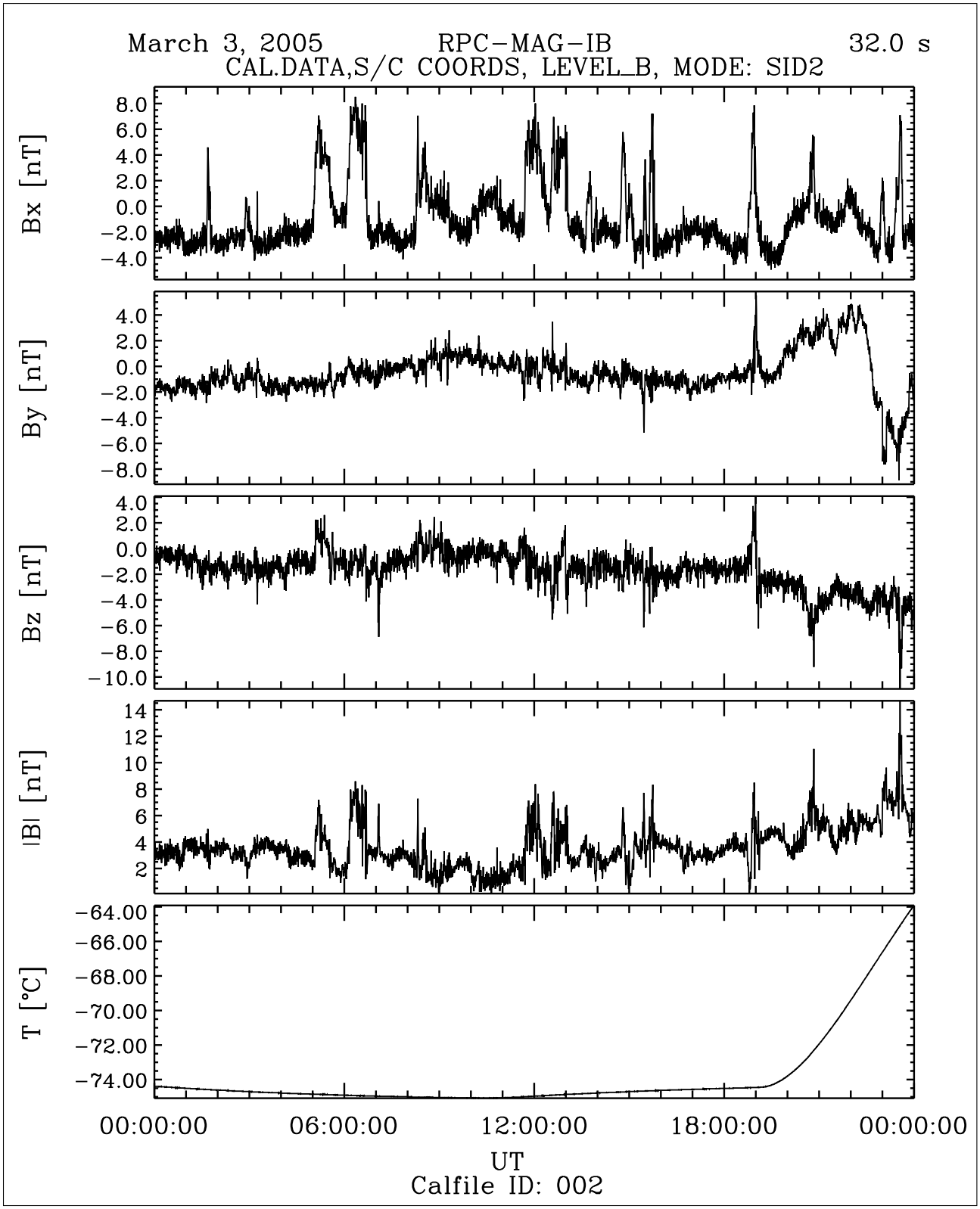

Figure 26: File: RPCMAG050303T0000_CLB_IB_M2_T0000_2400_002

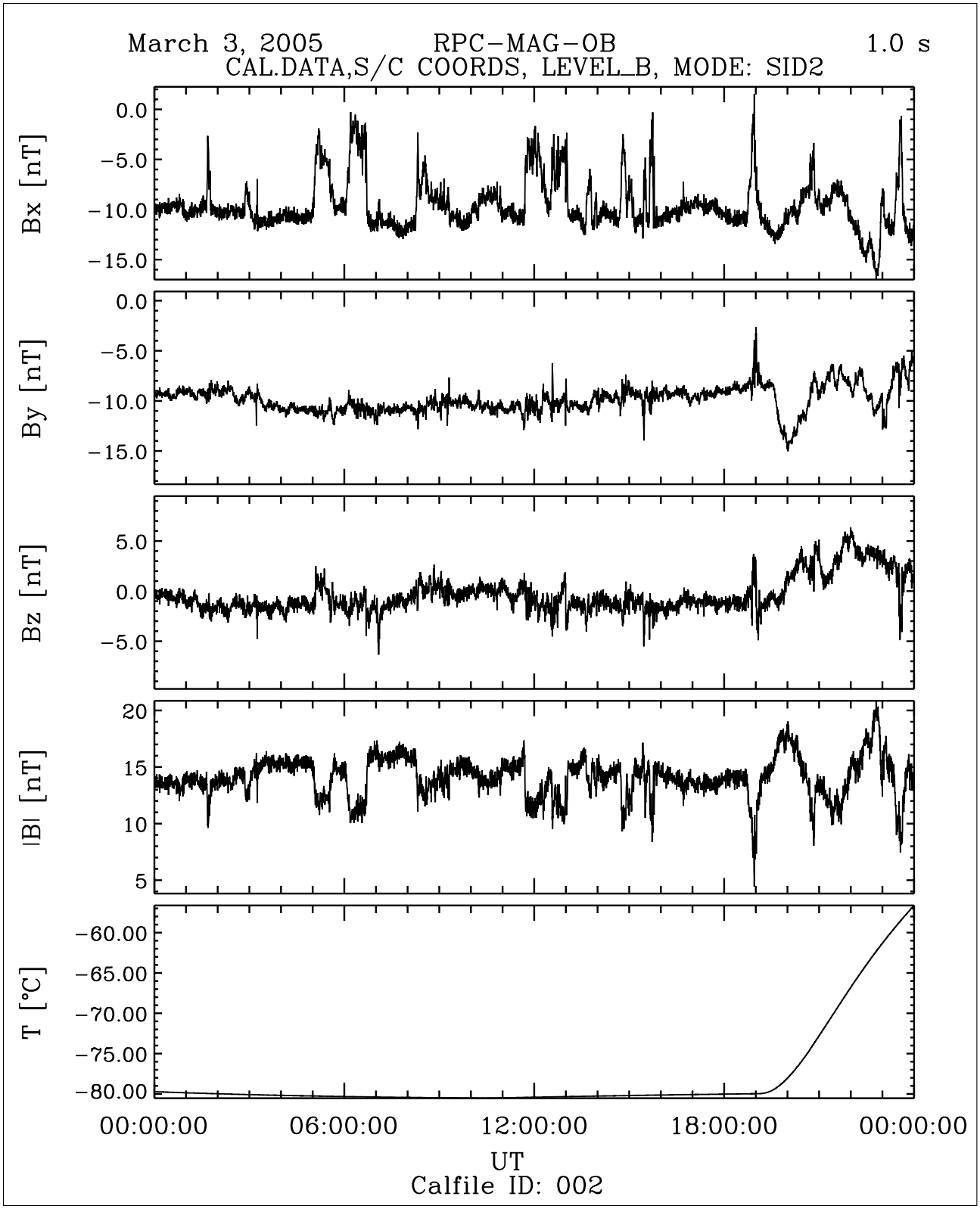

Figure 27: File: RPCMAG050303T0000_CLB_OB_M2_T0000_2400_002

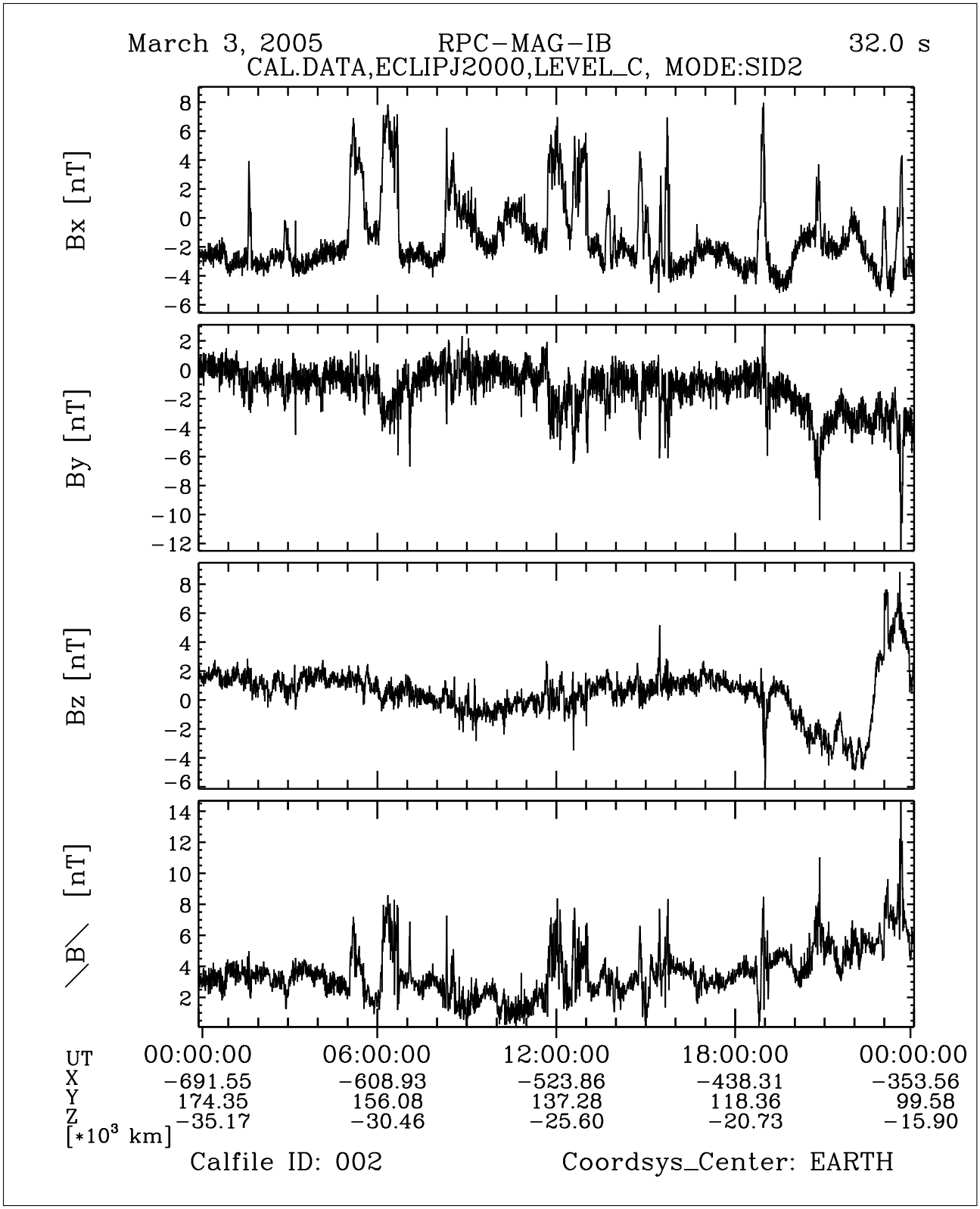

Figure 28: File: RPCMAG050303T0000_CLC_IB_M2_T0000_2400_002

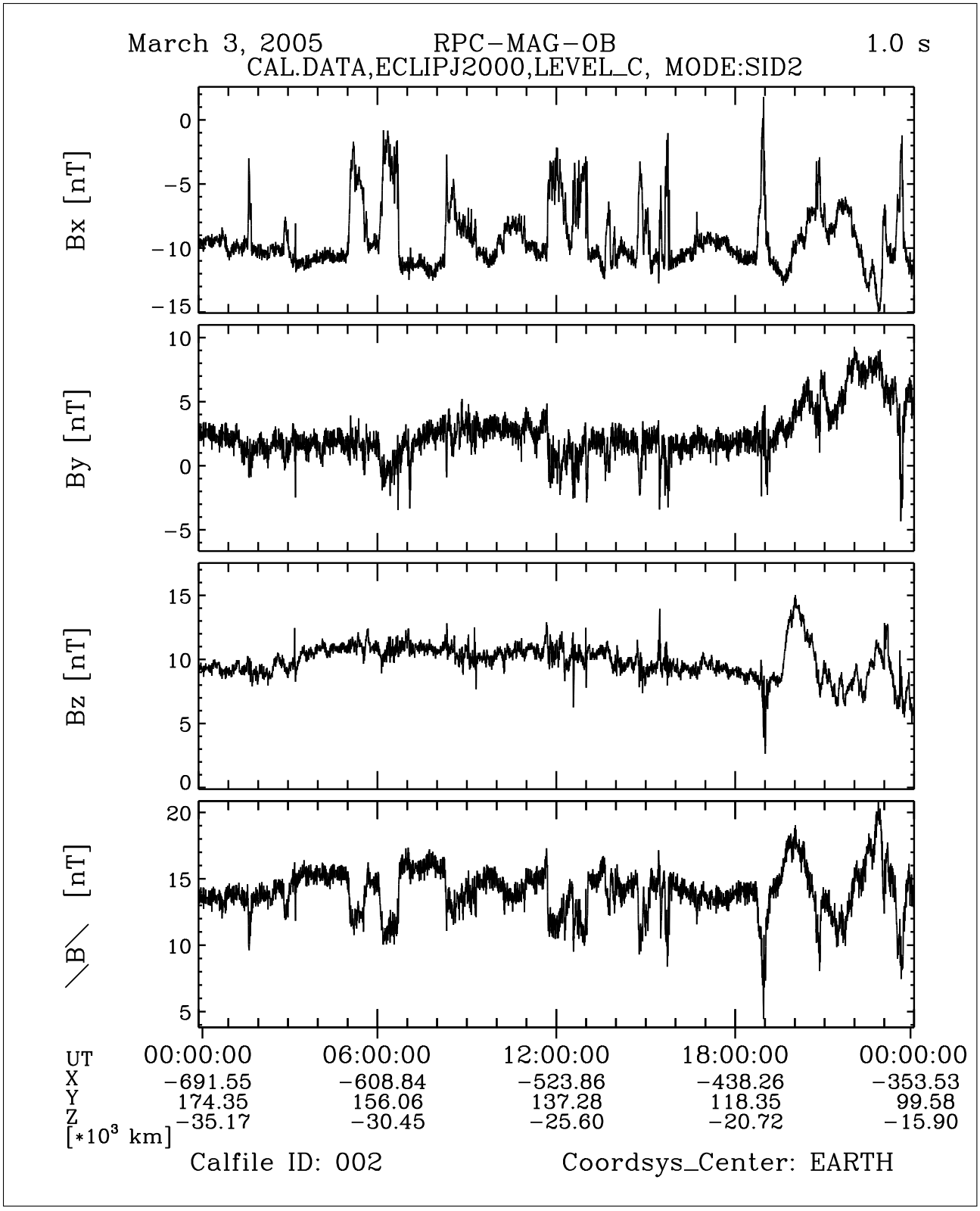

Figure 29: File: RPCMAG050303T0000_CLC_OB_M2_T0000_2400_002

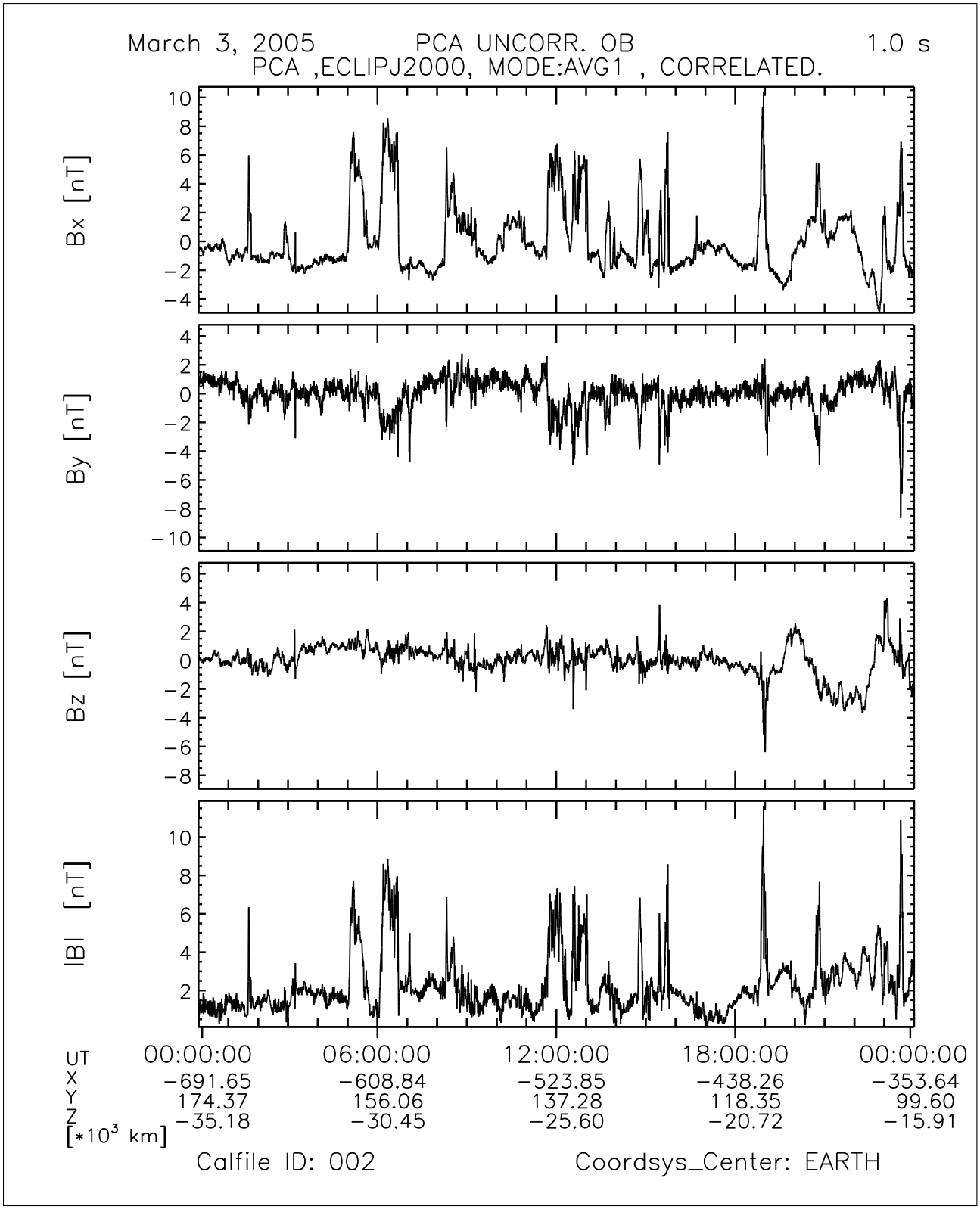

Figure 30: File: RPCMAG050303_CLJ_A1_C_T0000_2400_002

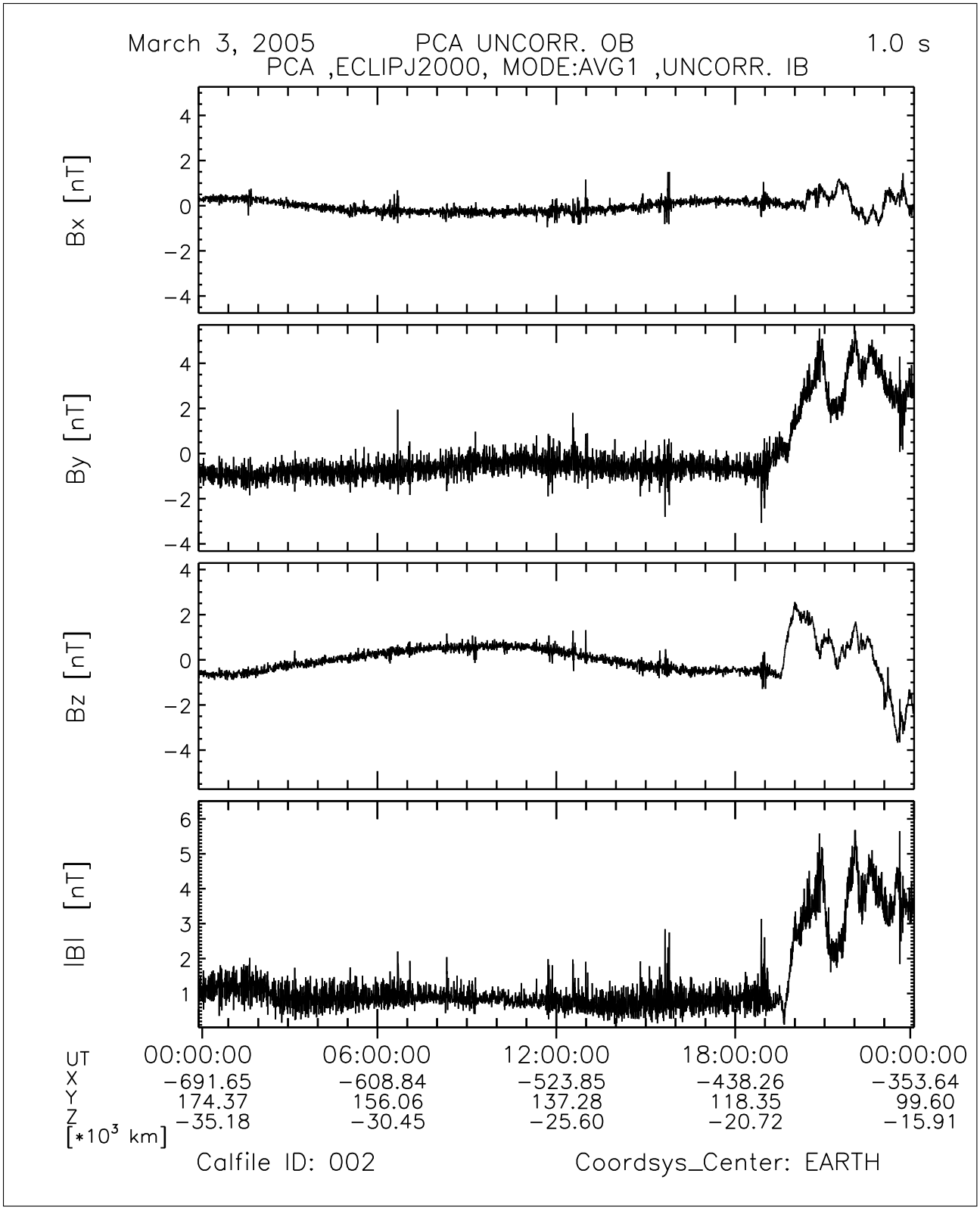

Figure 31: File: RPCMAG050303_CLJ_IB_A1_U_T0000_2400_002

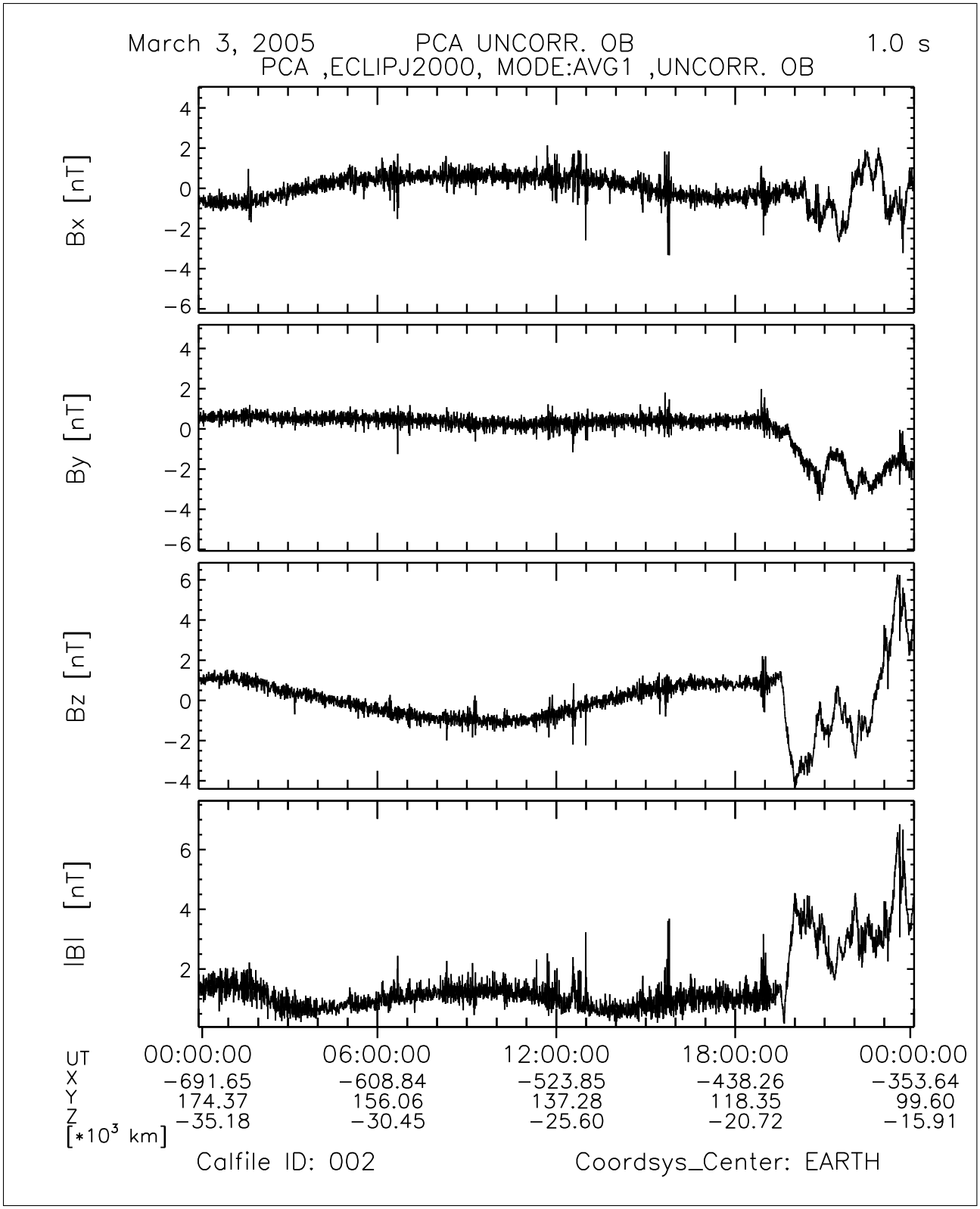

Figure 32: File: RPCMAG050303_CLJ_OB_A1_U_T0000_2400_002

3.5 March 04, 2005:

3.5.1 Actions

MAG stayed in SID 2. No problems occurred. The closest approach (CA) happened at 22:09.
ORER will be used instead of ORHR orbit files.

3.5.2 Plots of Calibrated Data

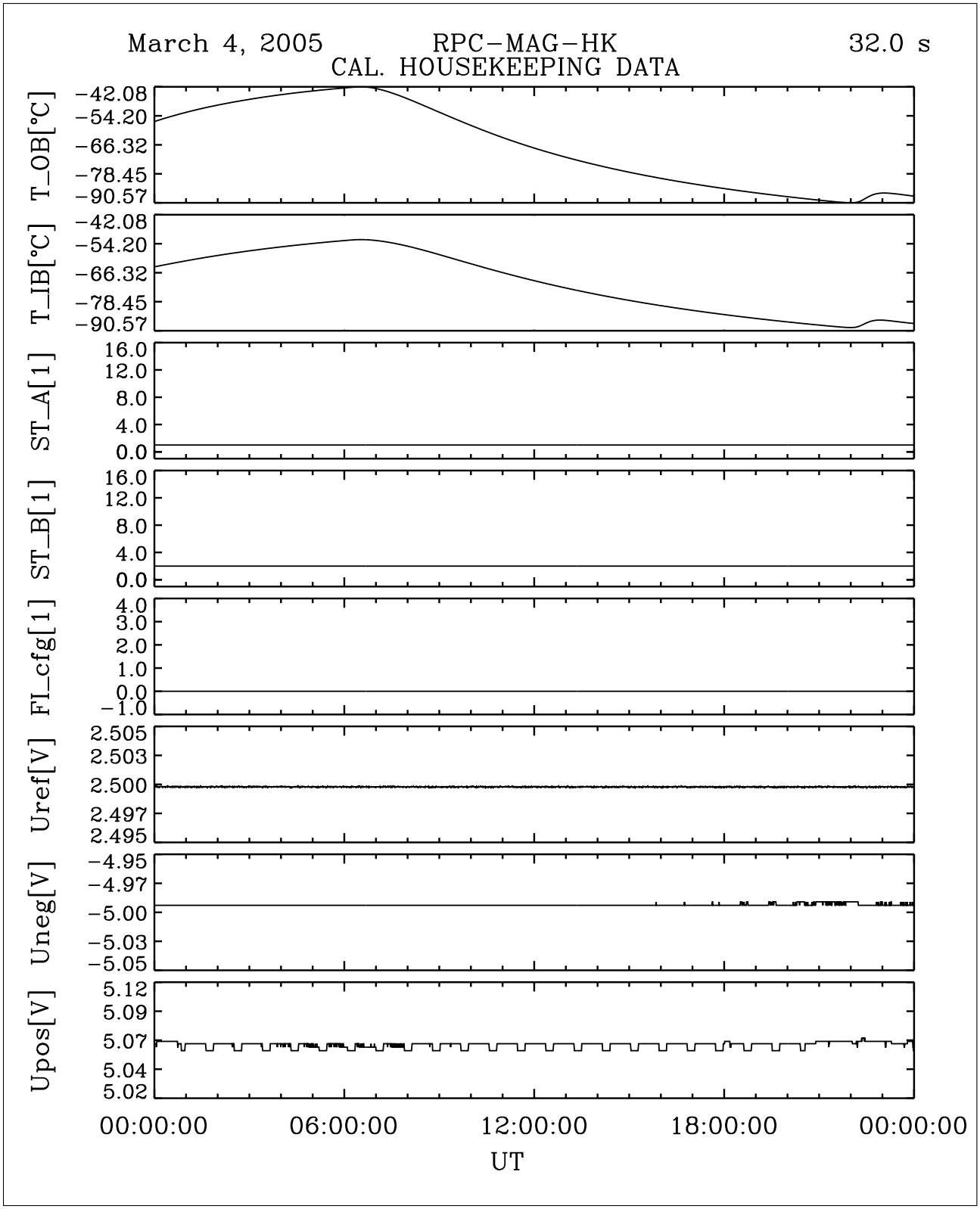

Figure 33: File: RPCMAG050304T0000_CLA_HK_P0000_2400

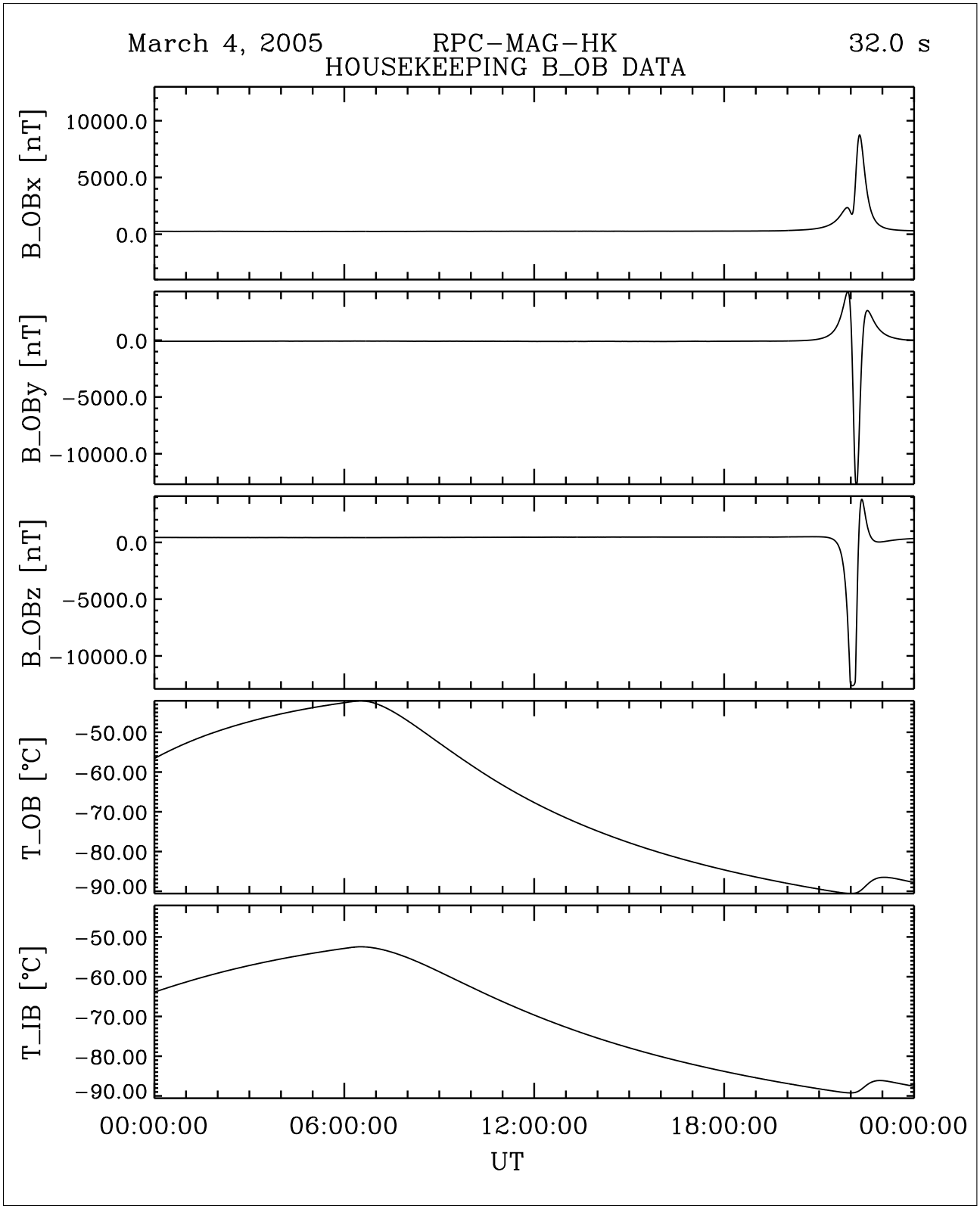

Figure 34: File: RPCMAG050304T0000_CLA_HK_B_P0000_2400

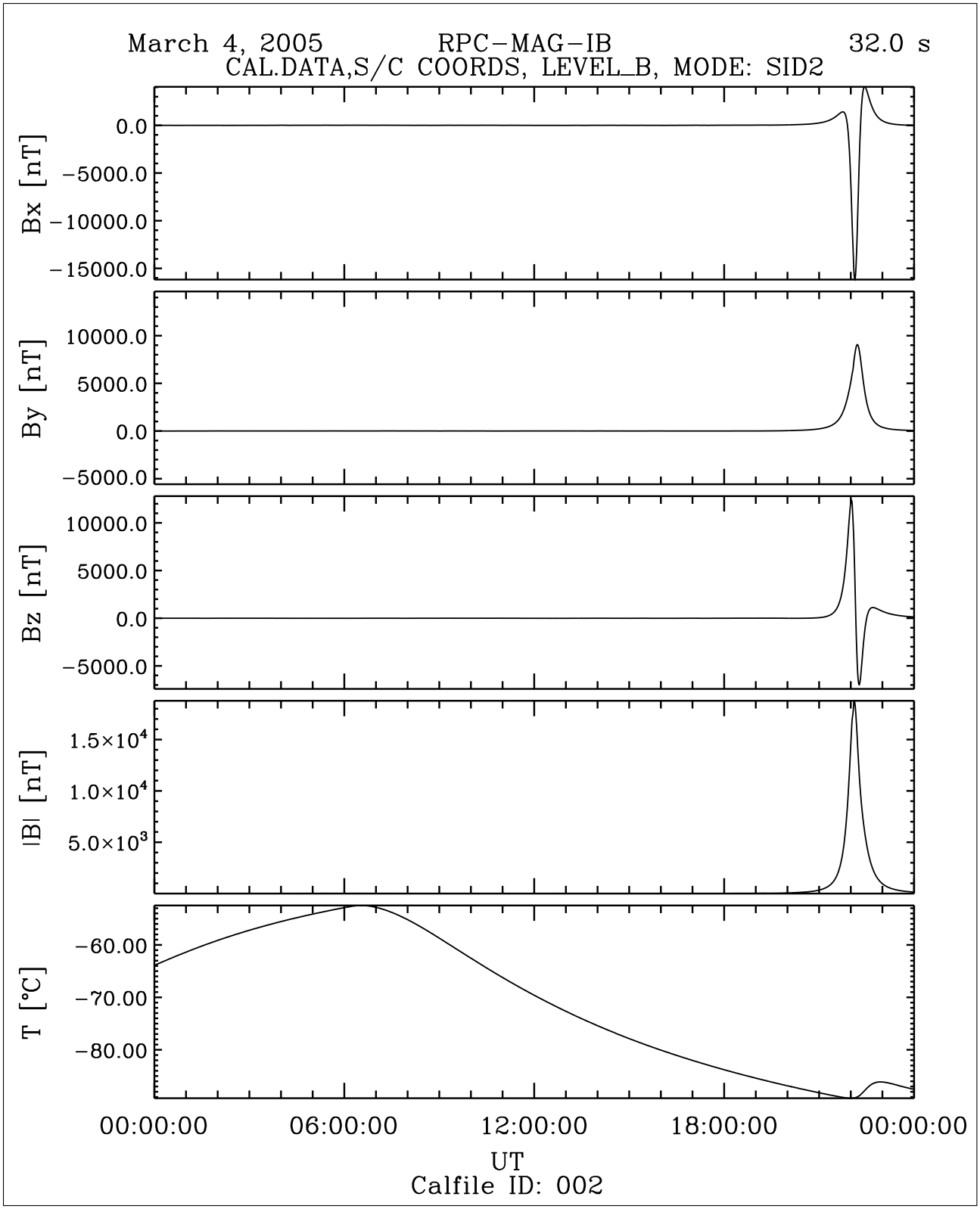

Figure 35: File: RPCMAG050304T0000_CLB_IB_M2_T0000_2400_002

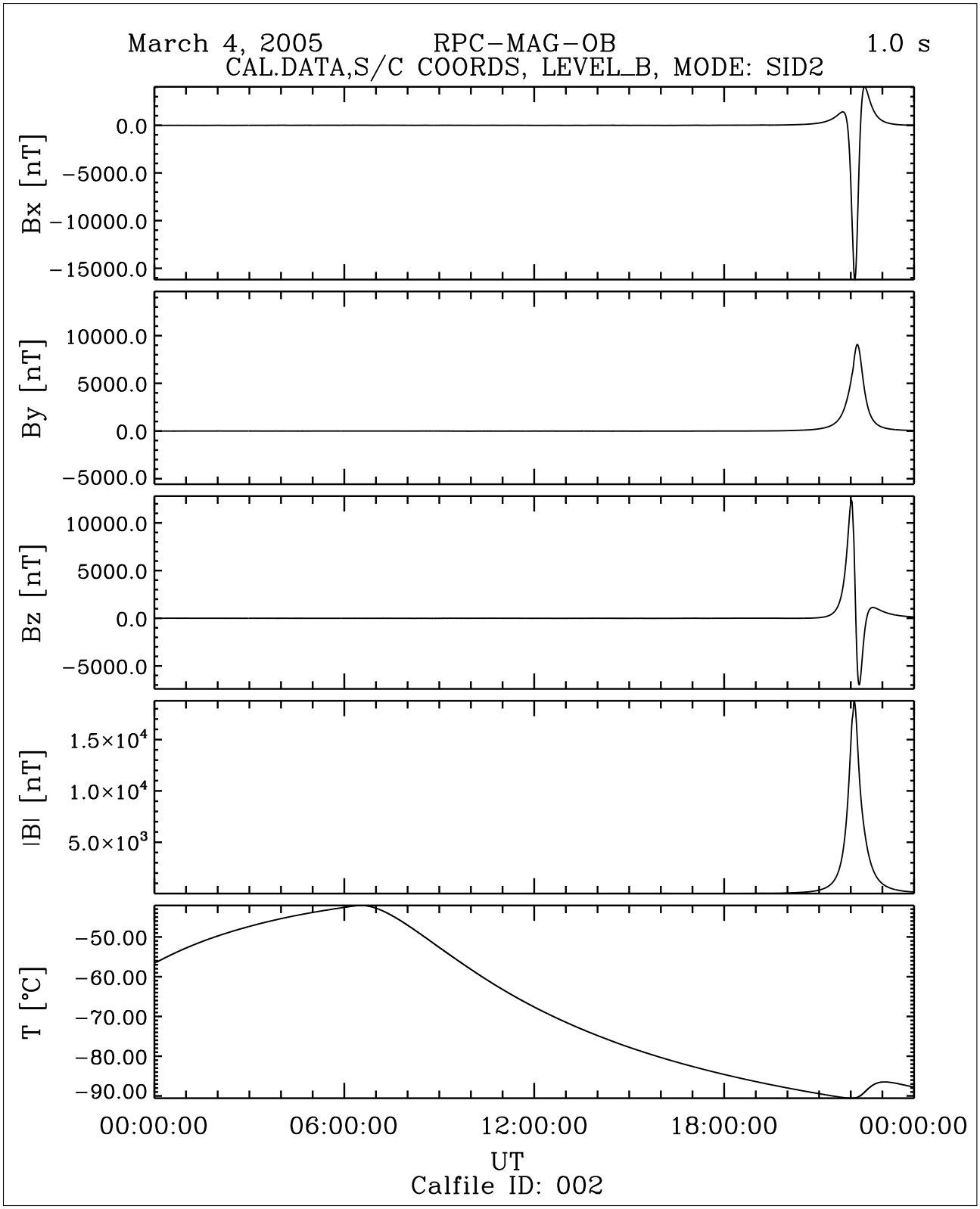

Figure 36: File: RPCMAG050304T0000_CLB_OB_M2_T0000_2400_002

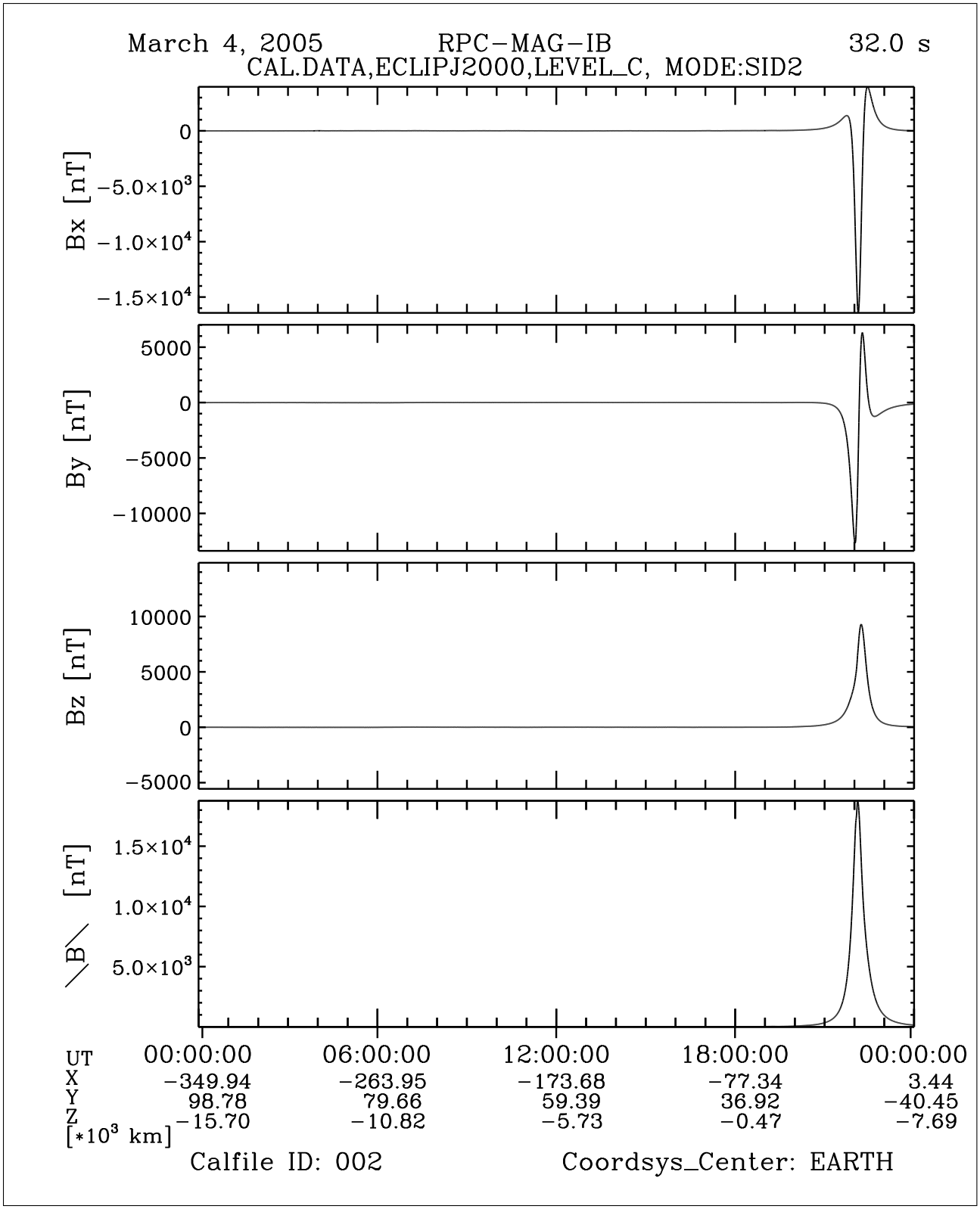

Figure 37: File: RPCMAG050304T0000_CLC_IB_M2_T0000_2400_002

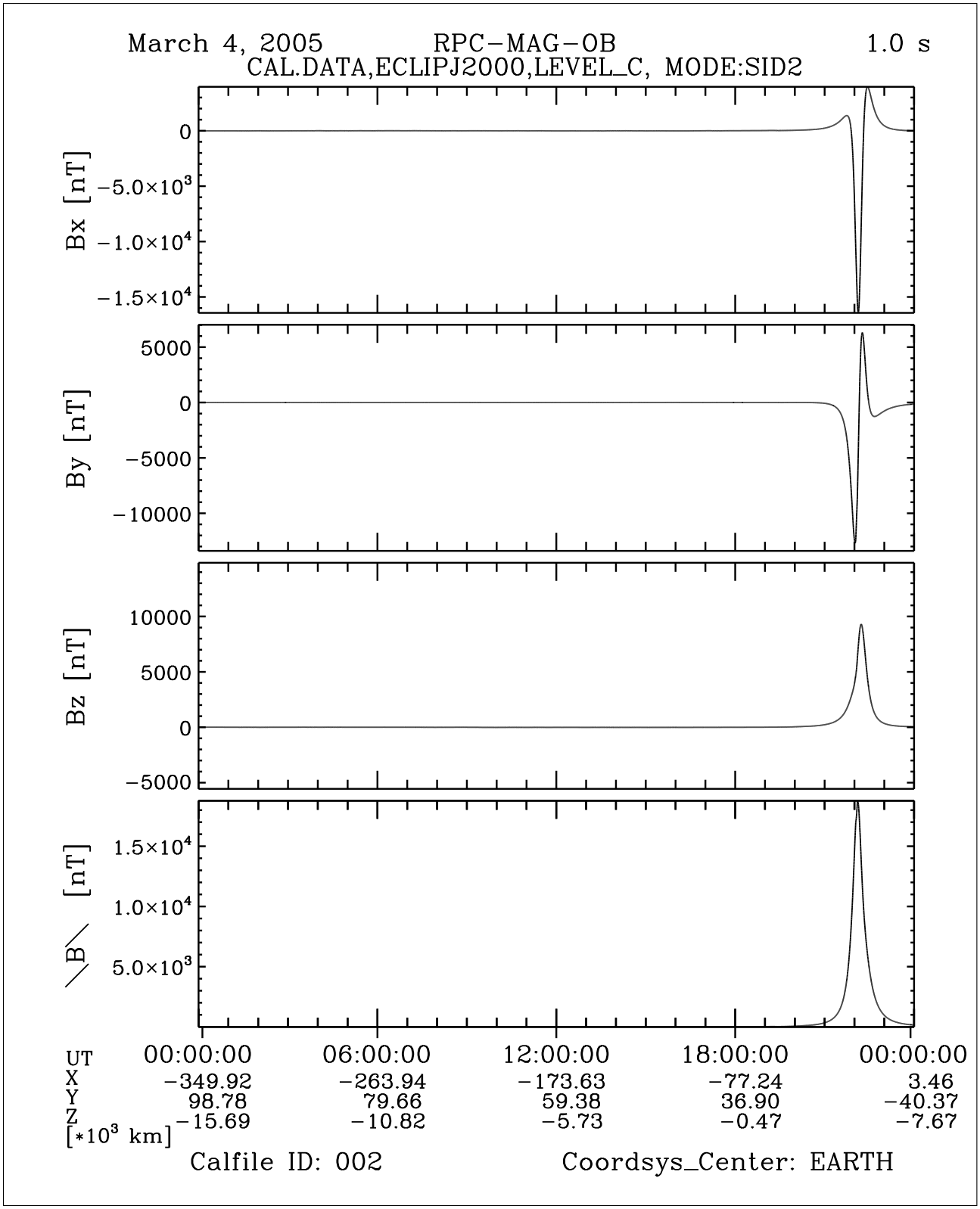

Figure 38: File: RPCMAG050304T0000_CLC_OB_M2_T0000_2400_002

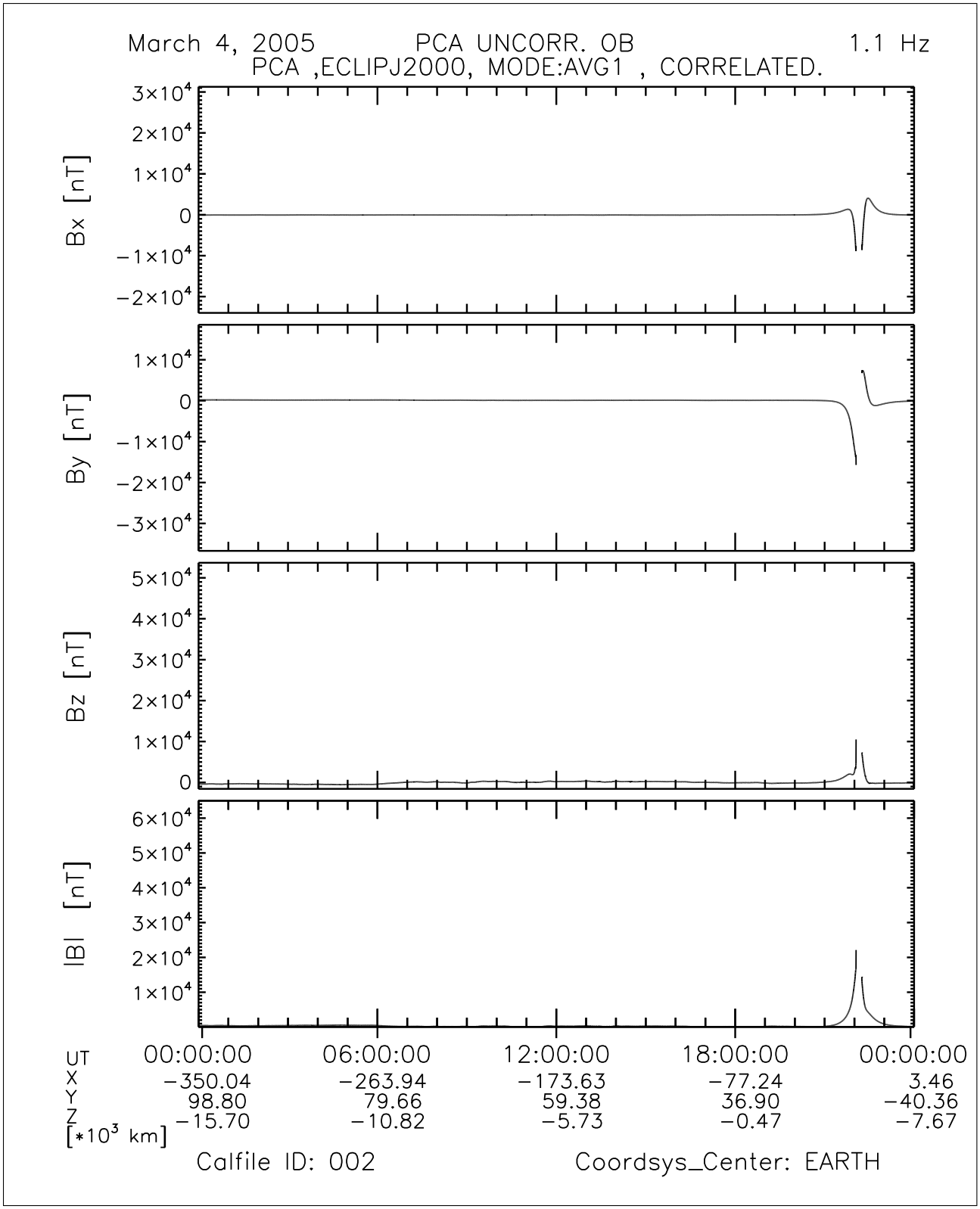

Figure 39: File: RPCMAG050304_CLJ_A1_C_T0000_2400_002

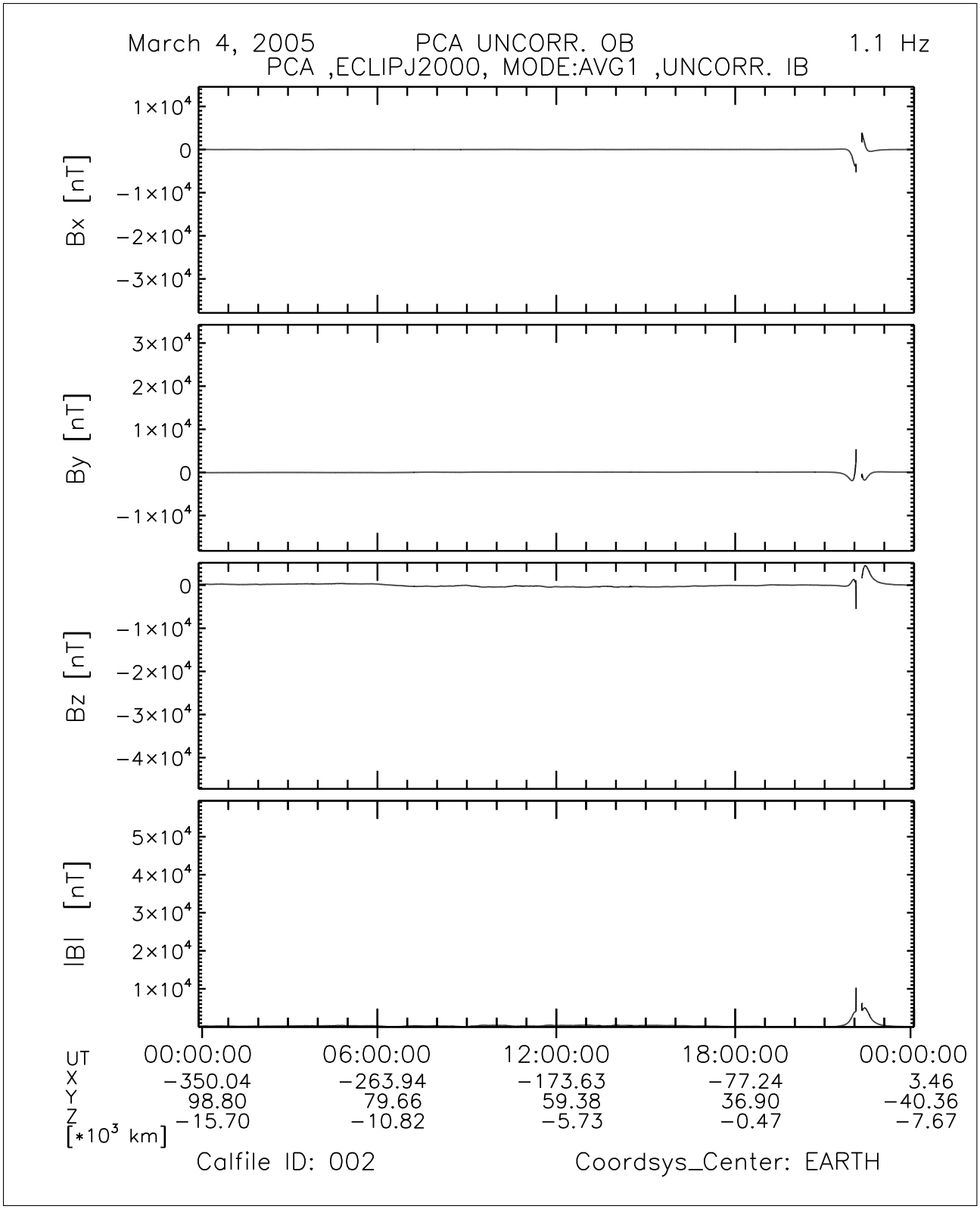

Figure 40: File: RPCMAG050304_CLJ_IB_A1_U_T0000_2400_002

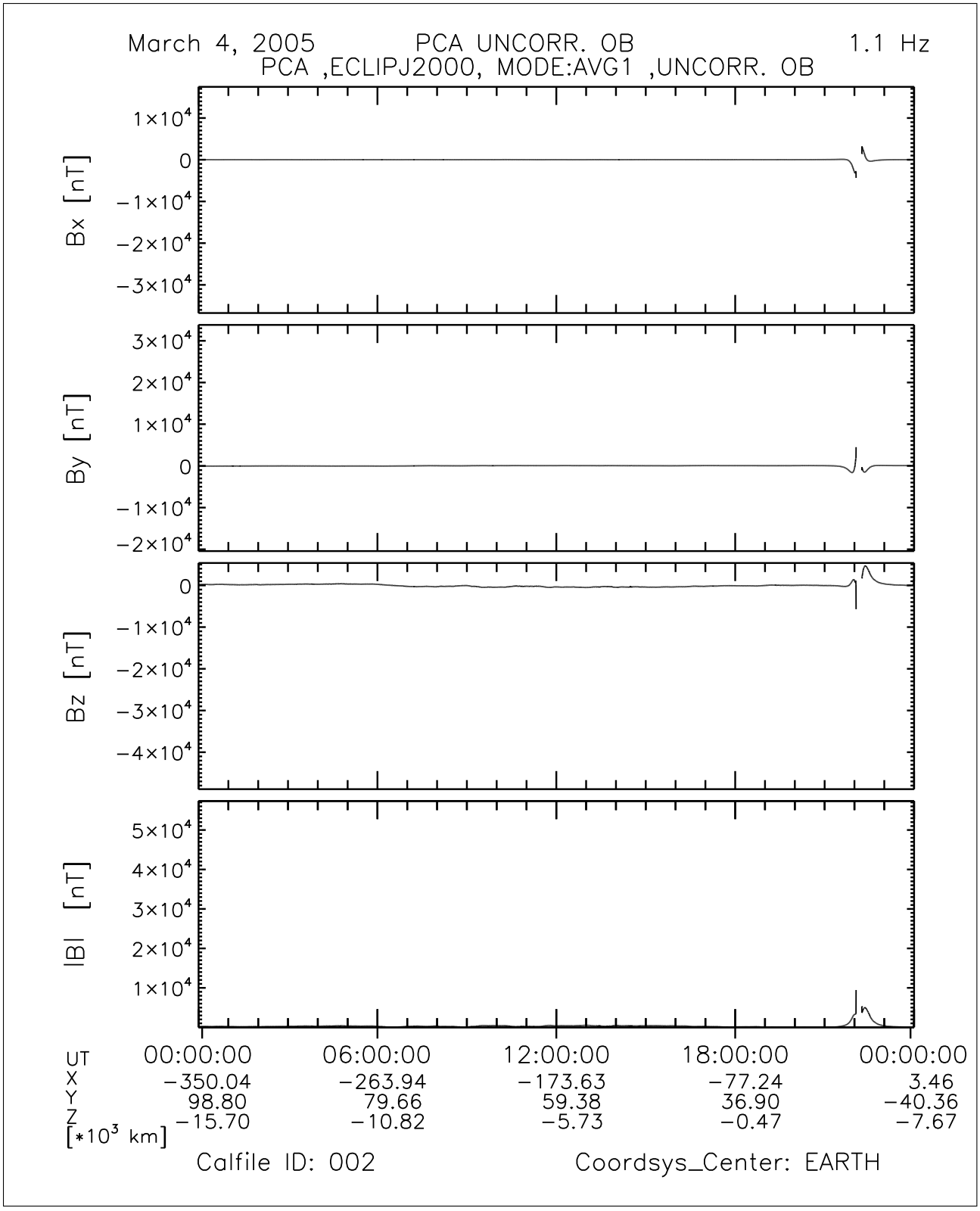

Figure 41: File: RPCMAG050304_CLJ_OB_A1_U_T0000_2400_002

3.6 March 05, 2005:

3.6.1 Actions

MAG stayed nominally in SID 2. At 00:03:25 16 bad vectors occurred on the OB data. The IB data remained in good condition. Additionally at 12:49:35.00 some SID6 vectors appeared until 12:49:36.55. Besides these minor events no problems arose.
ORER data will be used instead of ORHR orbit files.

3.6.2 Plots of Calibrated Data

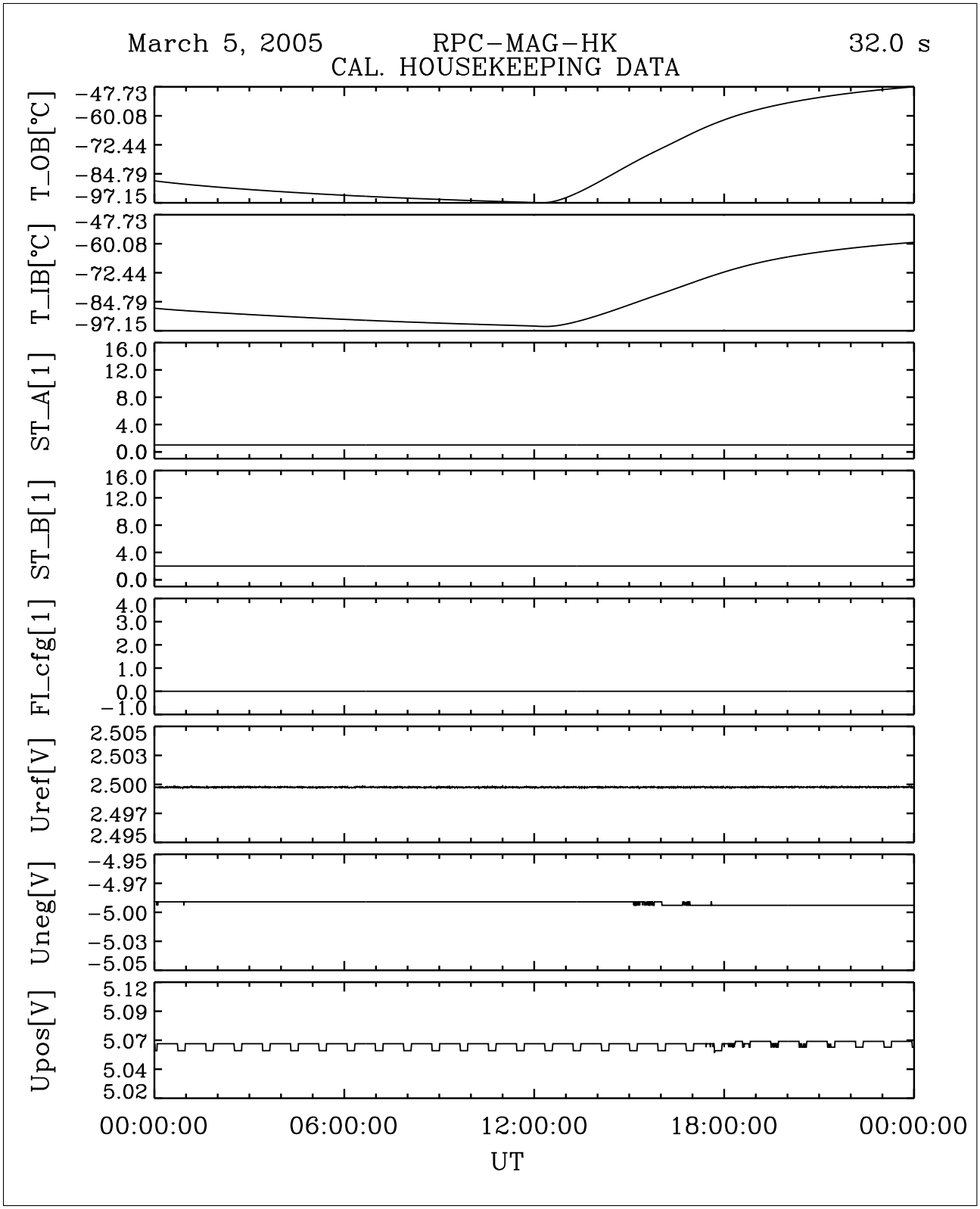

Figure 42: File: RPCMAG050305T0000_CLA_HK_P0000_2400

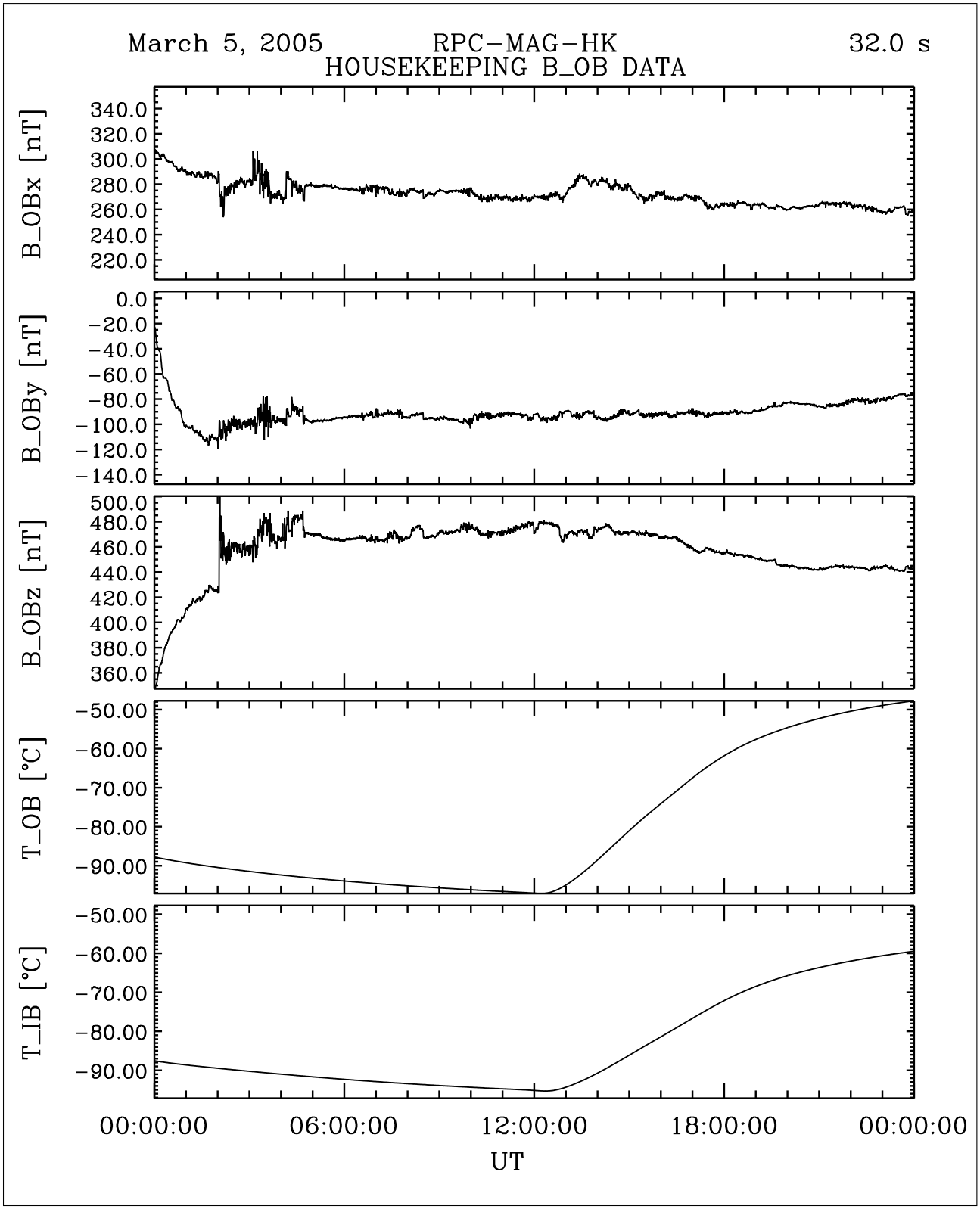

Figure 43: File: RPCMAG050305T0000_CLA_HK_B_P0000_2400

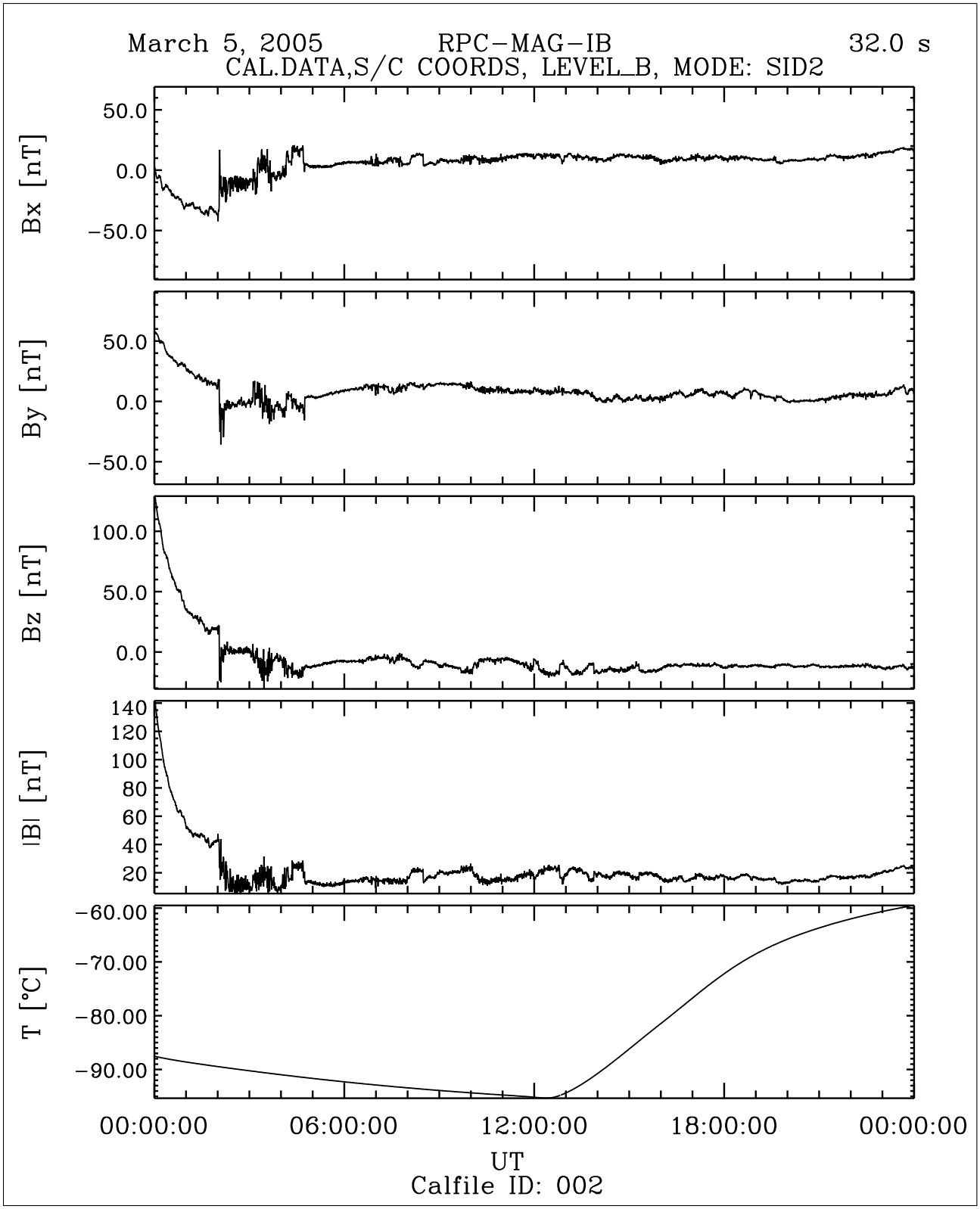

Figure 44: File: RPCMAG050305T0000_CLB_IB_M2_T0000_2400_002

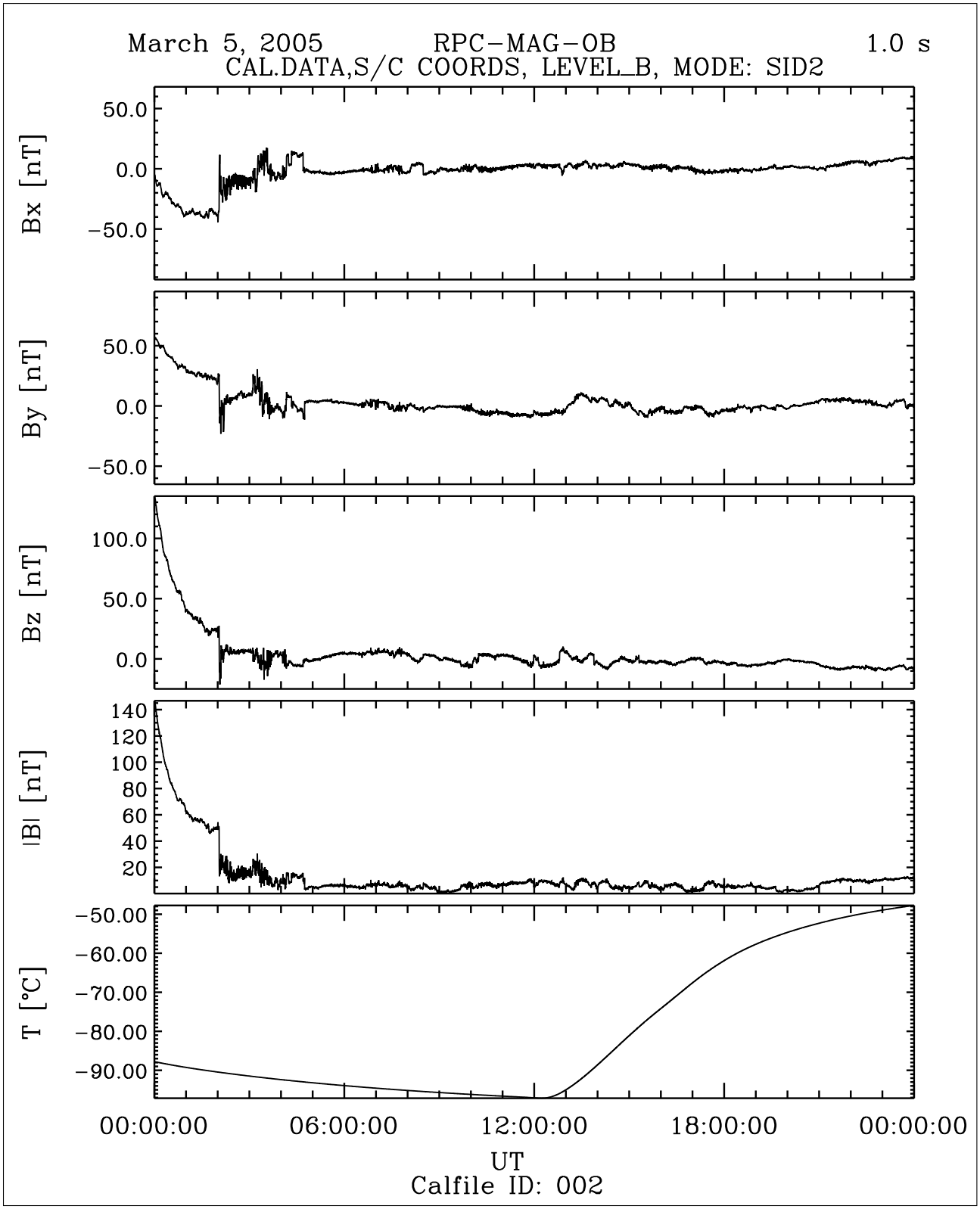

Figure 45: File: RPCMAG050305T0000_CLB_OB_M2_T0000_2400_002

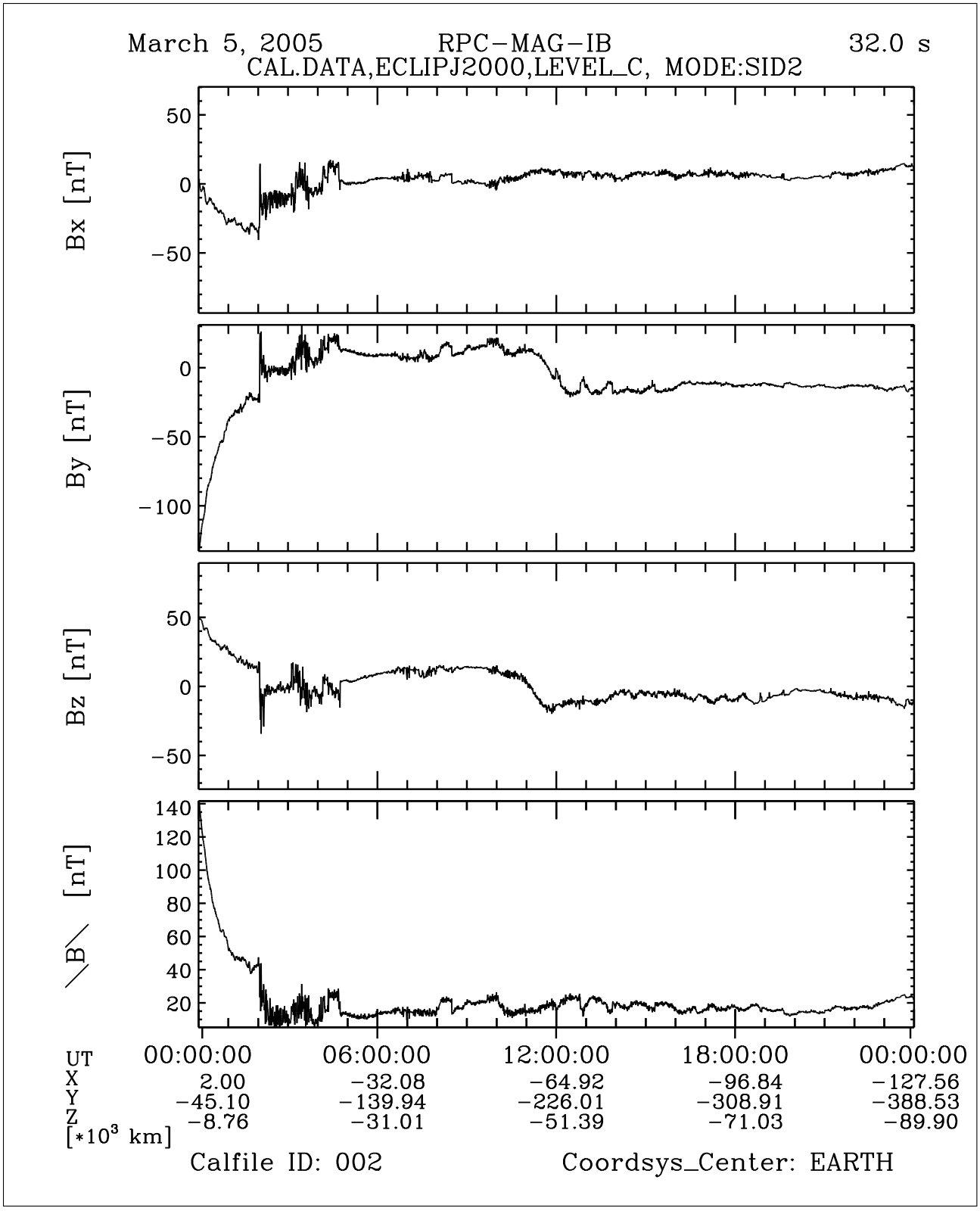

Figure 46: File: RPCMAG050305T0000_CLC_IB_M2_T0000_2400_002

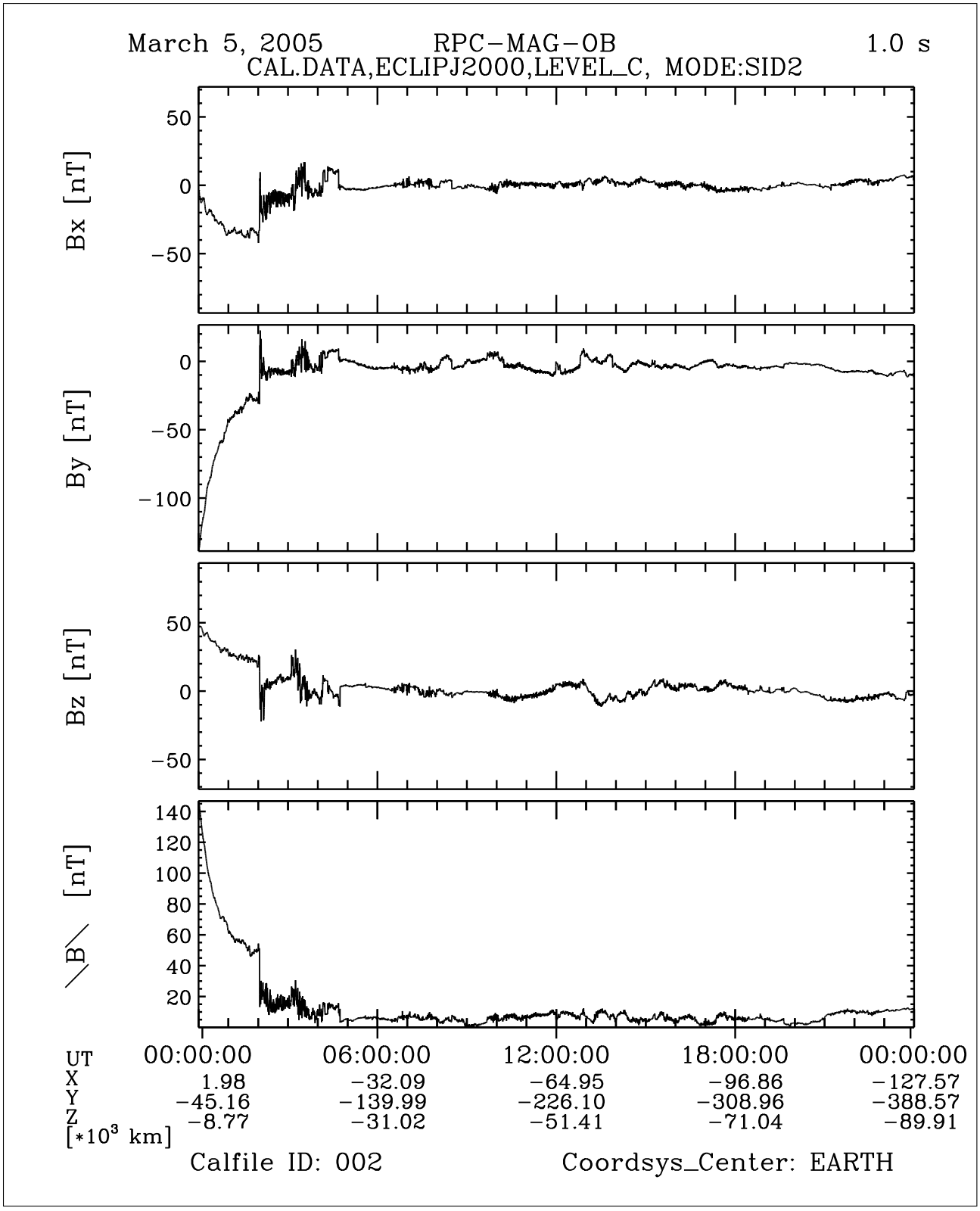

Figure 47: File: RPCMAG050305T0000_CLC_OB_M2_T0000_2400_002

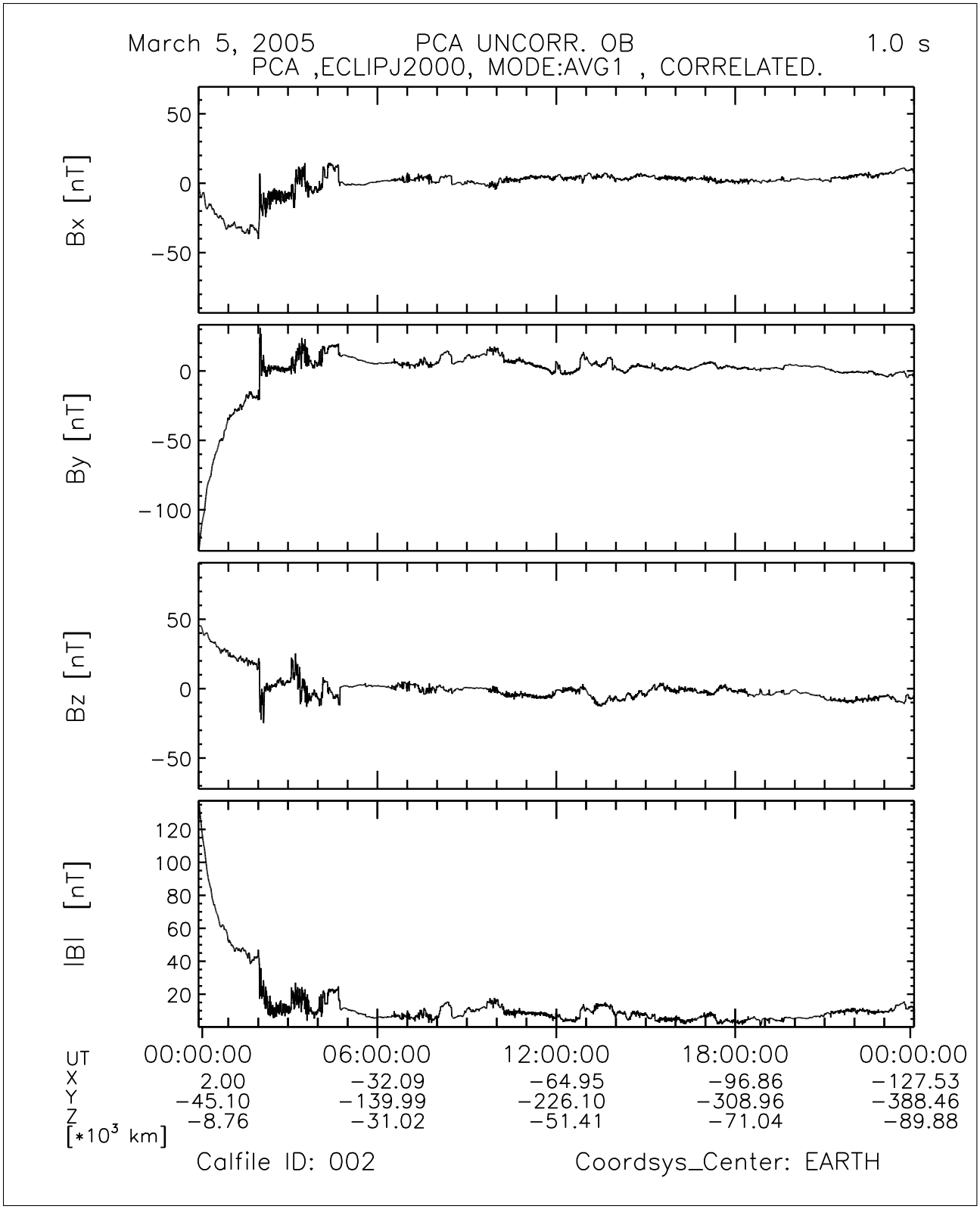

Figure 48: File: RPCMAG050305_CLJ_A1_C_T0000_2400_002

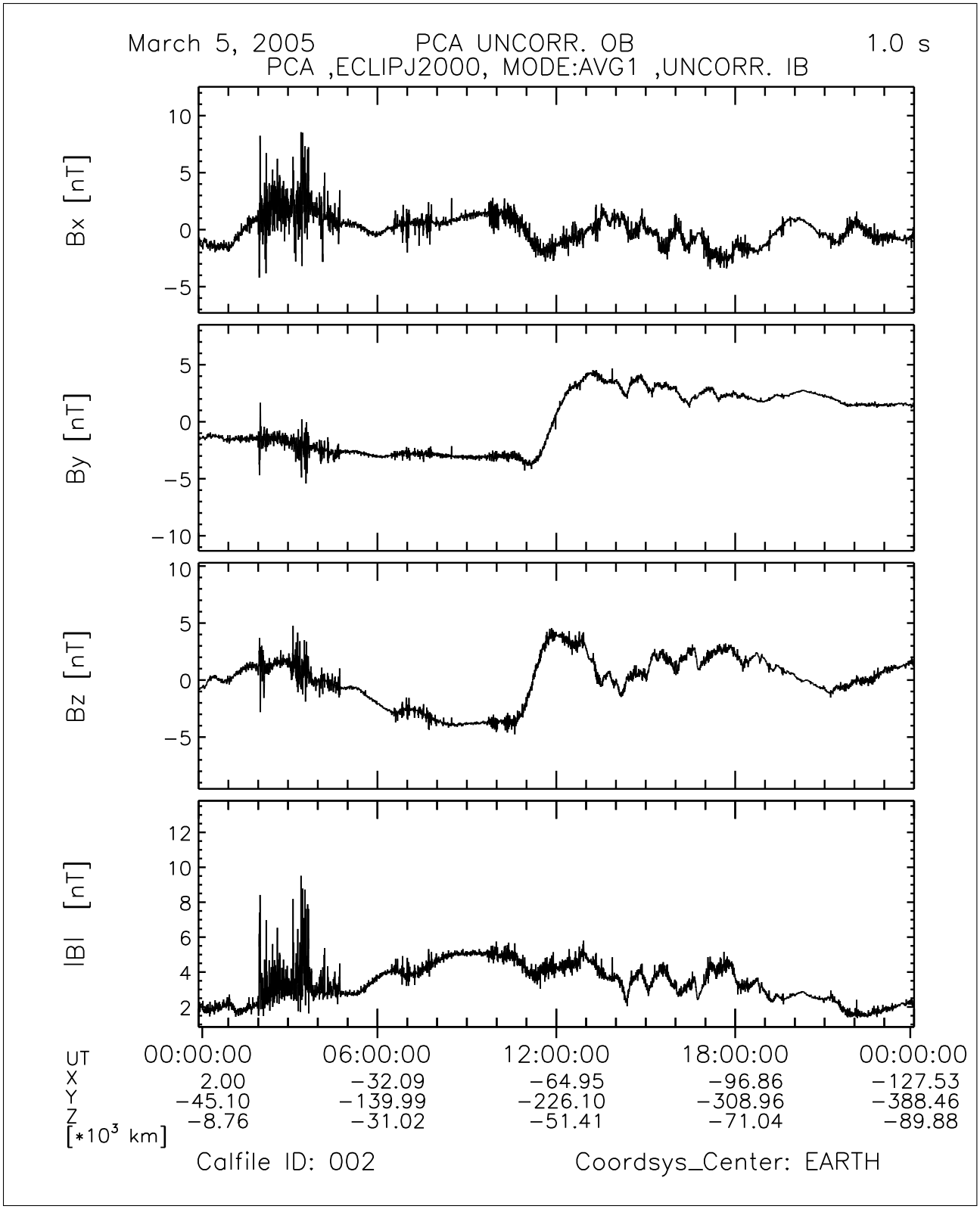

Figure 49: File: RPCMAG050305_CLJ_IB_A1_U_T0000_2400_002

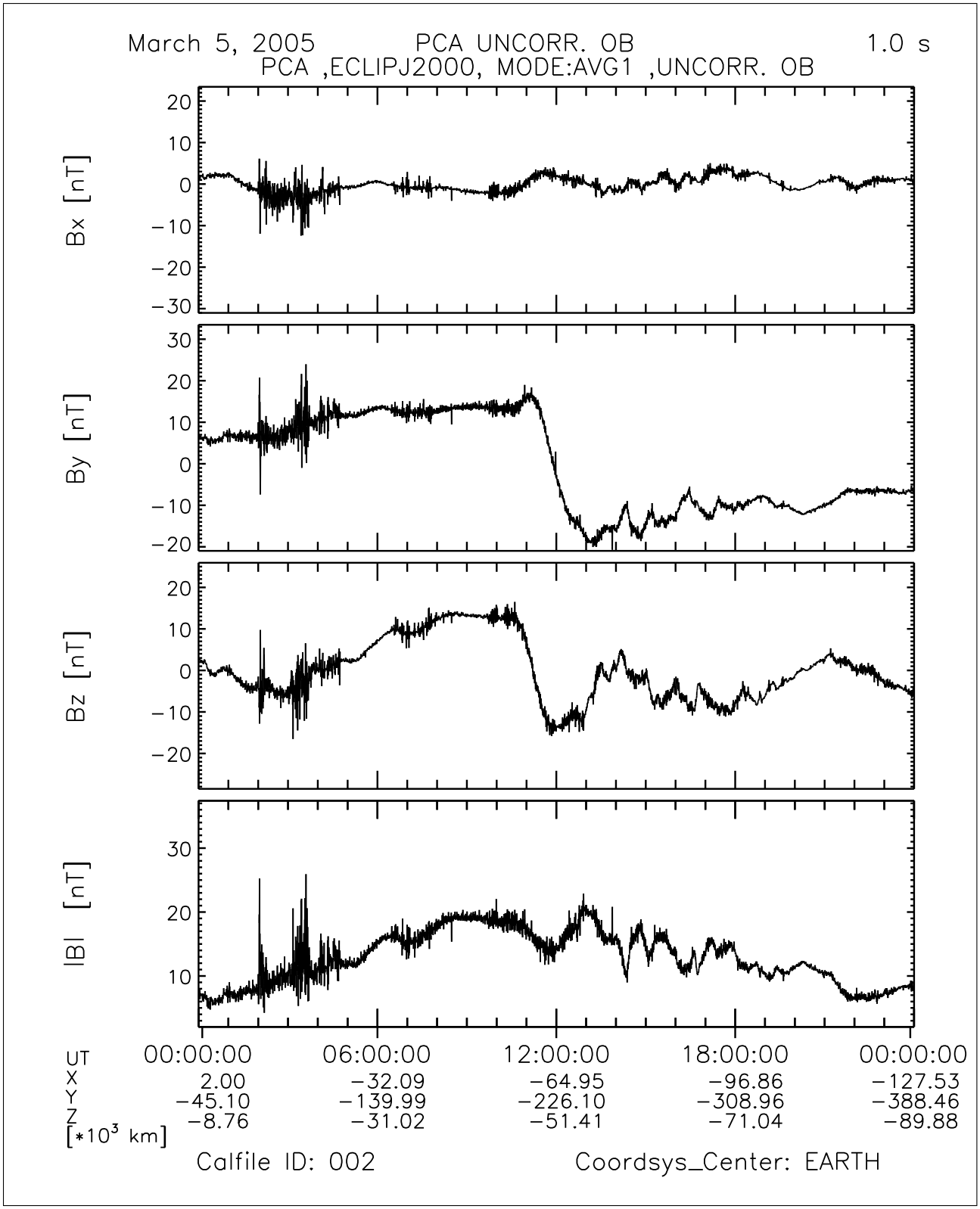

Figure 50: File: RPCMAG050305_CLJ_OB_A1_U_T0000_2400_002

3.7 March 06, 2005:

3.7.1 Actions

MAG stayed in SID 2. No problems occurred.
ORER will be used instead of ORHR orbit files.

3.7.2 Plots of Calibrated Data

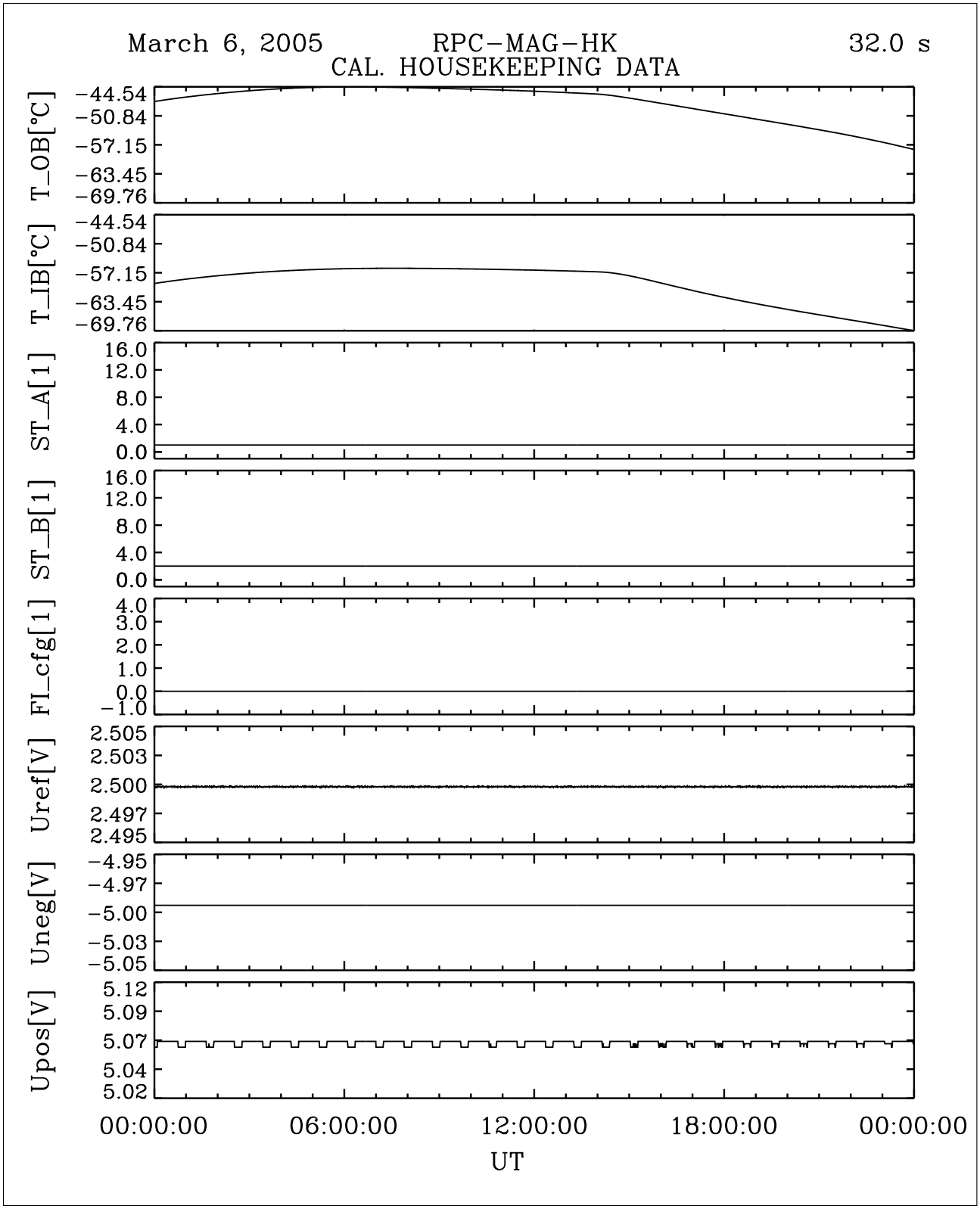

Figure 51: File: RPCMAG050306T0000_CLA_HK_P0000_2400

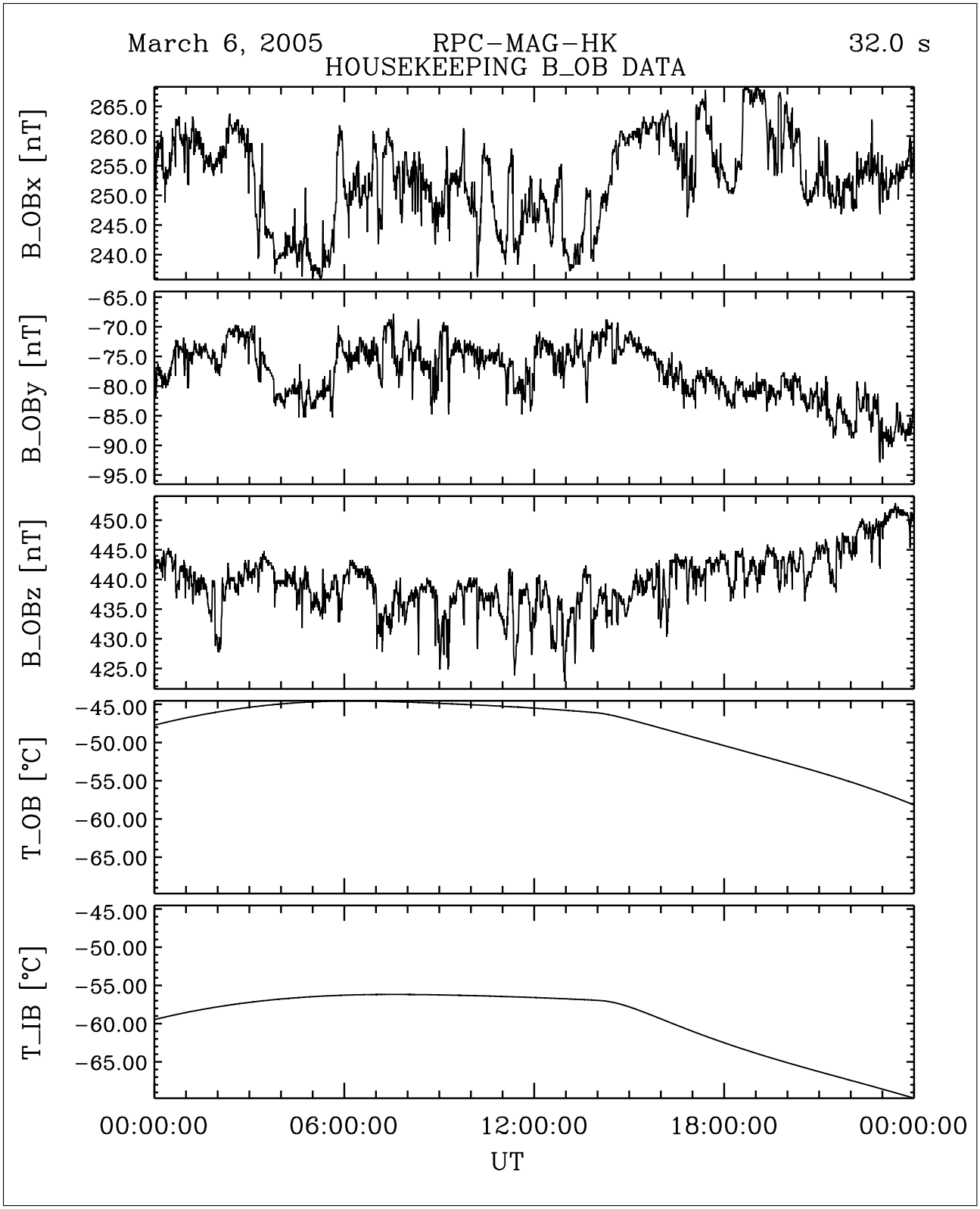

Figure 52: File: RPCMAG050306T0000_CLA_HK_B_P0000_2400

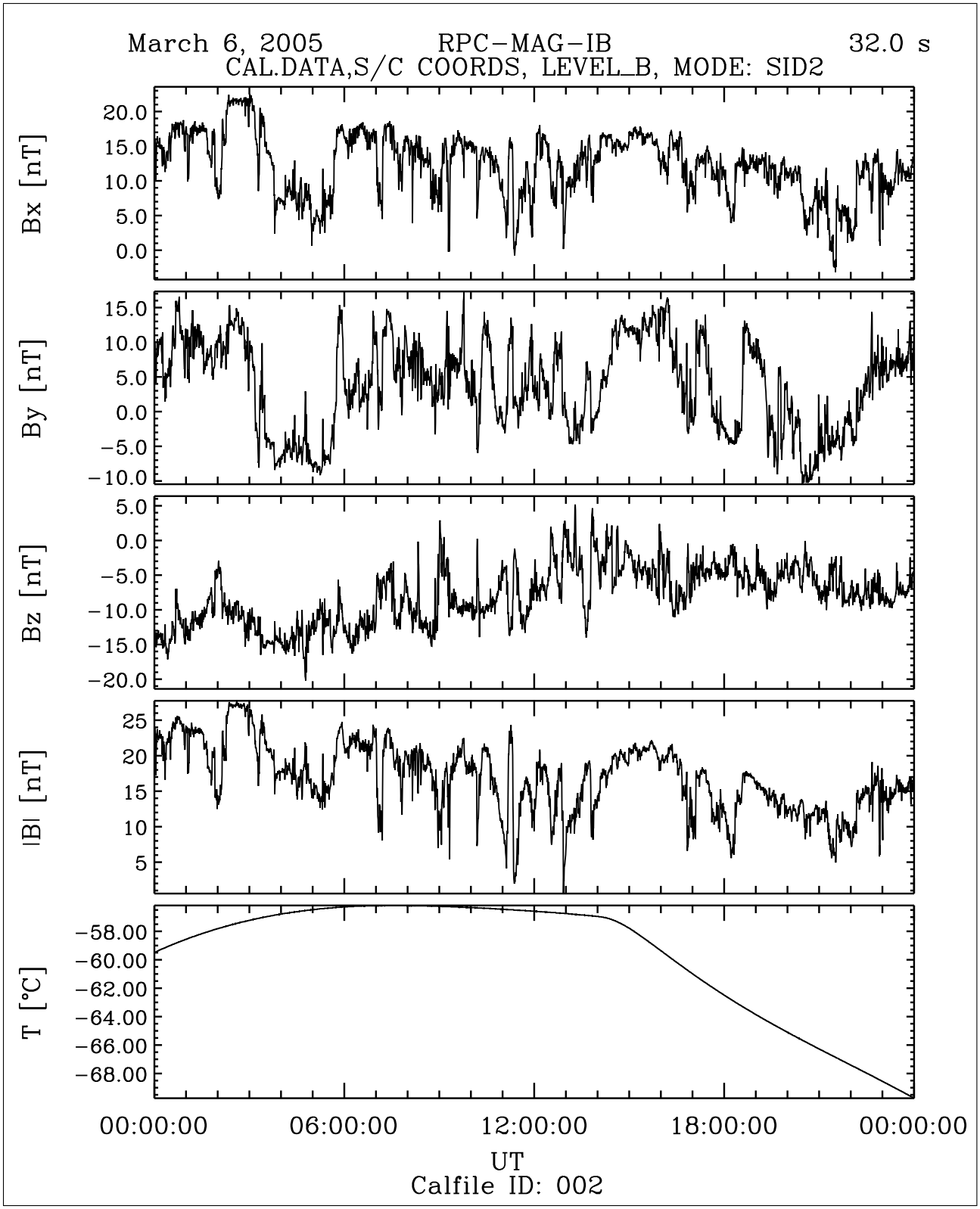

Figure 53: File: RPCMAG050306T0000_CLB_IB_M2_T0000_2400_002

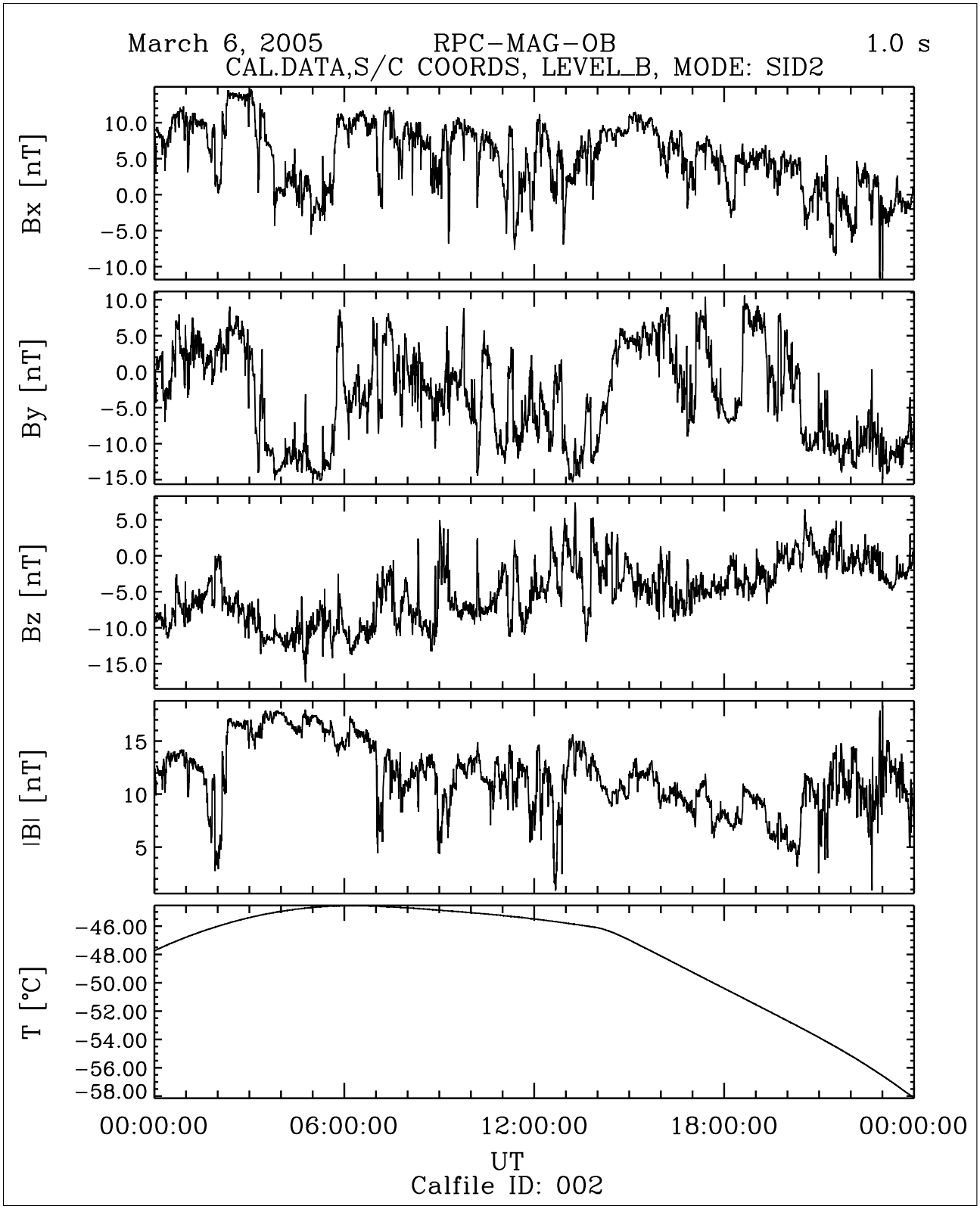

Figure 54: File: RPCMAG050306T0000_CLB_OB_M2_T0000_2400_002

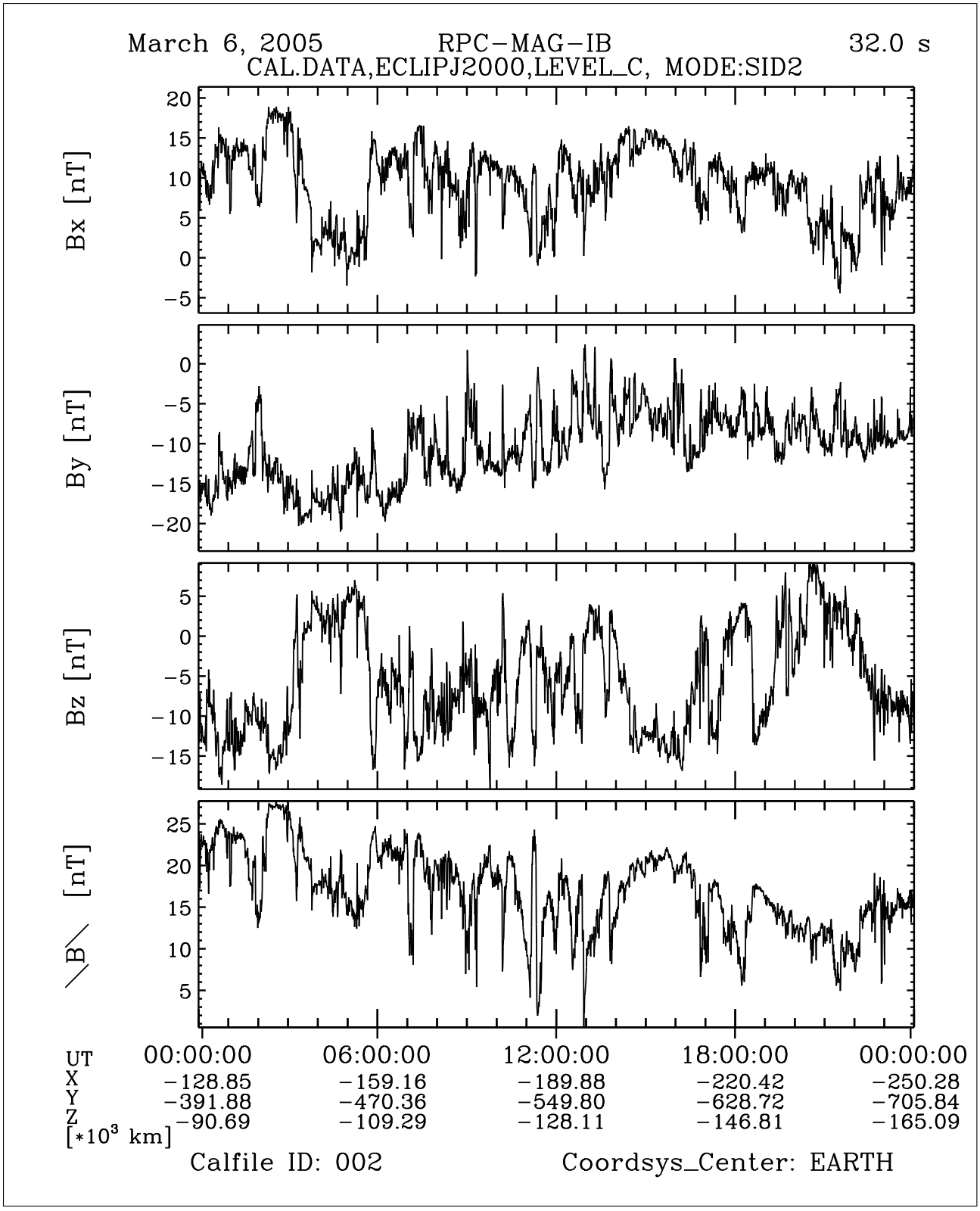

Figure 55: File: RPCMAG050306T0000_CLC_IB_M2_T0000_2400_002

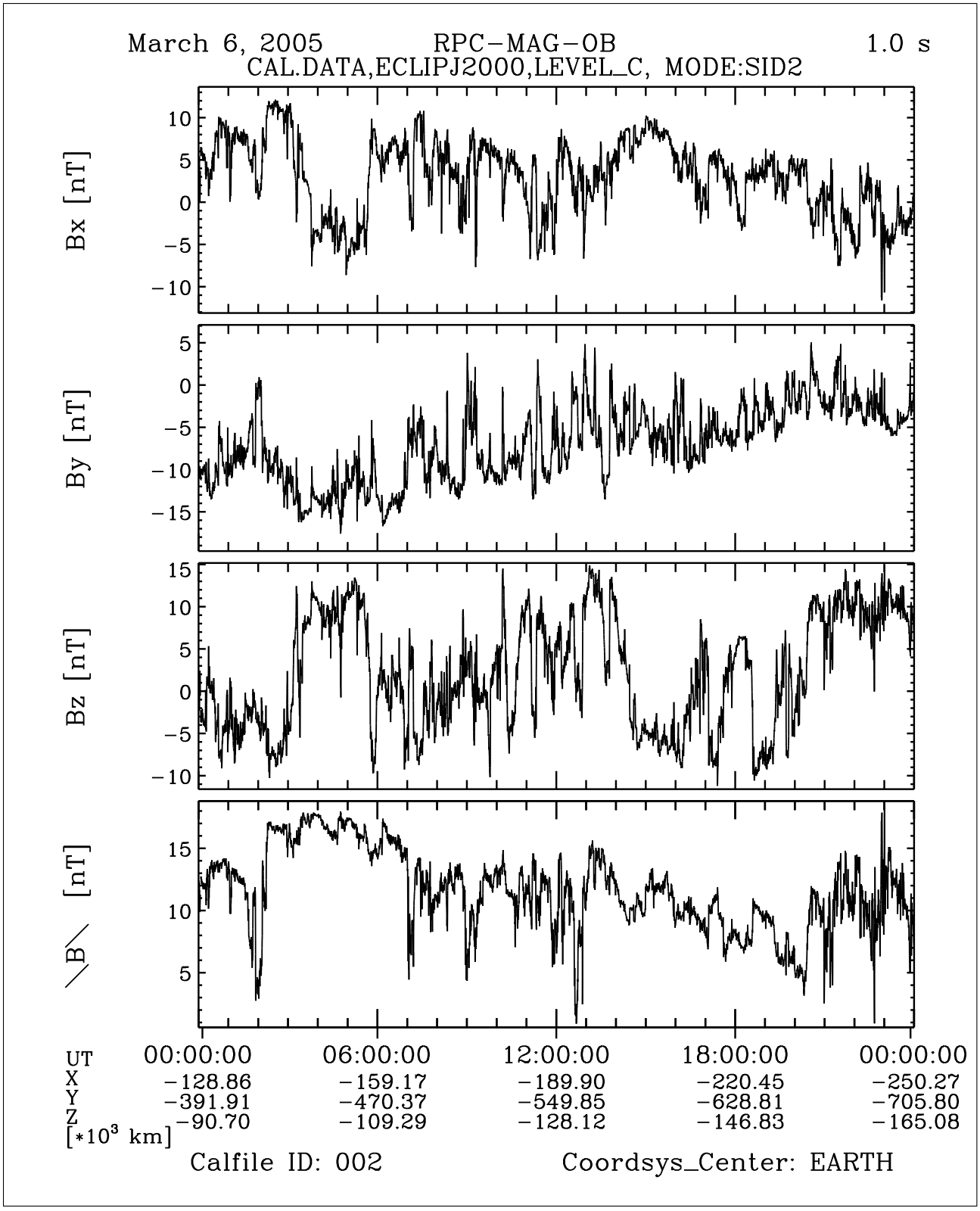

Figure 56: File: RPCMAG050306T0000_CLC_OB_M2_T0000_2400_002

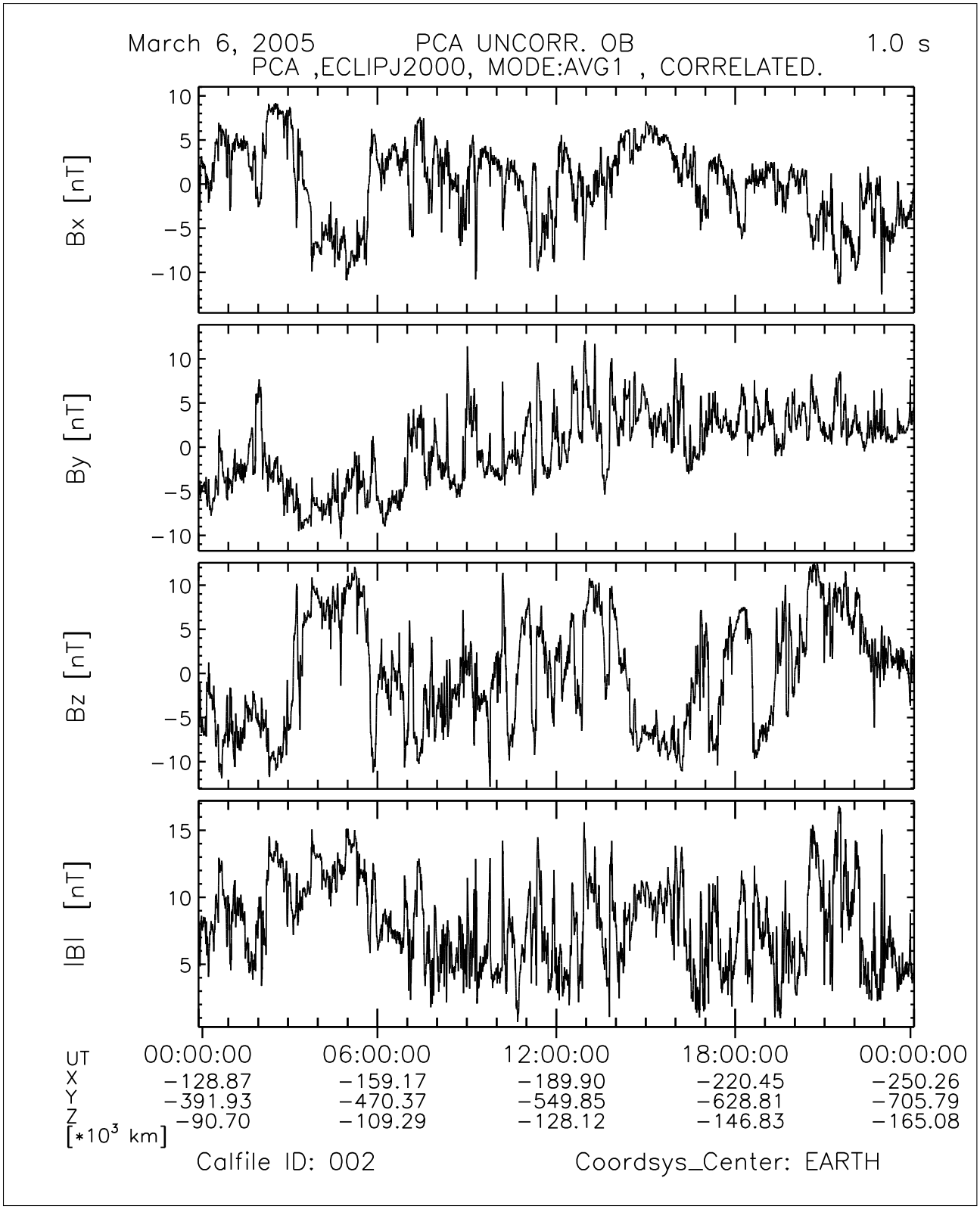

Figure 57: File: RPCMAG050306_CLJ_A1_C_T0000_2400_002

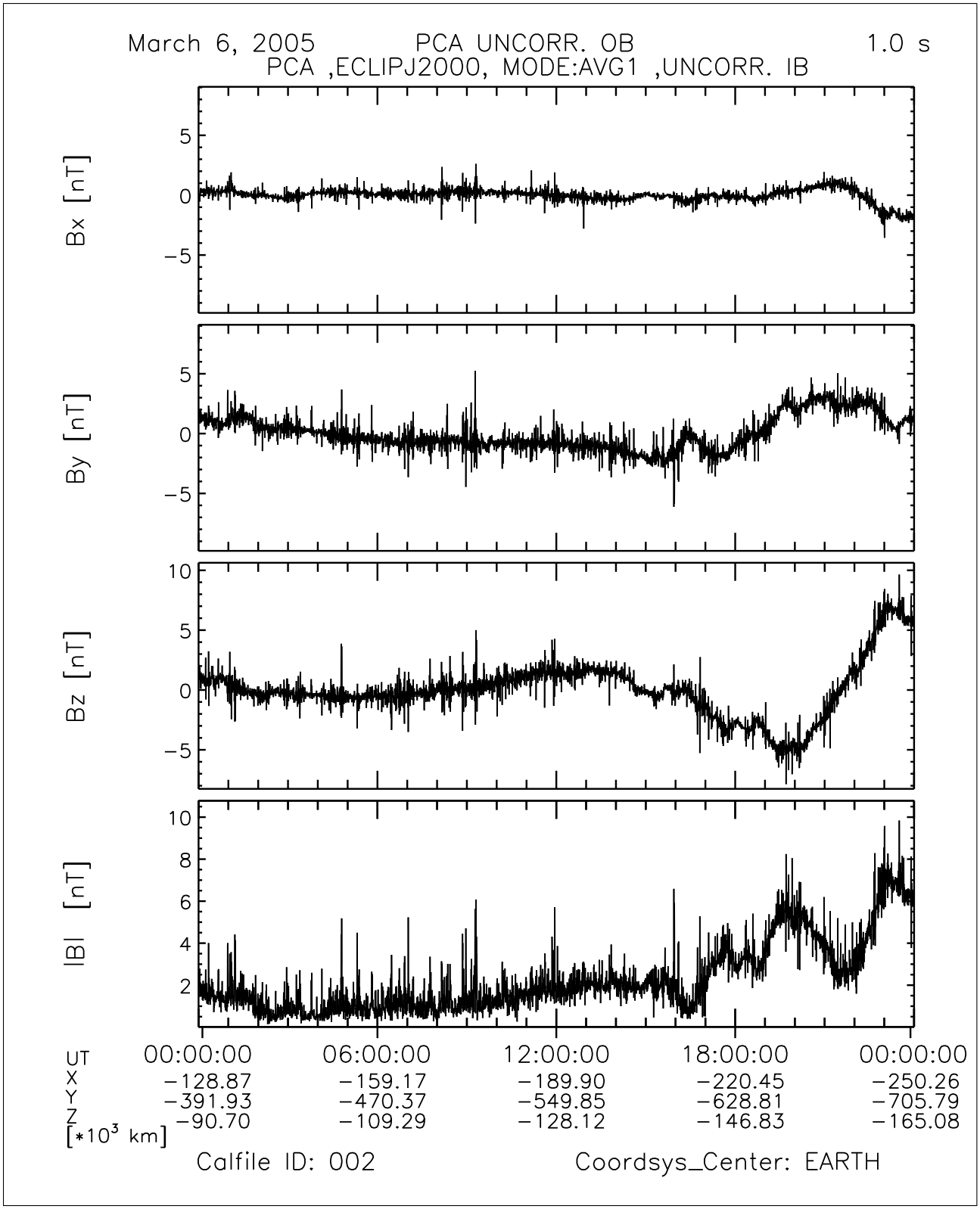

Figure 58: File: RPCMAG050306_CLJ_IB_A1_U_T0000_2400_002

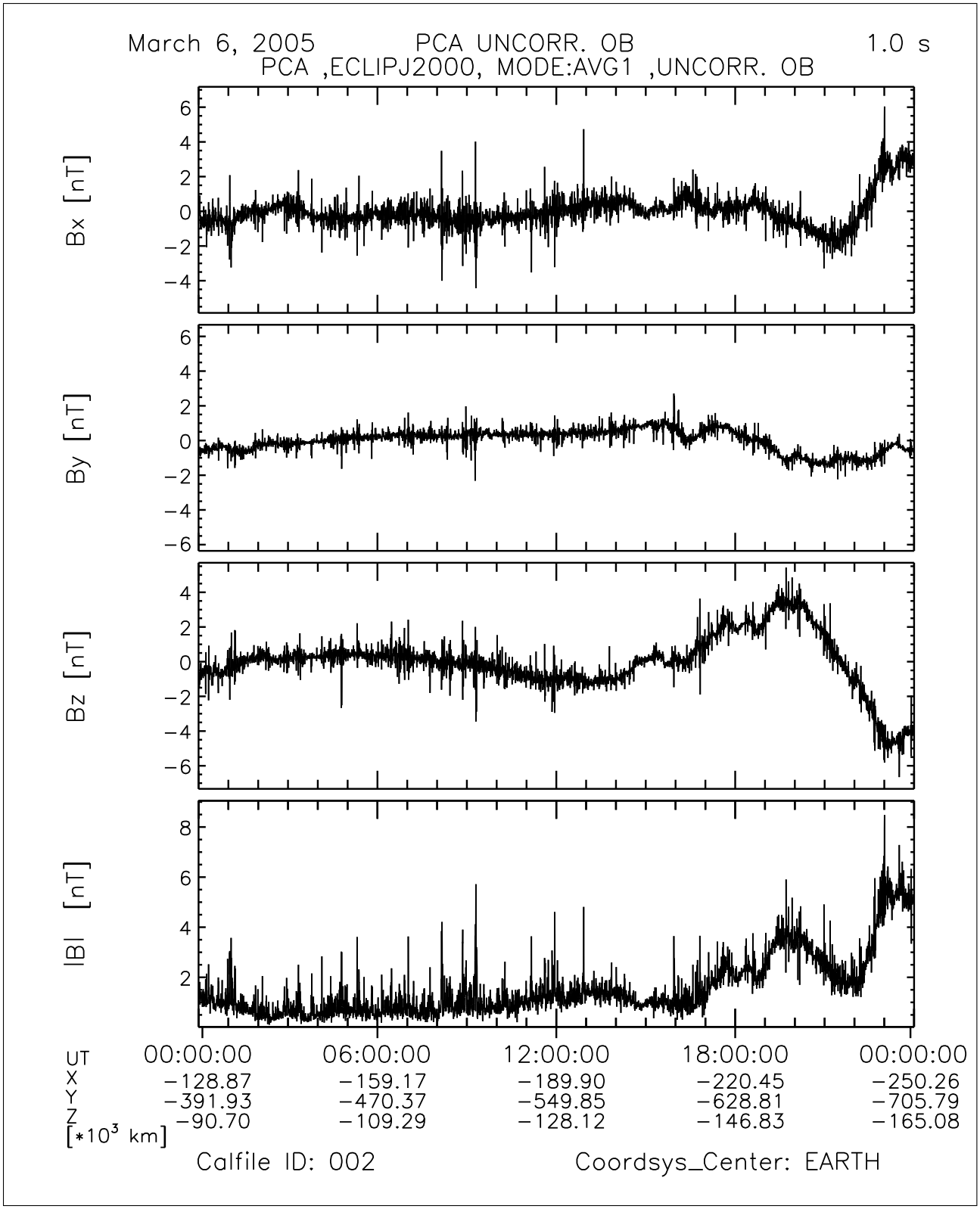

Figure 59: File: RPCMAG050306_CLJ_OB_A1_U_T0000_2400_002

3.8 March 07, 2005:

3.8.1 Actions

MAG stayed in SID 2 until 23:55. Then RPC was switched off. No problems occurred. The ORER file ended. Therefore, data will be plotted in the usual SUN centered system, using the standard ORHR orbit file.

3.8.2 Plots of Calibrated Data

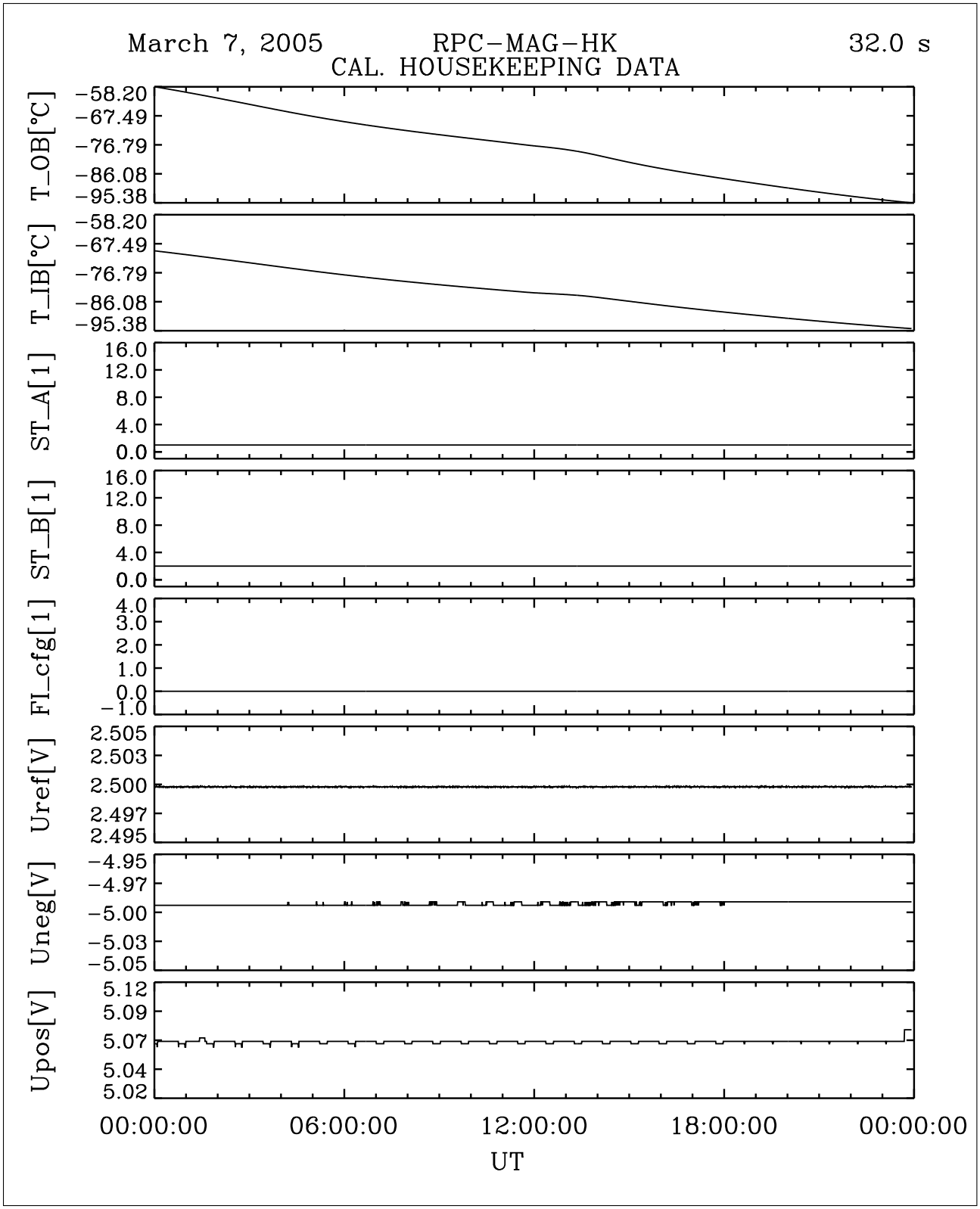

Figure 60: File: RPCMAG050307T0000_CLA_HK_P0000_2400

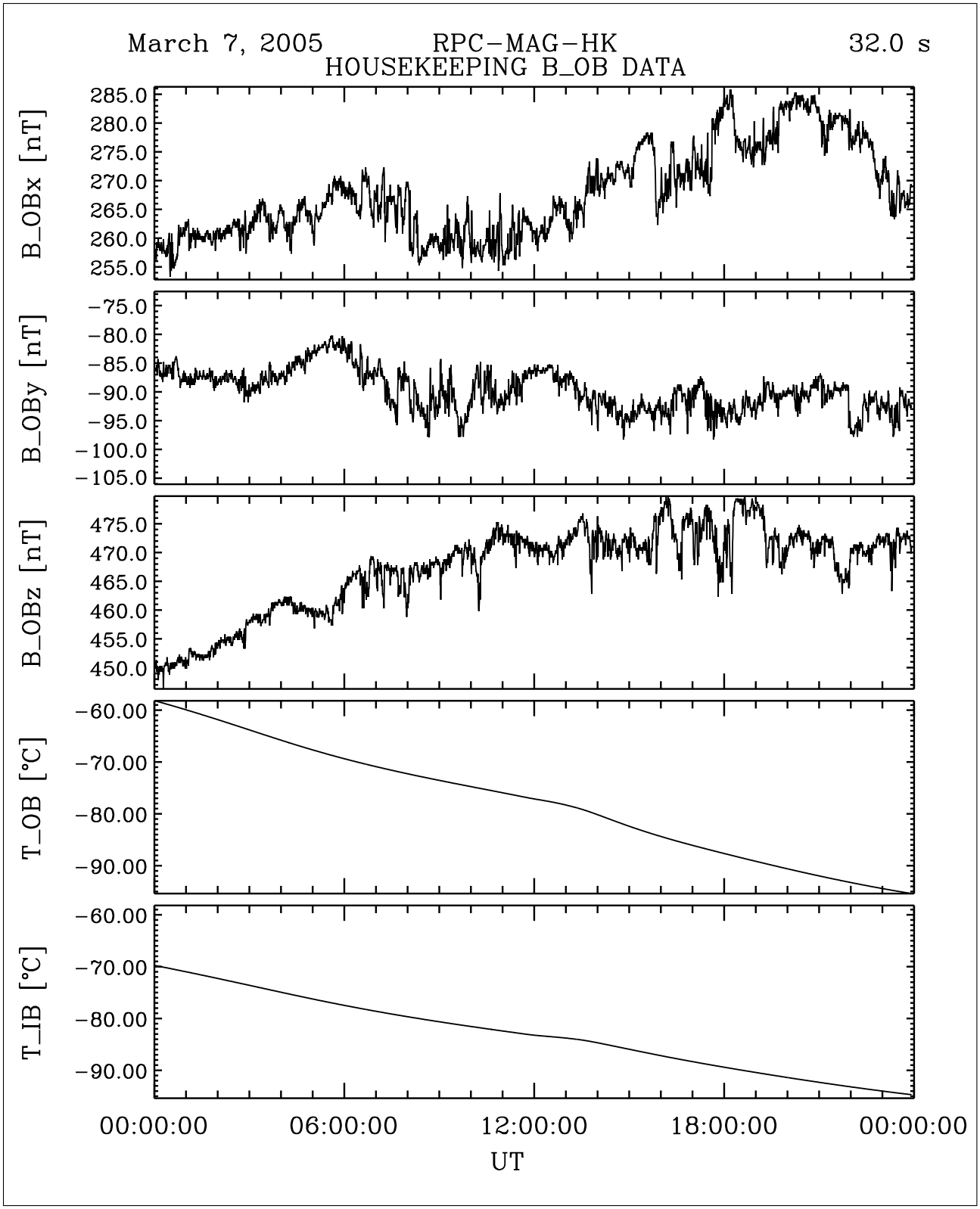

Figure 61: File: RPCMAG050307T0000_CLA_HK_B_P0000_2400

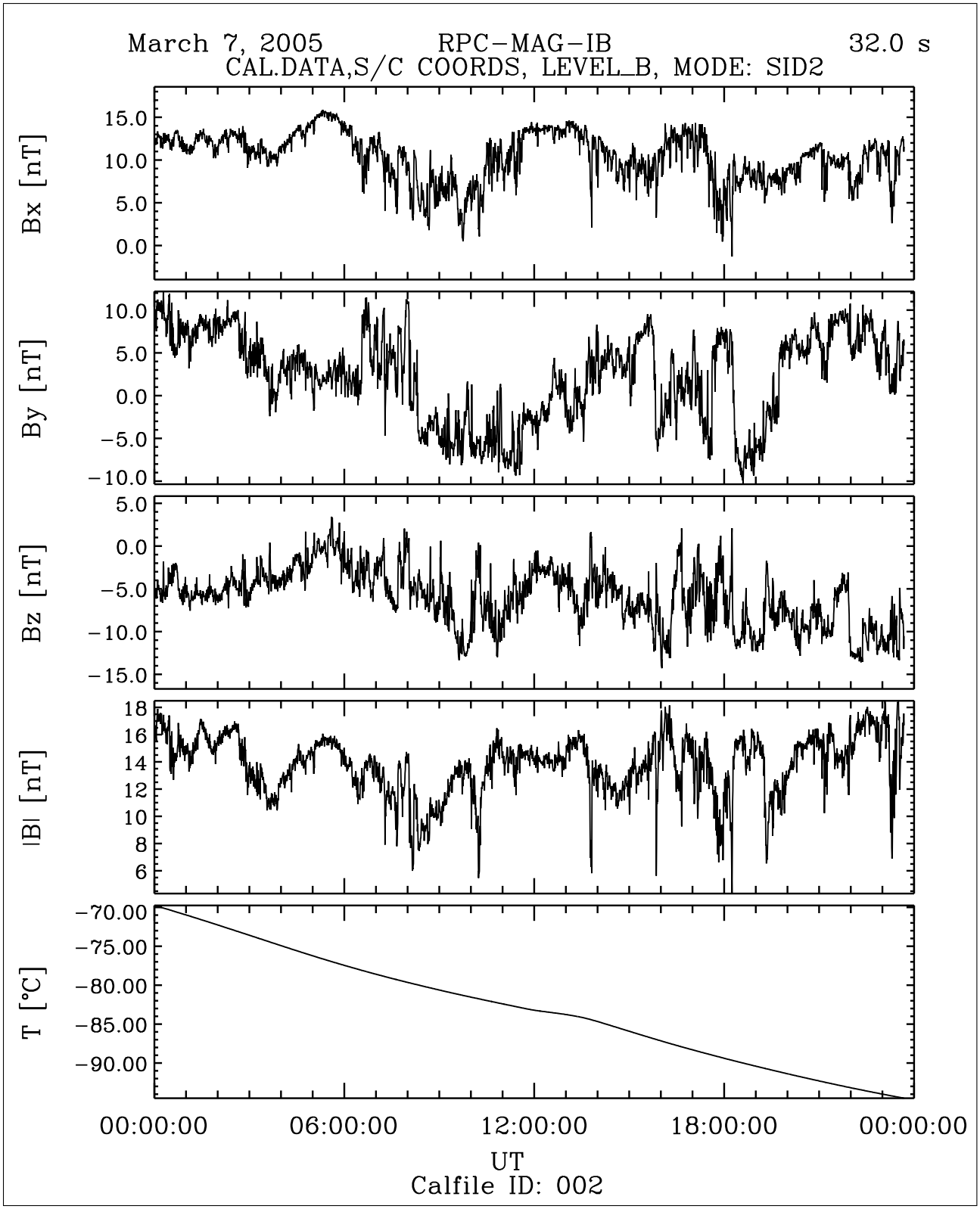

Figure 62: File: RPCMAG050307T0000_CLB_IB_M2_T0000_2400_002

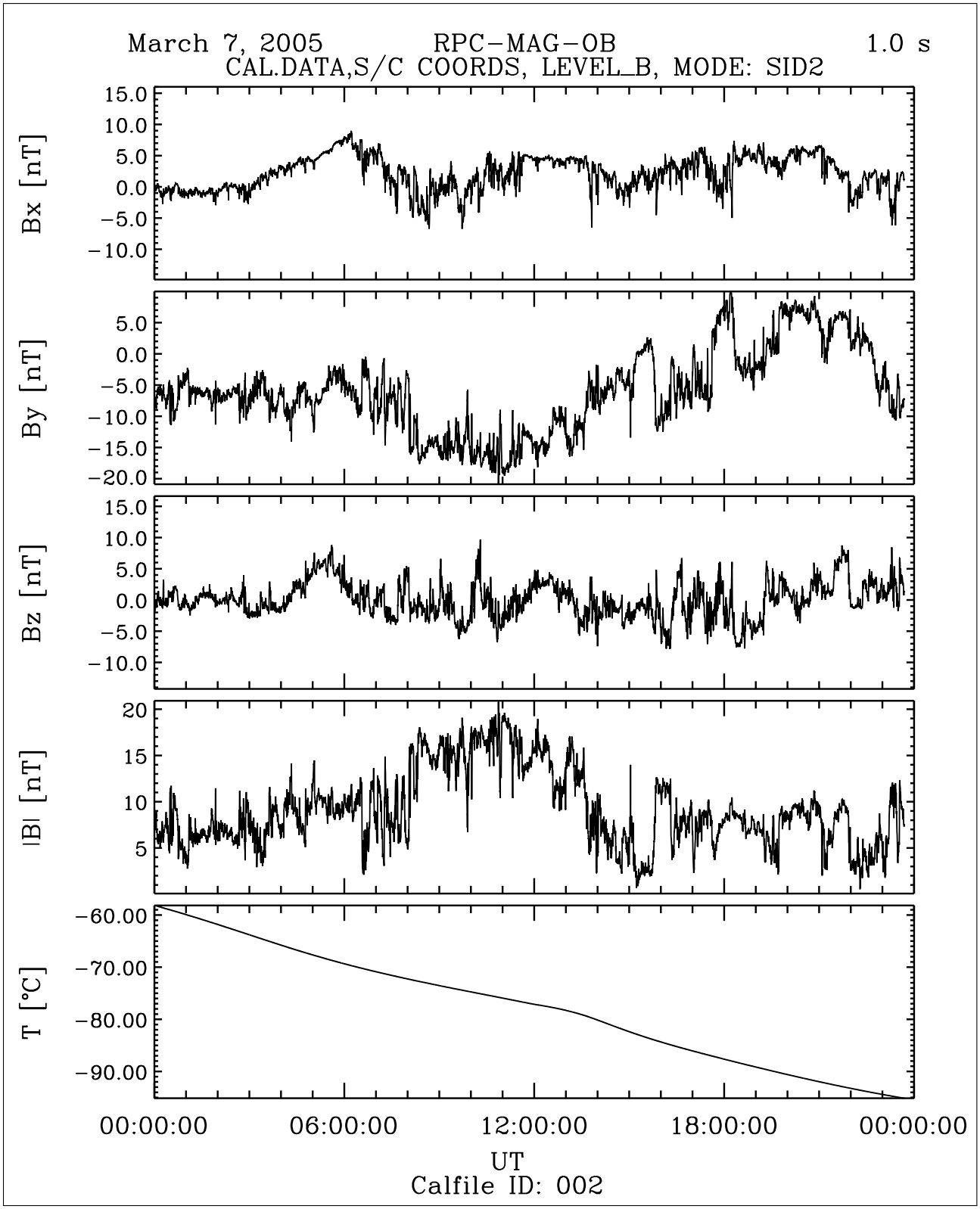

Figure 63: File: RPCMAG050307T0000_CLB_OB_M2_T0000_2400_002

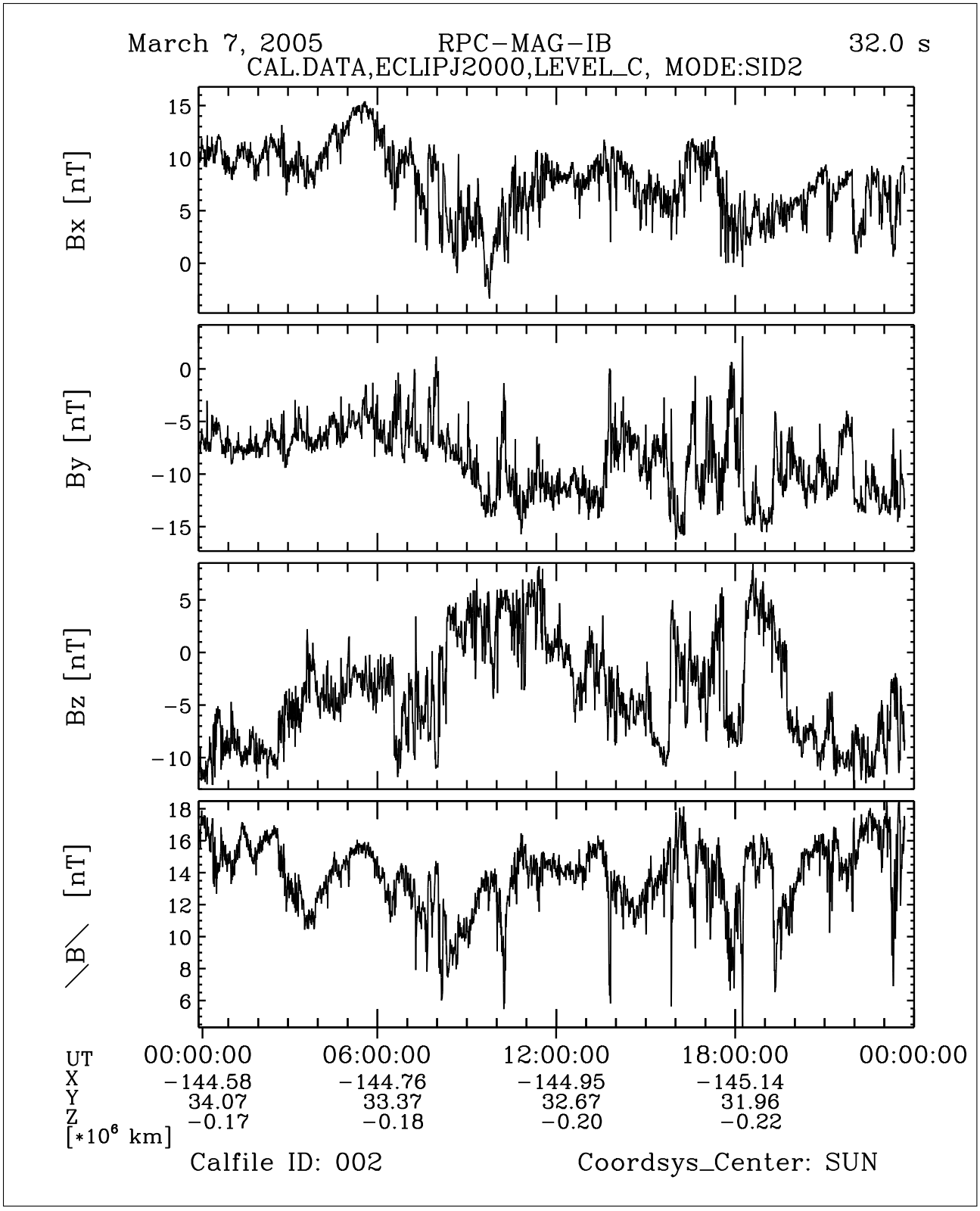

Figure 64: File: RPCMAG050307T0000_CLC_IB_M2_T0000_2400_002

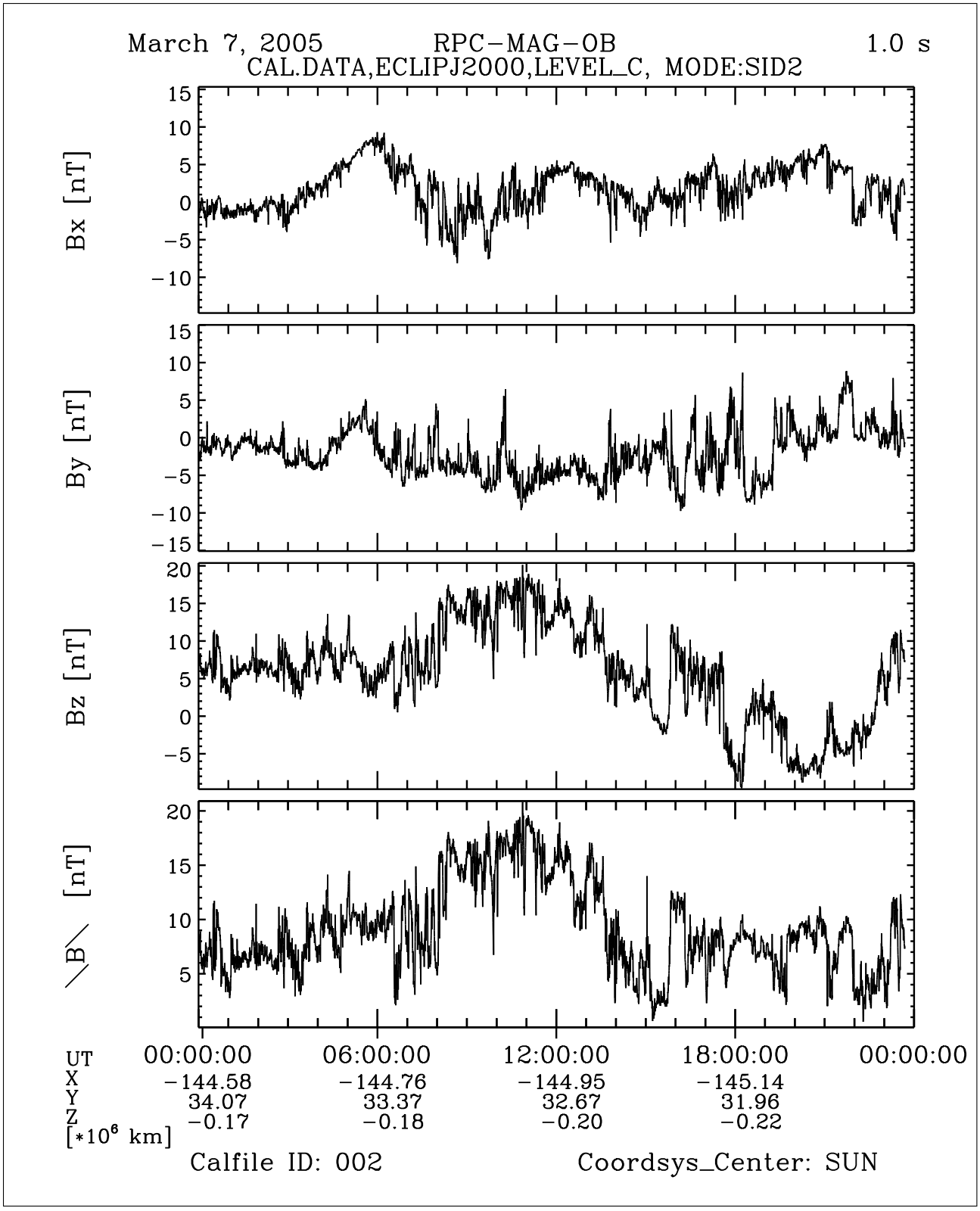

Figure 65: File: RPCMAG050307T0000_CLC_OB_M2_T0000_2400_002

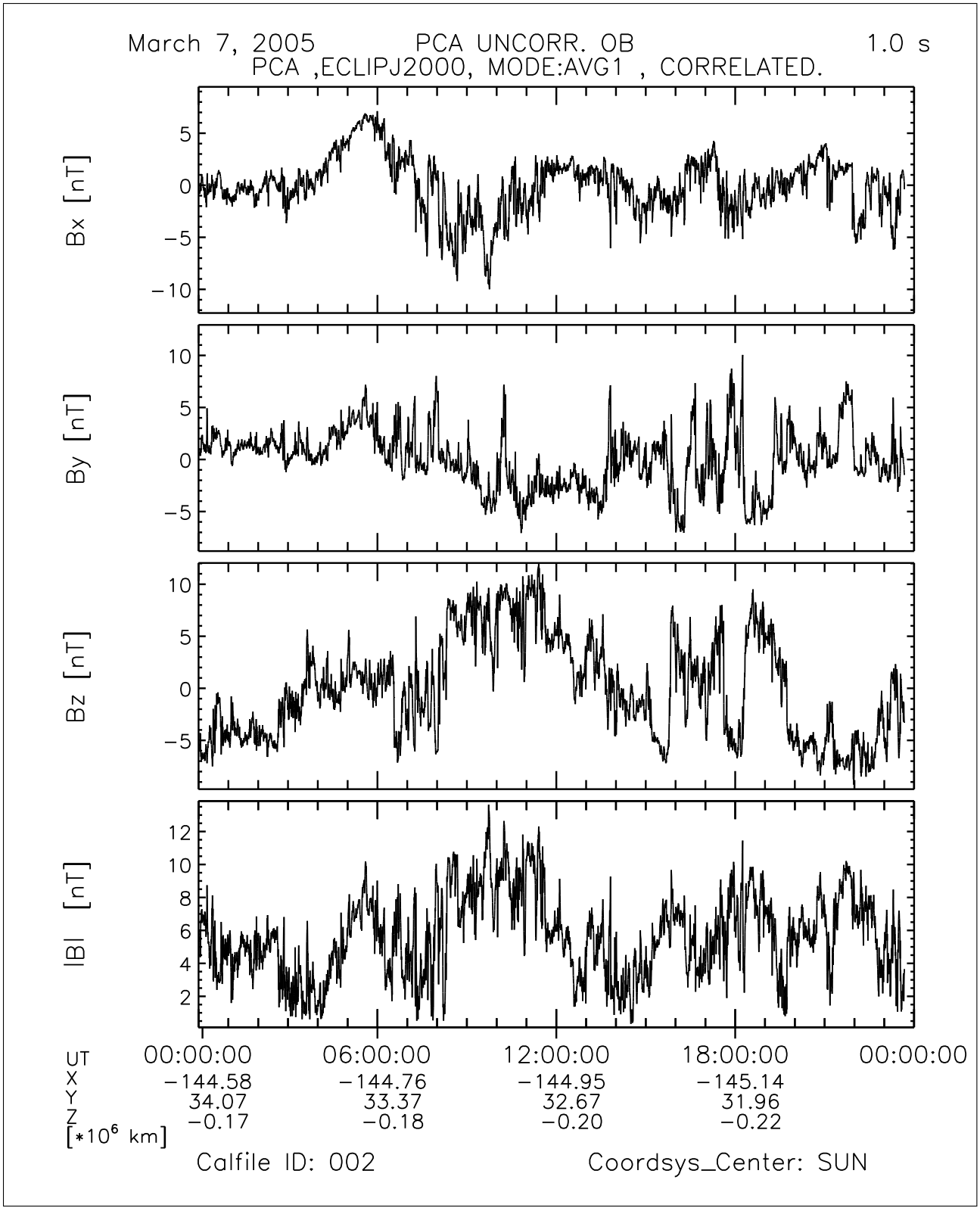

Figure 66: File: RPCMAG050307_CLJ_A1_C_T0000_2400_002

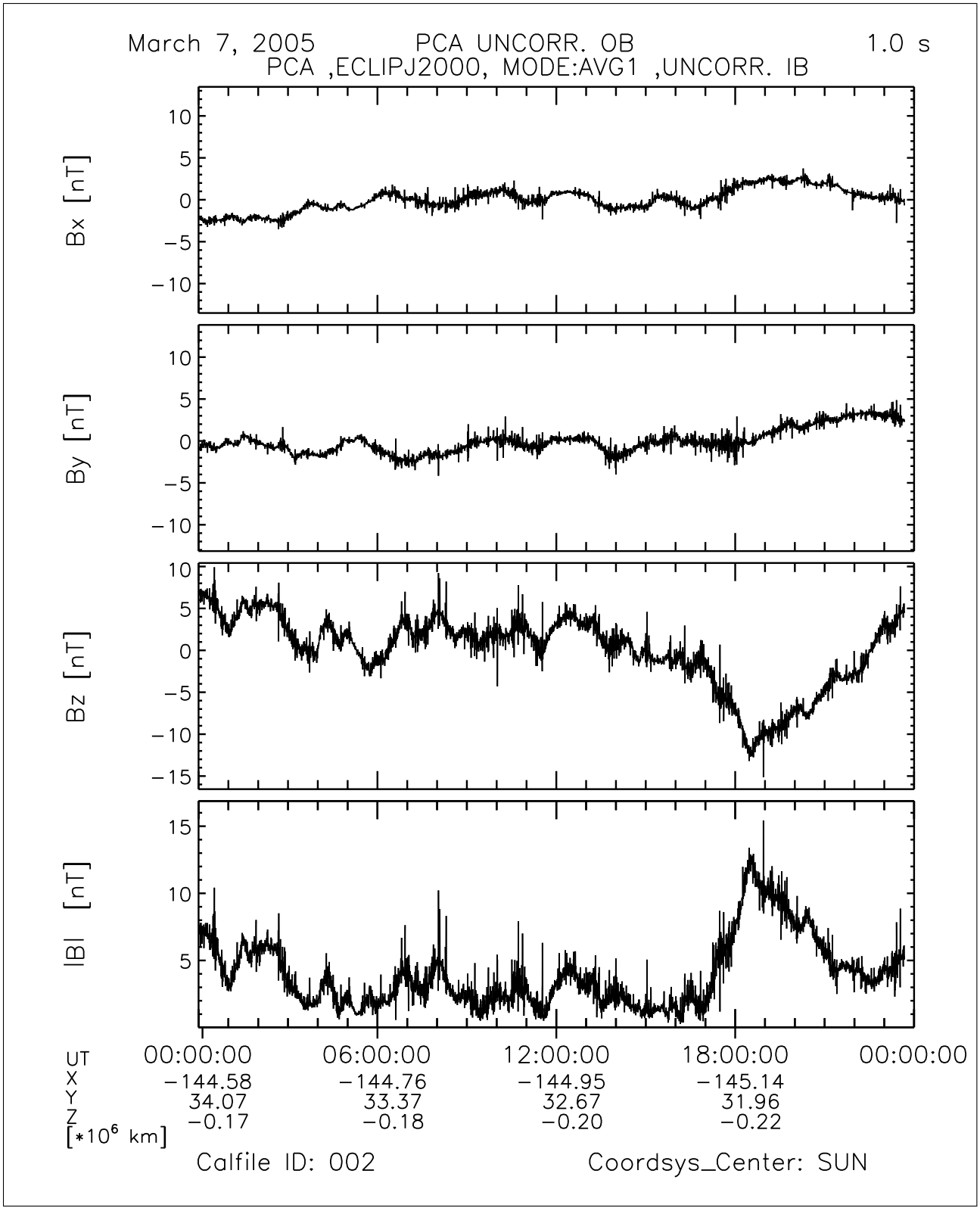

Figure 67: File: RPCMAG050307_CLJ_IB_A1_U_T0000_2400_002

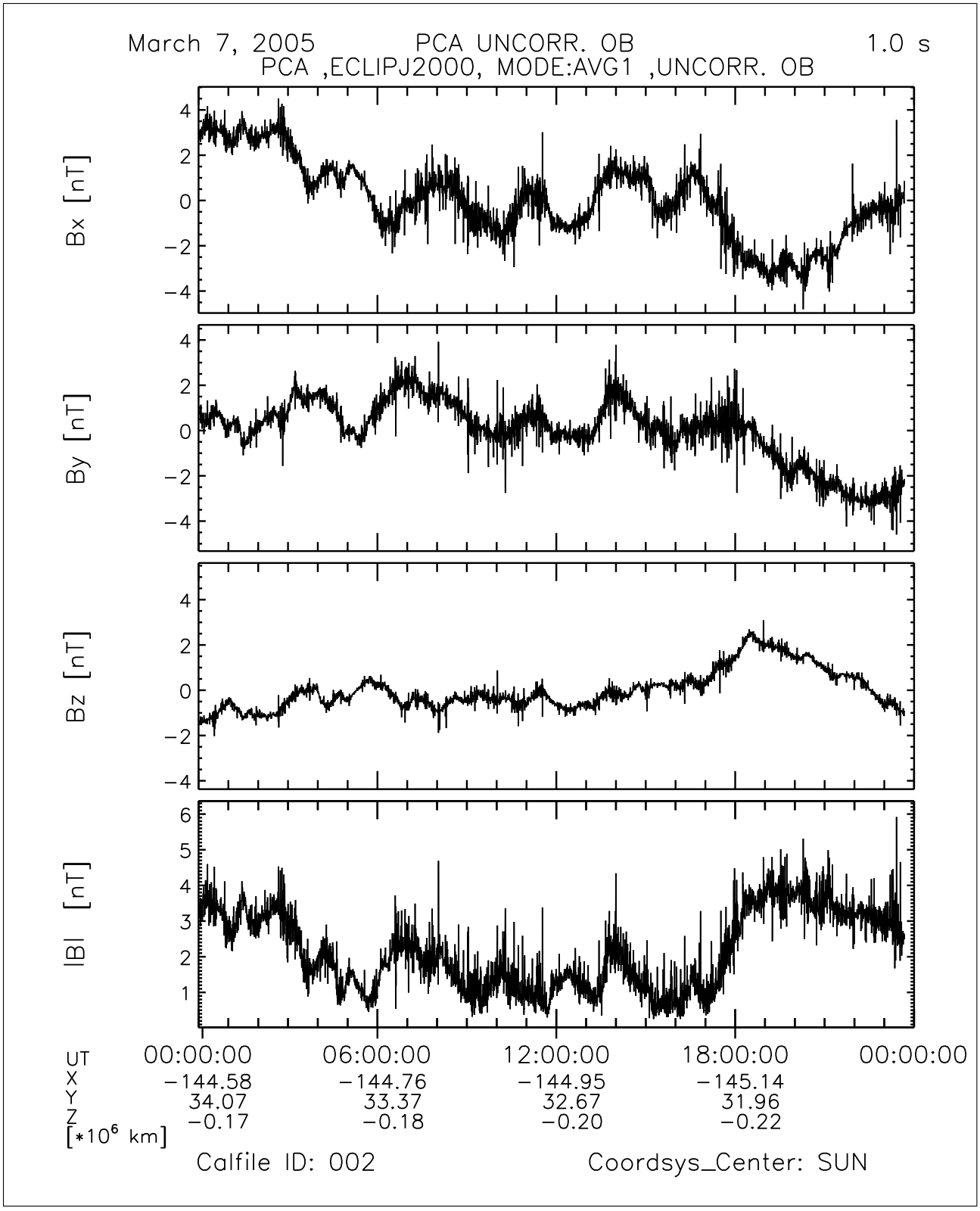

Figure 68: File: RPCMAG050307_CLJ_OB_A1_U_T0000_2400_002

4 Comparison between OB and IB: The Influence of the Sensor Temperature to the Data Quality

In this section we compare the measured data of the OB Sensor with the IB ones. The investigation is done with 1 s averaged LEVEL_F data (s/c coordinates) for various days.

Figure 69 shows the magnetic field data and the sensor temperatures of March 3. The differences for the same day are plotted in Figure 70. The data for March 5, and March 6 have been plotted in Figures 71 – 74.

One can clearly see, that the OB and IB data match very well at times where the both sensors feel the same temperature *variation*. When the temperature changes are different, then the magnetic field data diverge as well. We do see this effect although a 3rd order temperature calibration has been applied. On short time scales, however, different heat capacities and micro physical hysteresis effects of the sensors core material may cause this behavior.

From this analysis we can derive a "Data Quality Indicator" based on the temperature difference between OB and IB. The data quality is expected to be good if this difference is constant. If it varies with time, however, the data quality will most likely be poor.
For the future a more sophisticated temperature calibration and maybe a more convenient s/c attitude, with unique sun illumination of both sensor, might improve the measurements.

Remark:
The "bursts" in the differences at certain times are most likely caused by the non perfect time handling of the differences of 1 s OB data and averaged 32 s IB data.

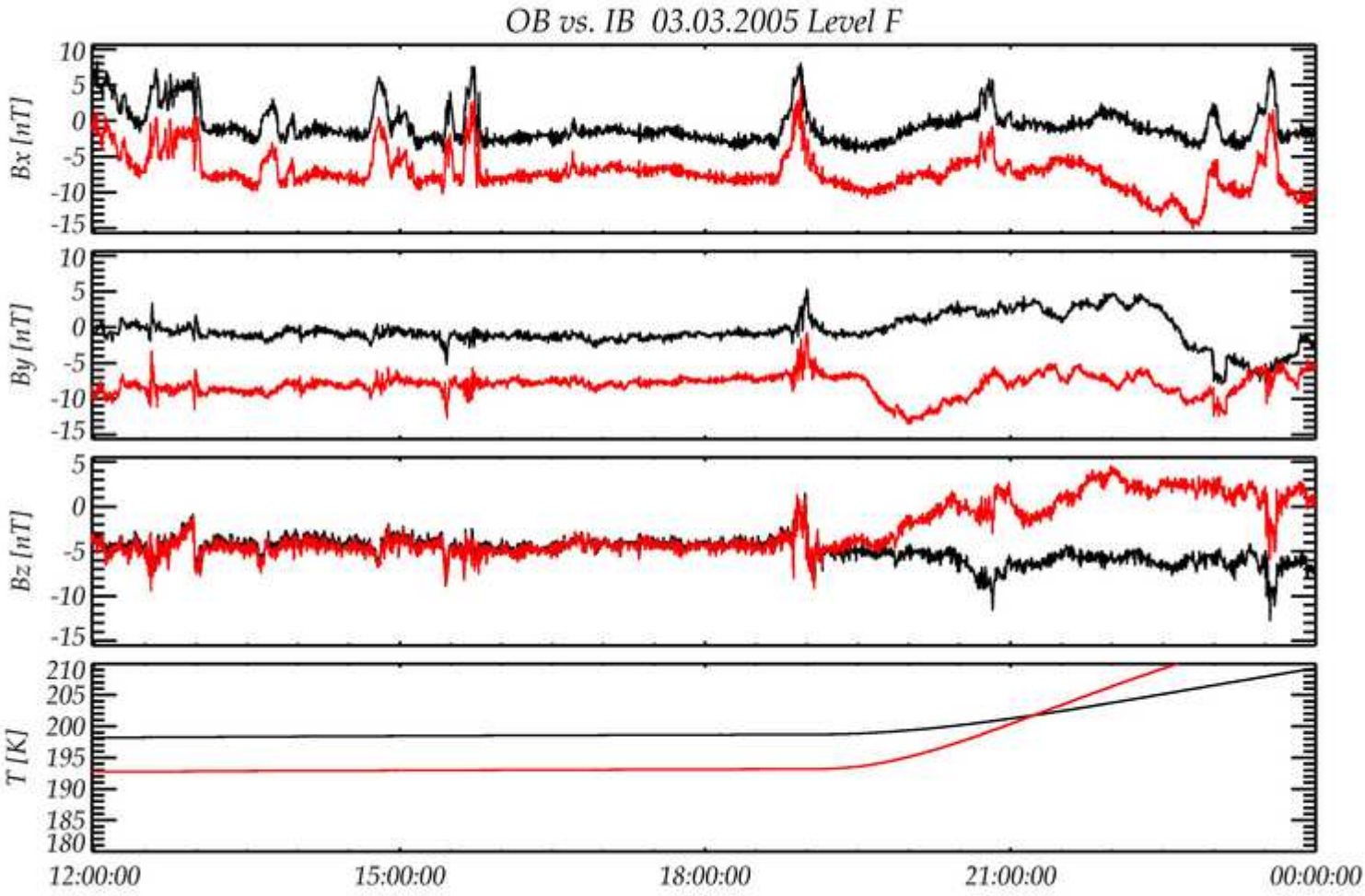

Figure 69: OB versus IB: Data of March 3, 2005

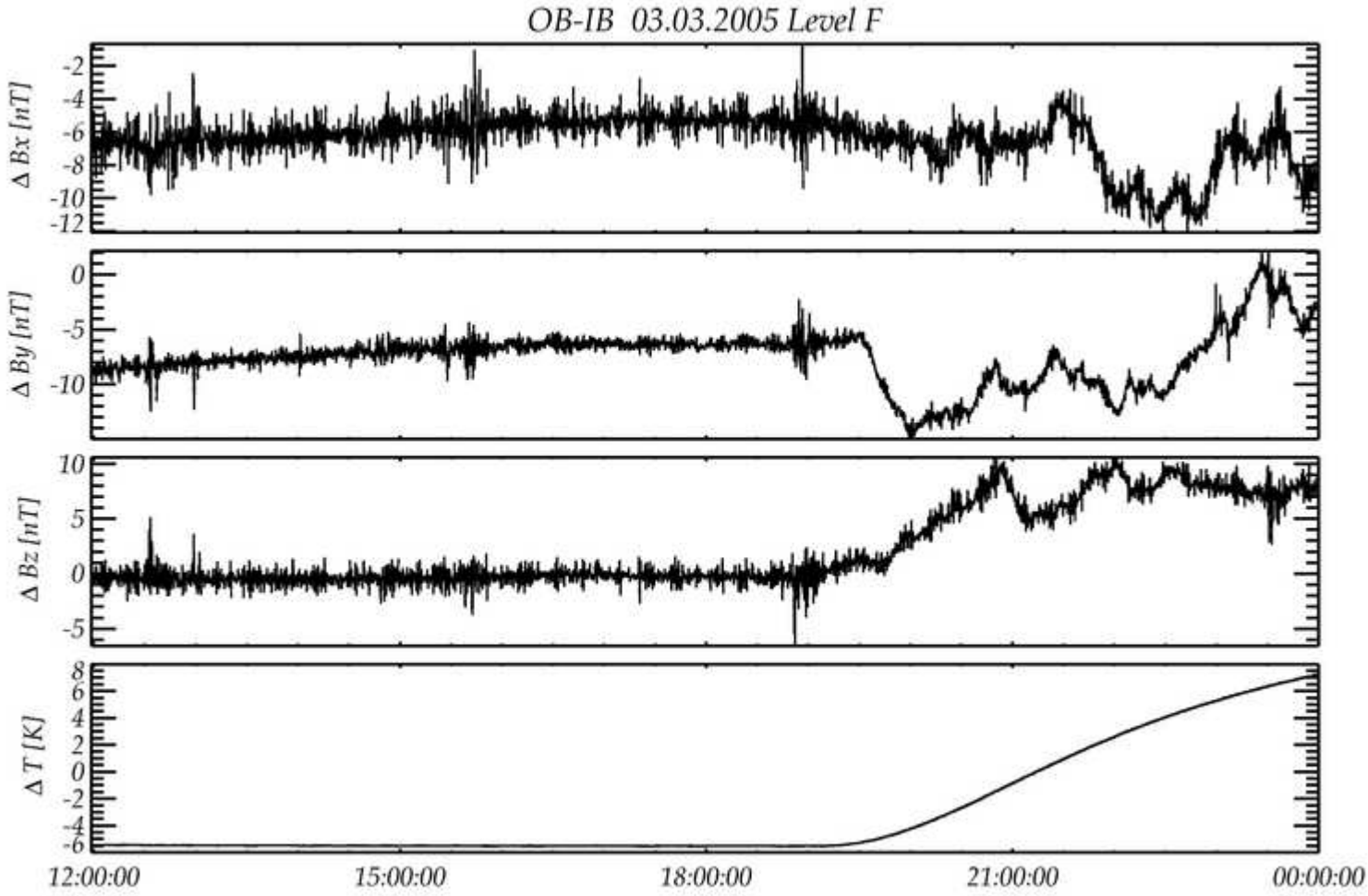

Figure 70: OB versus IB: Data of March 3, 2005, Differences

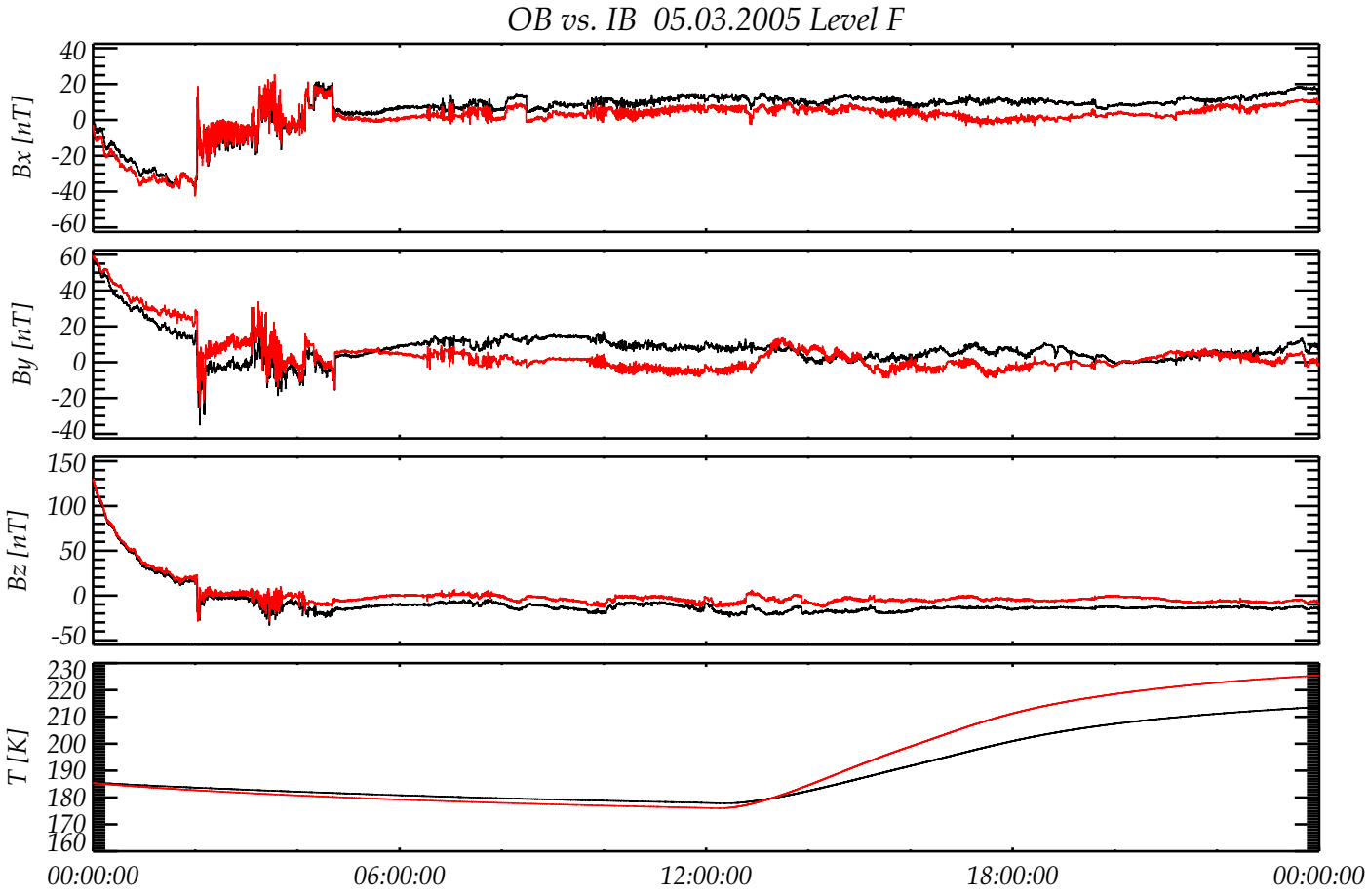

Figure 71: OB versus IB: Data of March 5, 2005

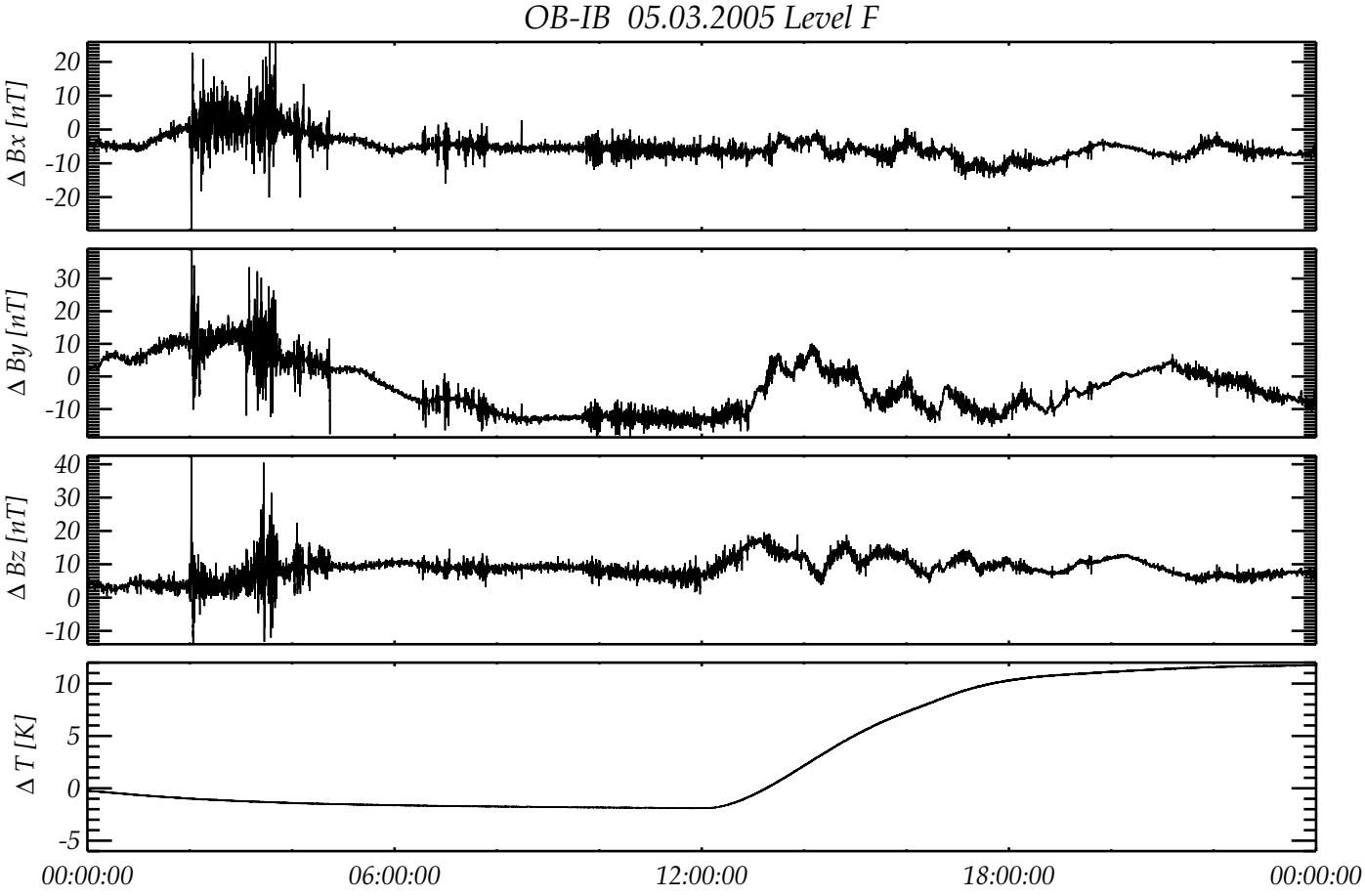

Figure 72: OB versus IB: Data of March 5, 2005, Differences

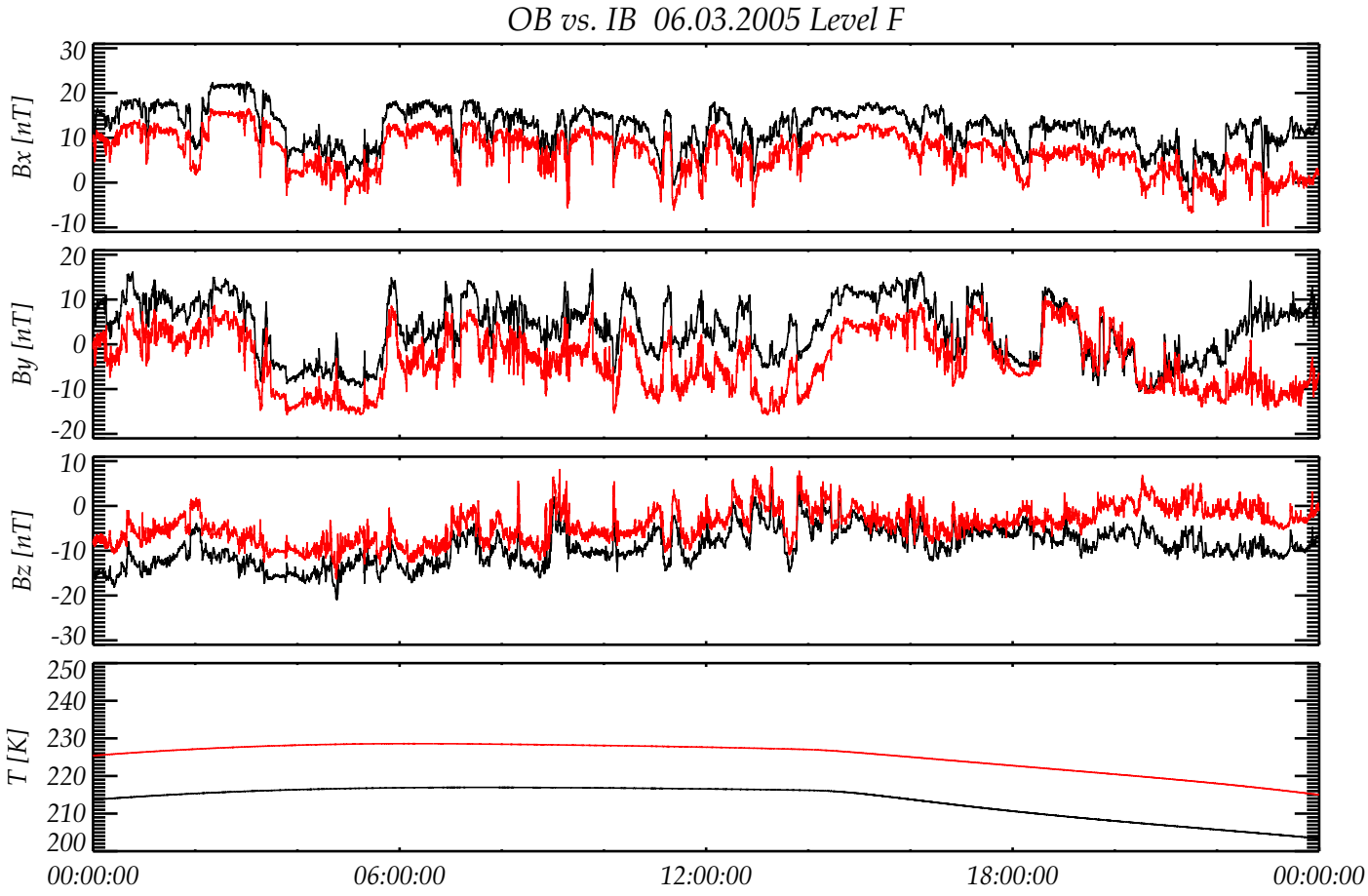

Figure 73: OB versus IB: Data of March 6, 2005

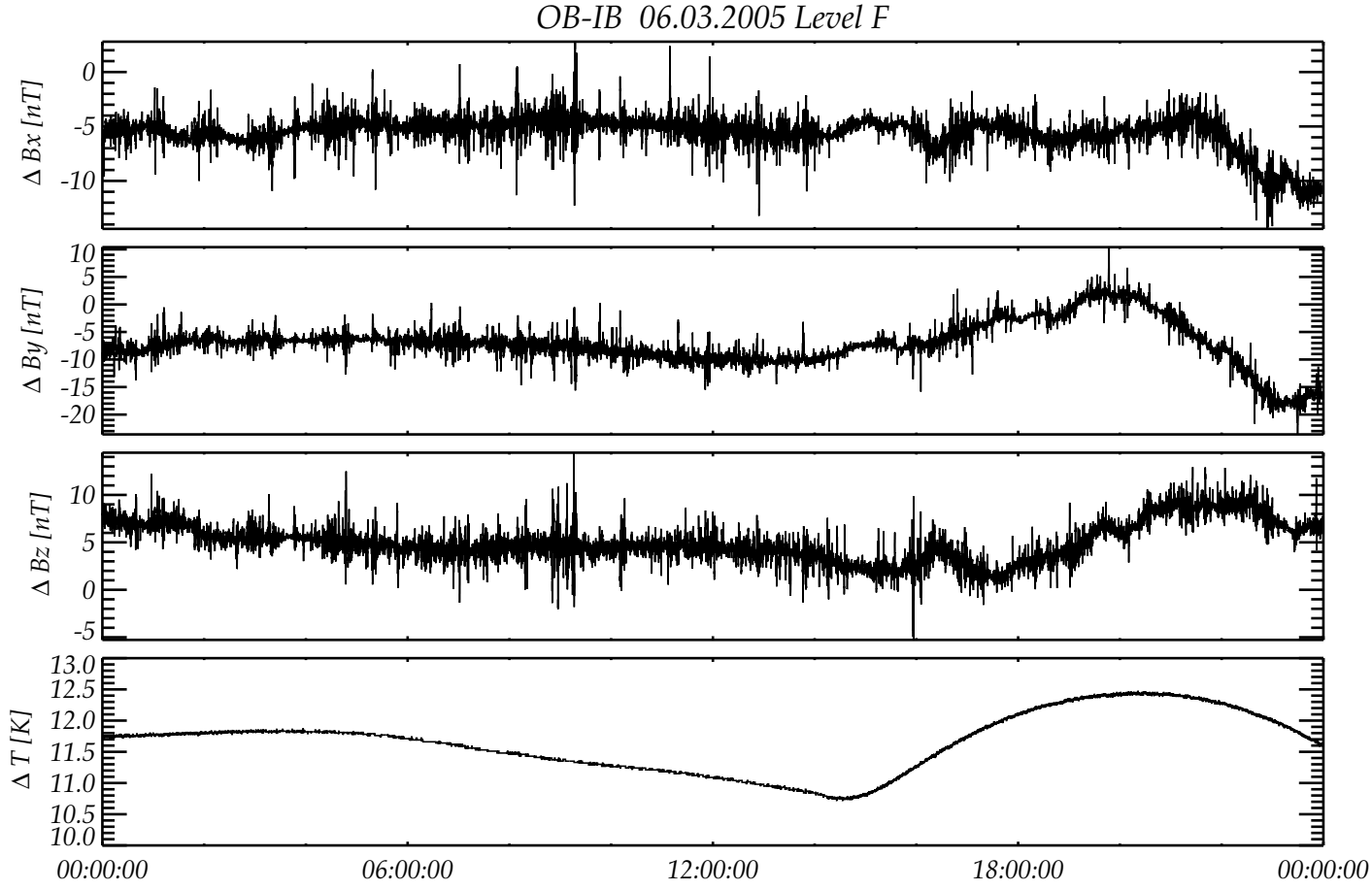

Figure 74: OB versus IB: Data of March 6, 2005,Differences

5 Comparison of the MAG data with the POMME Model

In this section we compare the RPCMAG data with a theoretical Earth field model. As model the so called POMME2-model (**Po**tsdam **M**agnetic **M**odel of the **E**arth) developed by the Geo–Forschungs–Zentrum (GFZ) Potsdam is used. This model is based on CHAMP and OERSTED data and includes the following geophysical features:

- Time varying core field
- Ring current (DST)
- Time averaged magnetospheric field
- Secular variations
- Taking into account Main field & Crust field model MF4
  (MF4 Model : crust field model, based on spherical harmonic analysis up to degree 90)

The comparison will be done for the total field and as well for the single components for a time intervall of ± 30 min around Closest Approach (CA).

5.1 Comparison with the OB–Sensor

Figure 75 shows the modulus of the OB sensor in the most upper panels and the total field calculated by the POMME model in the second panel. On this large scale the difference are negligible. The computed difference in the bottom panels, however reveals an error of about ± 150 nT for the most times. It is remarkable, that there is bump in the RPCMAG data for about 4 min just before CA (S/C passed from the Gulf of Mexico via Mexico to the Pacific ocean). There is no external explanation for this bump. We guess that there are movable parts on ROSETTA. An in depth analysis can be performed if all SPICE kernels for ROSETA are available. In the following investigation we will exclude this specific time interval.

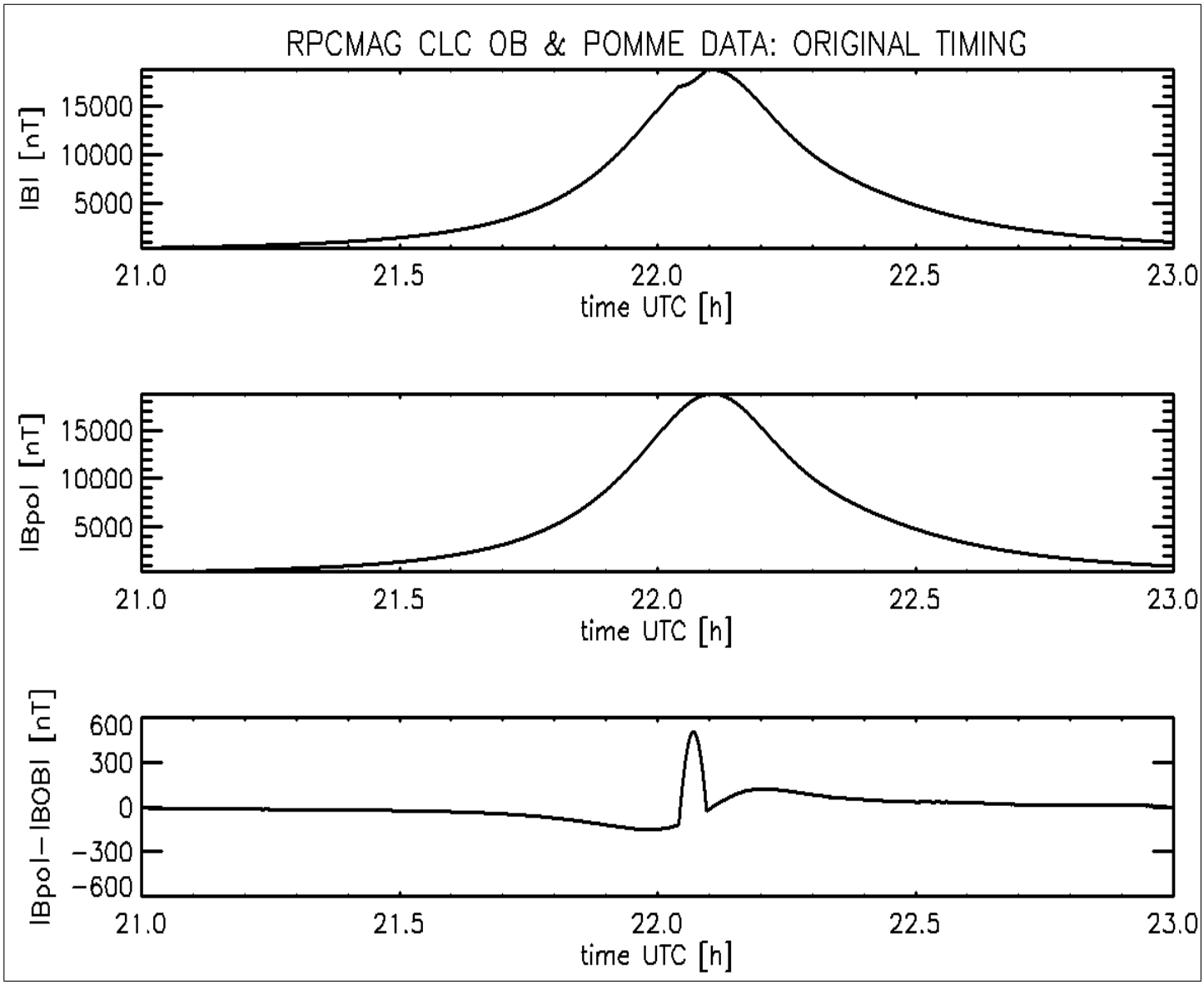

Figure 75: POMME versus OB: Total field, original timing

As the residua are higher than they should be we had the idea to minimize the difference by shifting the RPCMAG data in time domain. This was done using a minimization routine, minimizing the variance of the difference of both time series by shifting one time series in time domain. The result, shown in Figure 76, was that the OB data have to be shifted by -8.37 s against the POMME data. With this shift we can minimize the residual error to ± 10 nT.
The reason for this time shift is not absolutely clear. An upcoming investigation of the onboard filter software of RPCMAG will possibly reveal the secret.

Remark:
On the other hand we had a quick view to the different TSYGANENKO–96 model of the Earths magnetic field (which has some weaknesses compared to the POMME model). Here we found an optimal time shift of 14 s.

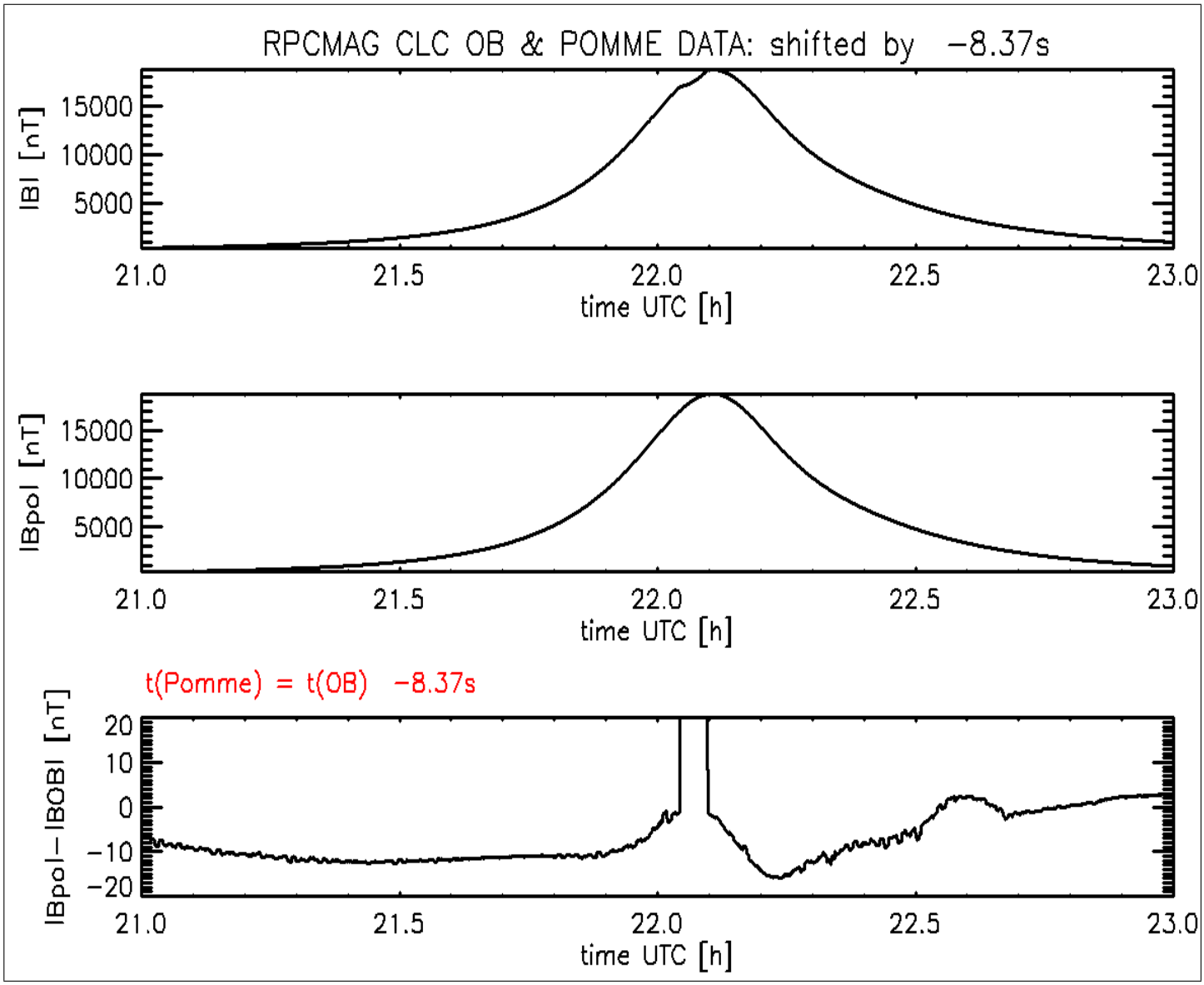

Figure 76: POMME versus OB: Total field, shifted timing

A comparison of the components of the OB sensor and POMME is displayed in Figure 77 for the original timing. At a first view this looks quite good as well. The differences of the model and the measurements are plotted in Figure 78 for the original timing and in Figure 79 for the time shifted data.

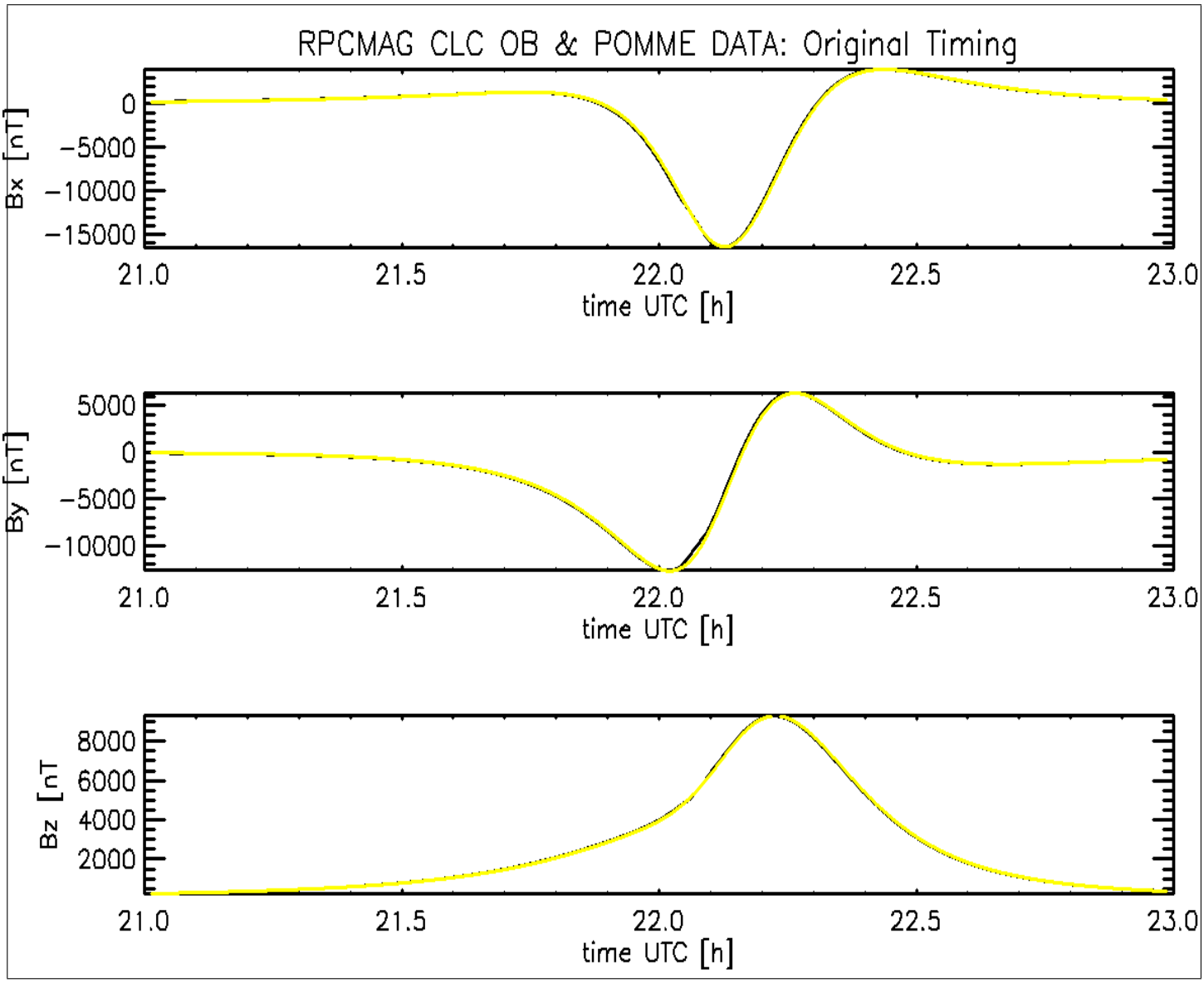

Figure 77: POMME versus OB: Components, original timing

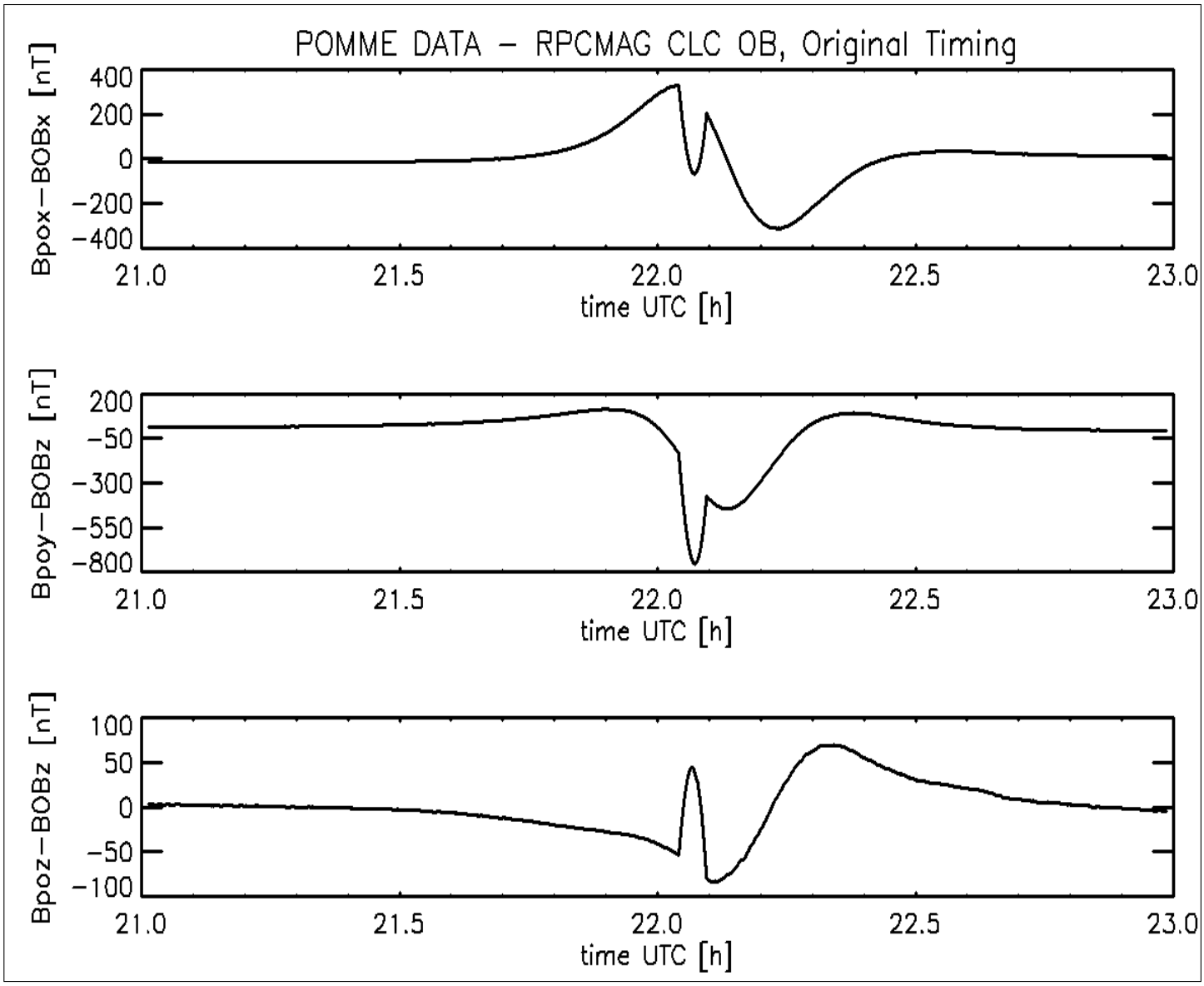

Figure 78: POMME versus OB: Differences of the Components, original timing

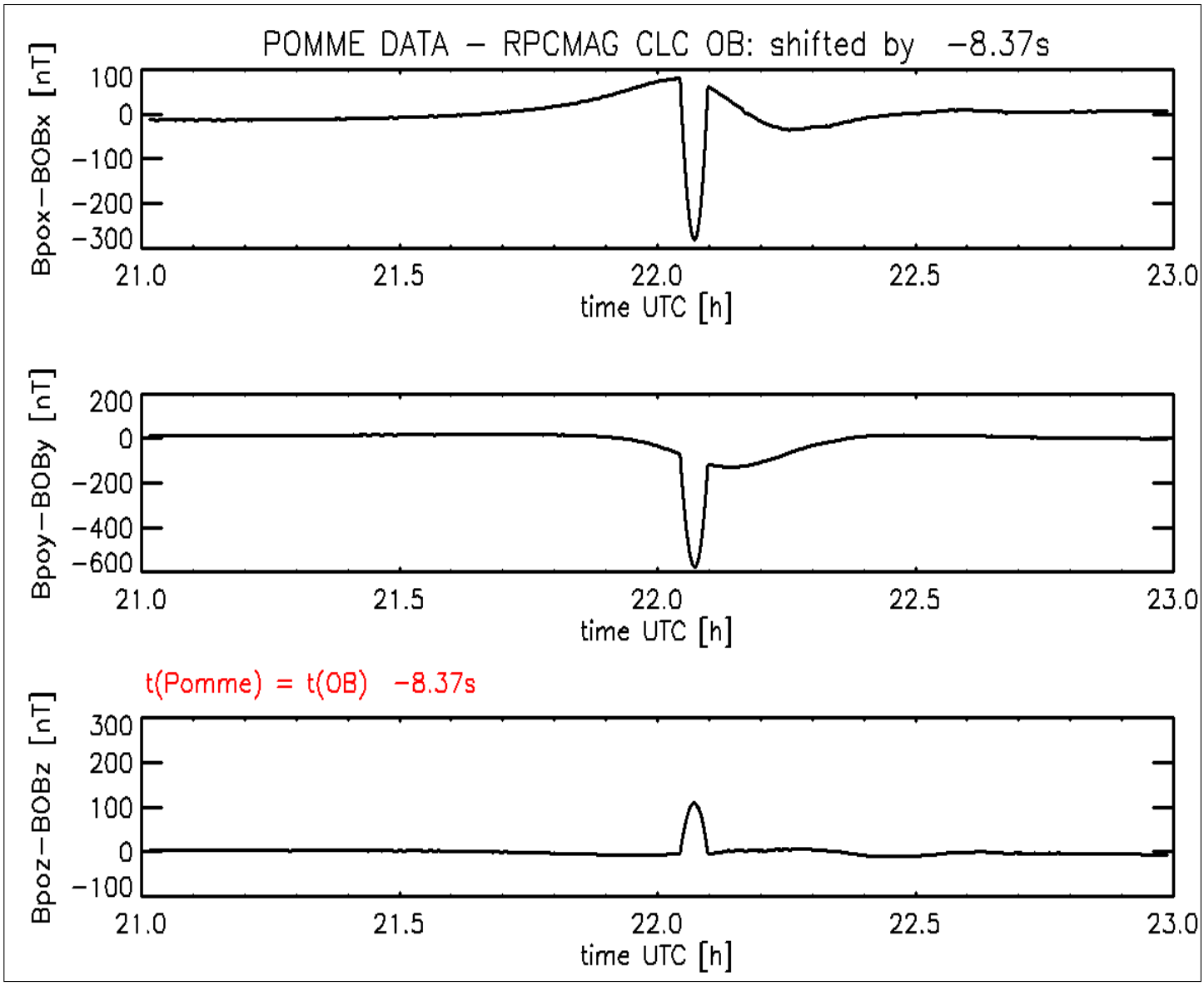

Figure 79: POMME versus OB: Differences of the Components, shifted timing

For the original timing we get residua in the order of ± 200 nT. The time shifted data are – as expected – much closer to the model data. Here we only see deviations of about ± 80 nT.
Analyzing the structure of the deviation the idea arose that the result could be improved drastically by rotation of the sensor reference frame. It could be that the actual orientation of the sensor does not perfectly coincide with the nominal build–in orientation.
To check this the RPCMAG data were feeded into an algorithm that minimizes the variance of the difference between measured and model data by applying three suitable rotations about the main axes. As output the three desired rotation angles are obtained.
The result of the procedure is displayed in Figure 80. This shows impressively that rotations of maximal 0.4° will reduce the error down to ±15 nT.

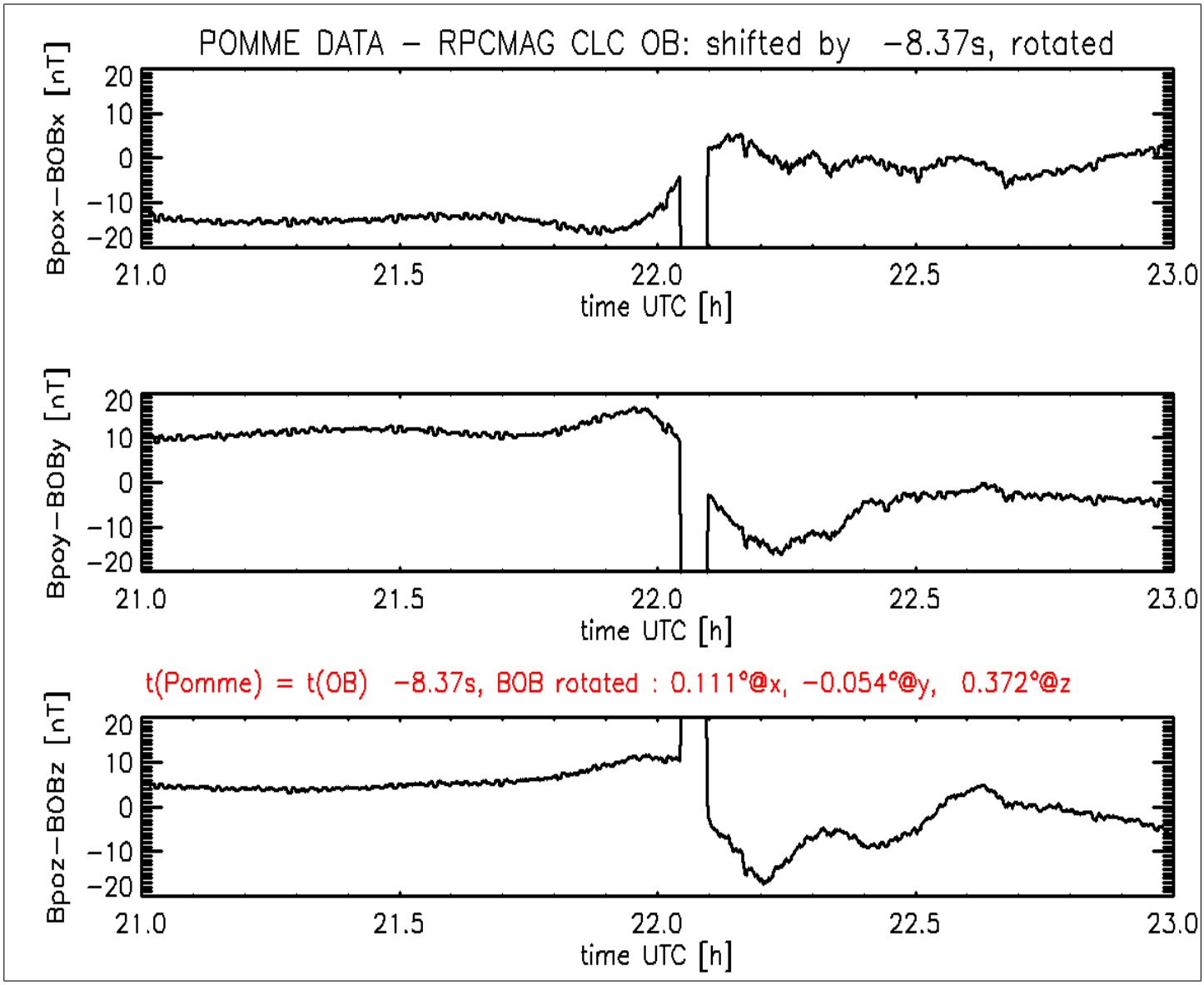

Figure 80: POMME versus OB: Differences of the Components, shifted timing, rotated URF

5.2 Comparison with the IB–Sensor

The same investigation as for the OB has been performed for the IB sensor.

Figure 81 shows the modulus of the IB sensor in the most upper panels and the total field calculated by the POMME model in the second panel. On this large scale the difference are negligible. The computed difference in the bottom panels, however reveals an error of about $\pm$ 600 nT for the most times. It is remarkable, that there is also a bump in the RPCMAG–IB data for about 4 min just before CA (S/C passed from the Gulf of Mexico via Mexico to the Pacific ocean). There is no external explanation for this bump. We guess that there are movable parts on ROSETTA. An in depth analysis can be performed if all SPICE kernels for ROSETA are available. In the following investigation we will exclude this specific time interval.

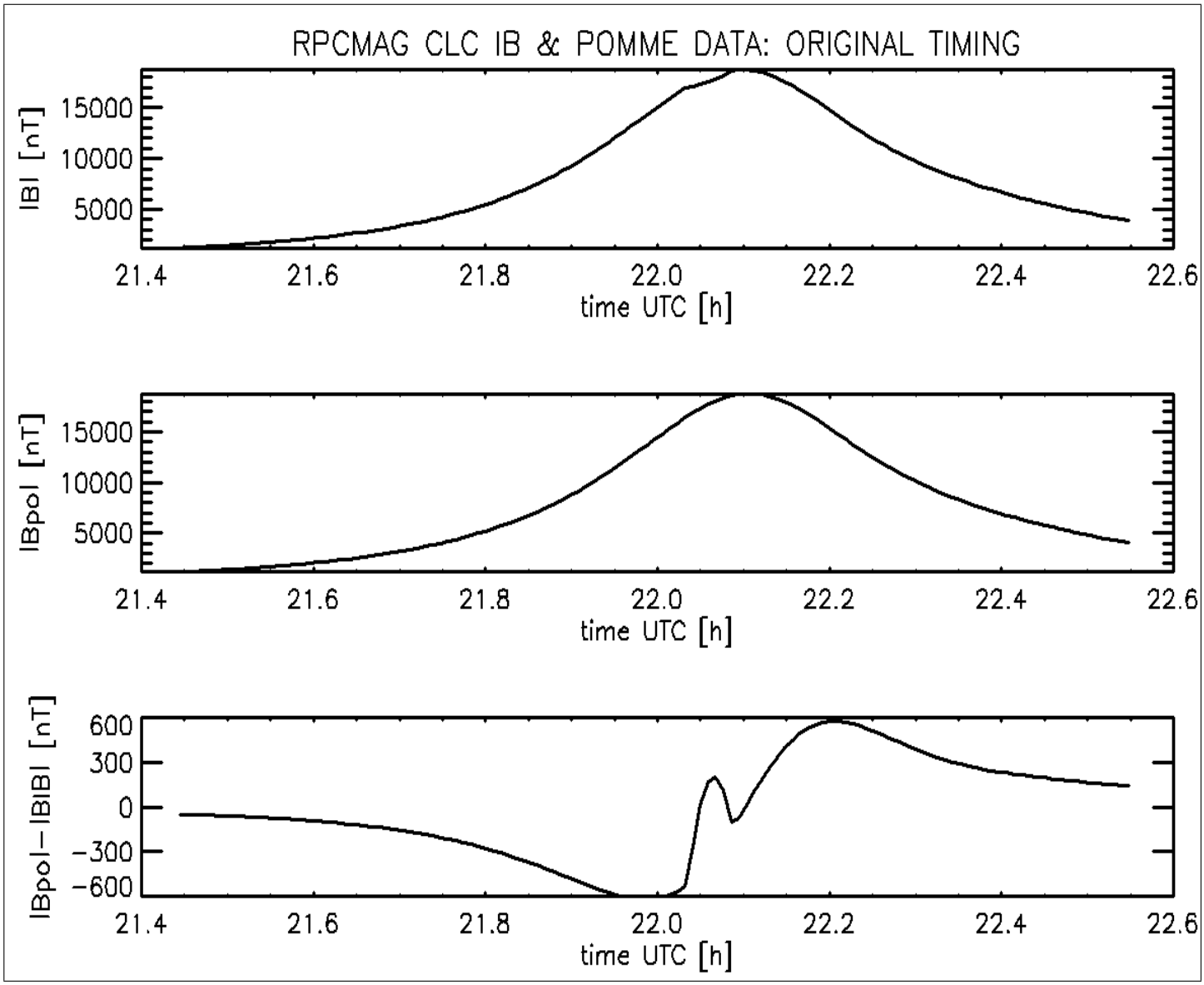

Figure 81: POMME versus IB: Total field, original timing

As the residua are higher than they should be we had the idea to minimize the difference by shifting the RPCMAG data in time domain. This was done using a minimization routine, minimizing the variance of the difference of both time series by shifting one time series in time domain. The result, shown in Figure 82, was that the IB data have to be shifted by -35.62 s against the POMME data. With this shift we can minimize the residual error to 10 nT.
The reason for this time shift is not absolutely clear. An upcoming investigation of the onboard filter software of RPCMAG will possibly reveal the secret.

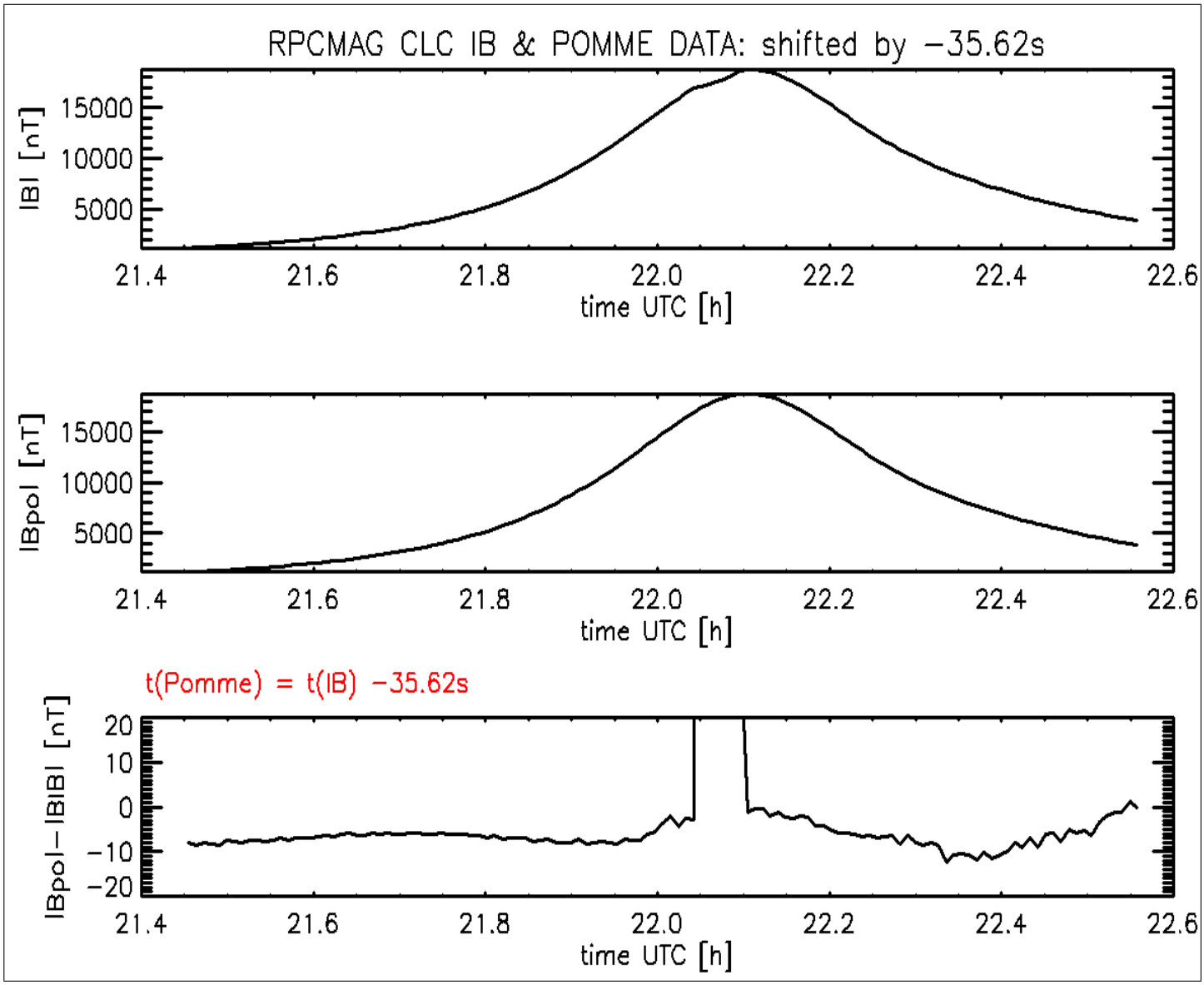

Figure 82: POMME versus IB: Total field, shifted timing

A comparison of the components of the IB sensor and POMME is displayed in Figure 83 for the original timing. At a first view this looks quite good as well. The differences of the model and the measurements are plotted in Figure 84 for the original timing and in Figure 85 for the time shifted data.

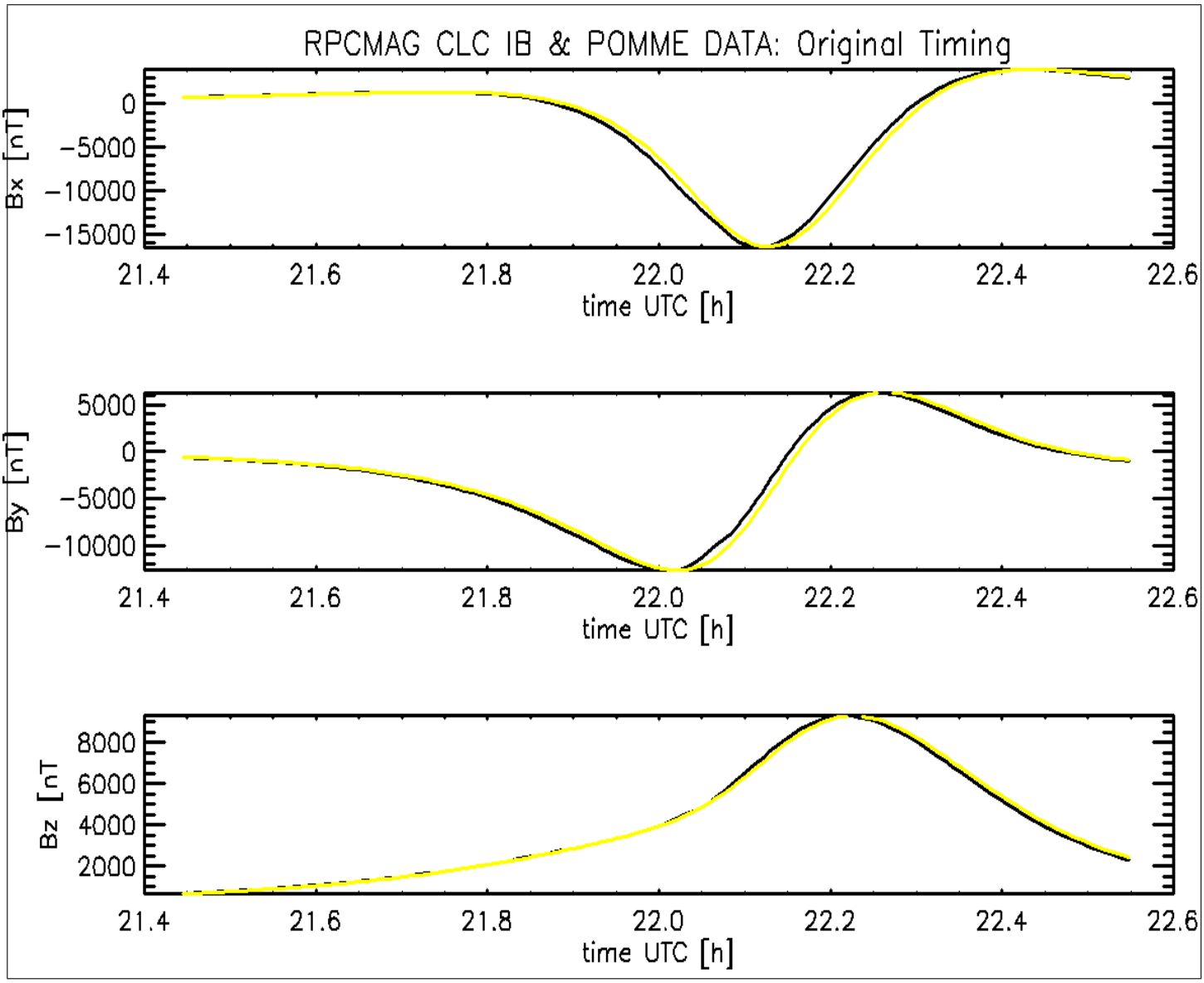

Figure 83: POMME versus IB: Components, original timing

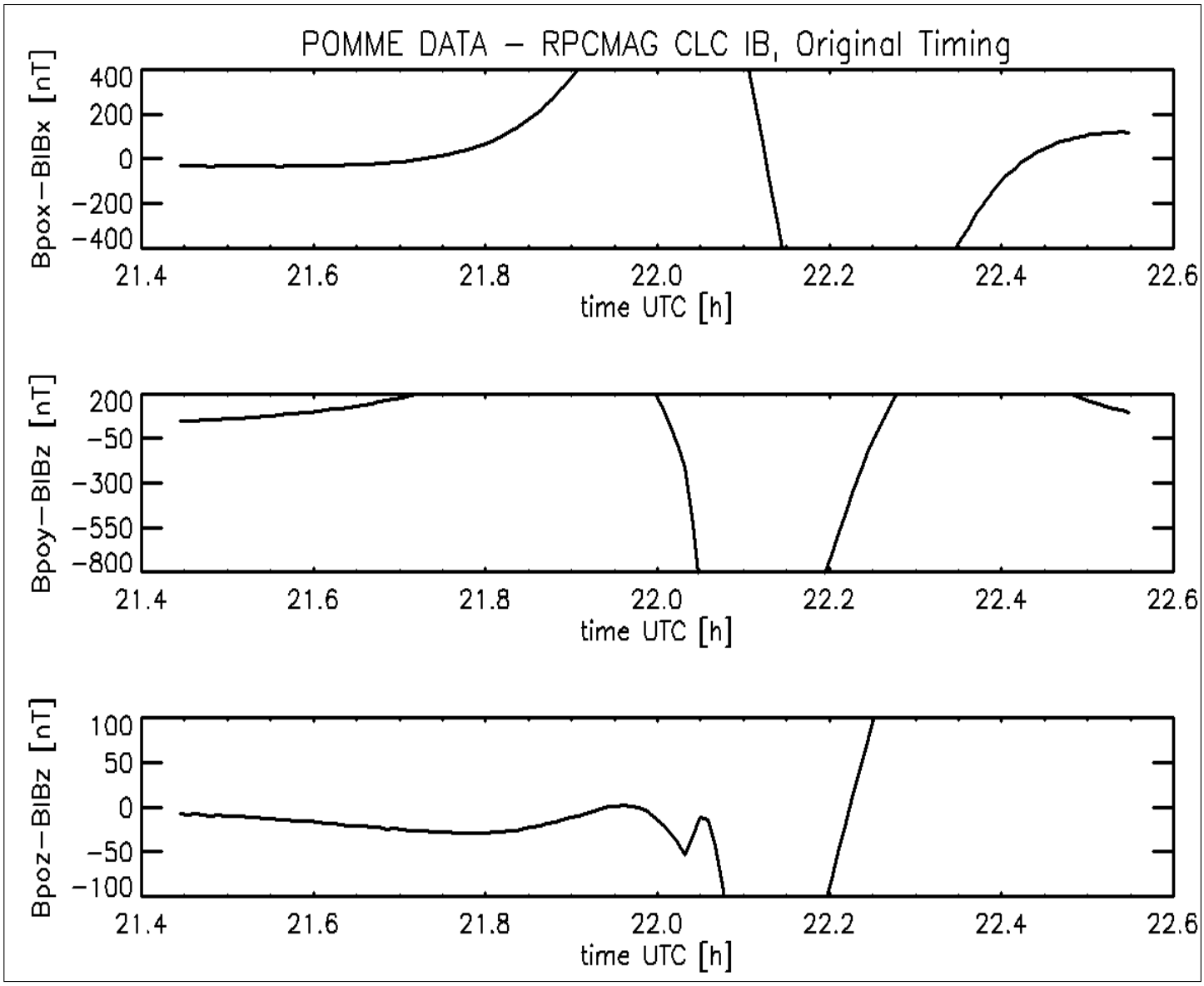

Figure 84: POMME versus IB: Differences of the Components, original timing

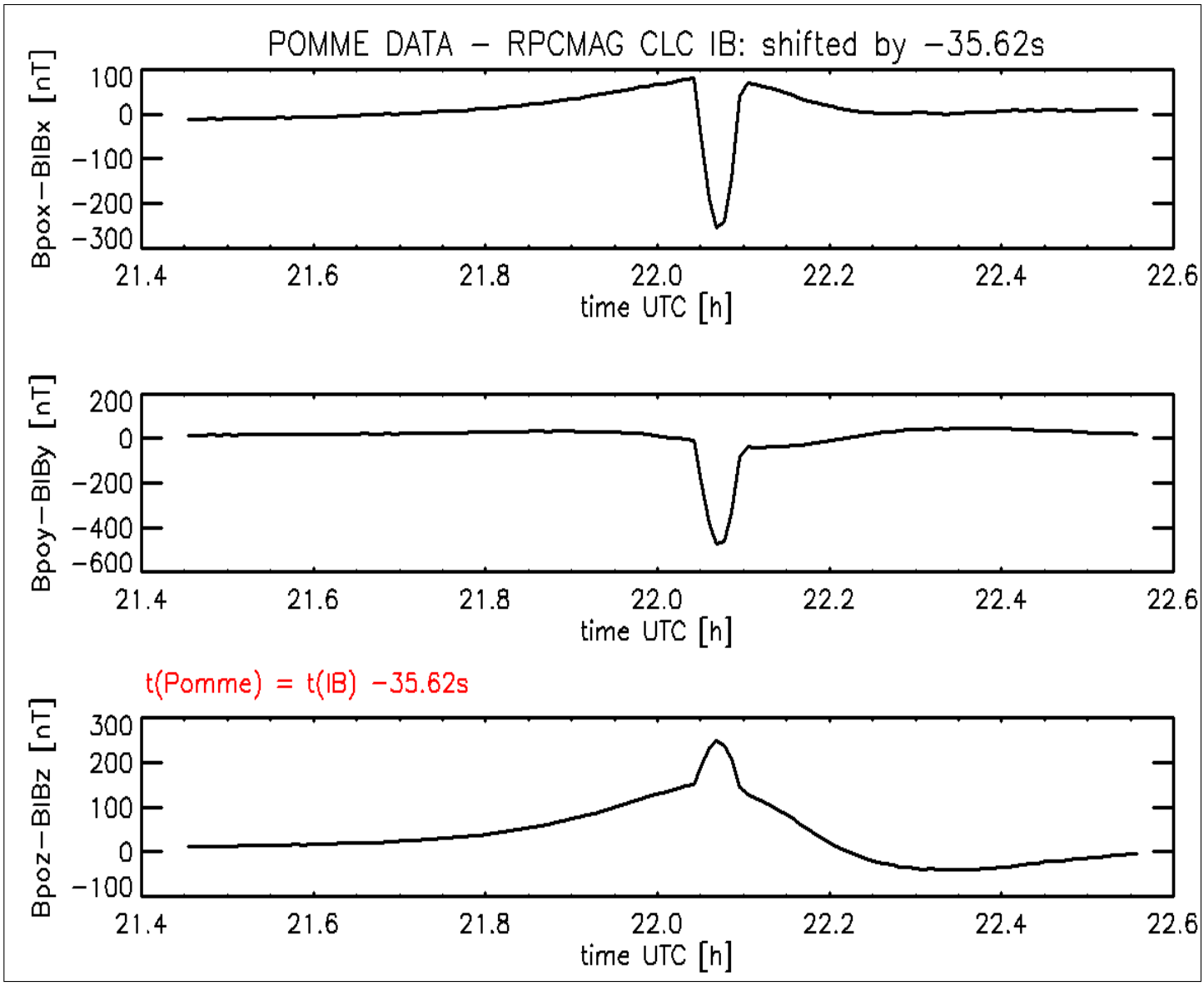

Figure 85: POMME versus IB: Differences of the Components, shifted timing

For the original timing we get residua in the order of ± 600 nT. The time shifted data are – as expected – much closer to the model data. Here we only see deviations of about ± 80 nT.
Analyzing the structure of the deviation the idea arose that the result could be improved drastically by rotation of the sensor reference frame. It could be that the actual orientation of the sensor does not perfectly coincide with the nominal build–in orientation.
To check this the RPCMAG data were feeded into an algorithm that minimizes the variance of the difference between measured and model data by applying three suitable rotations about the main axes. As output the three desired rotation angles are obtained.
The result of the procedure is displayed in Figure 86. This shows impressively that rotations of maximal 0.4° will reduce the error down to ±20 nT also for the IB sensor.

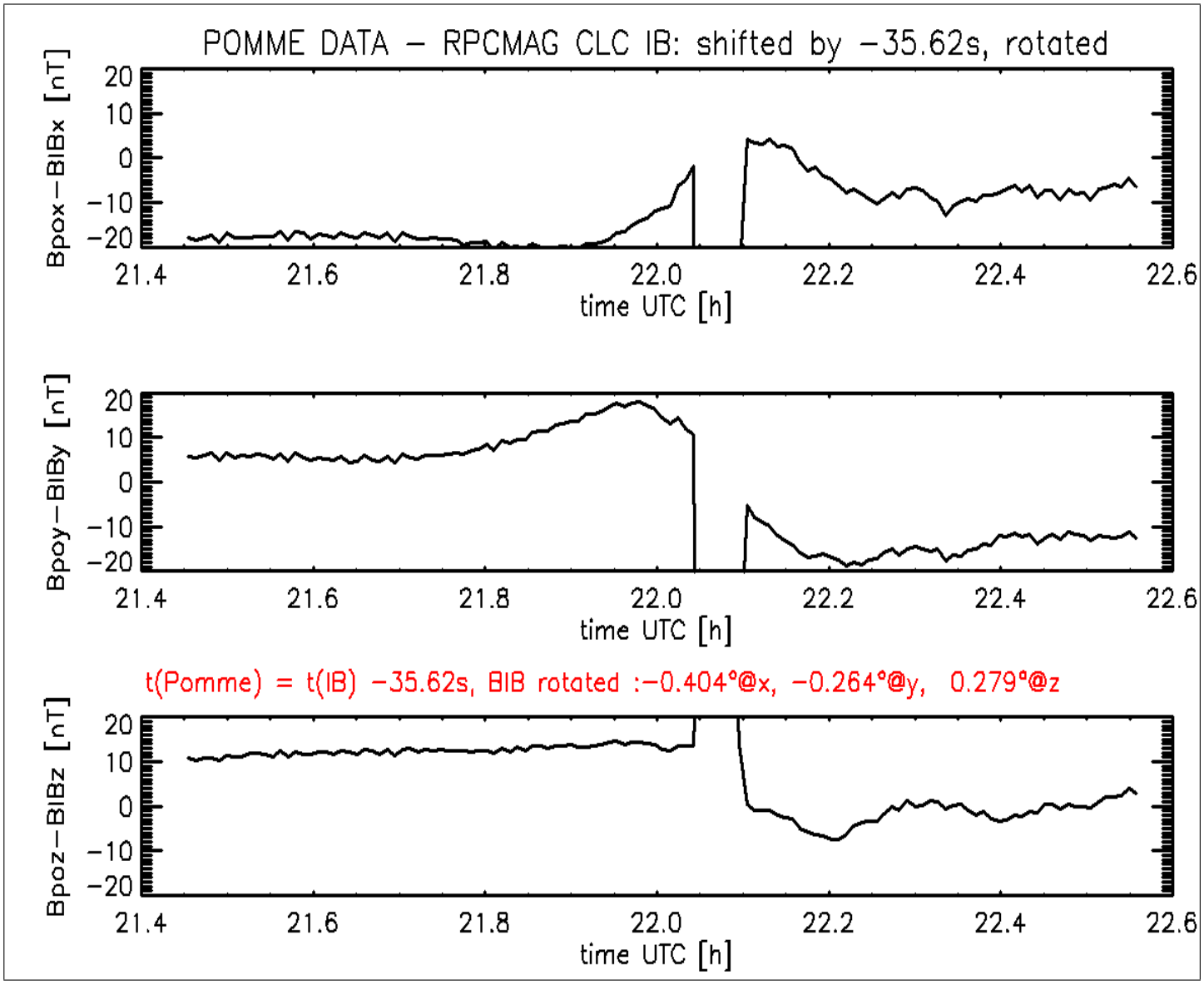

Figure 86: POMME versus IB: Differences of the Components, shifted timing, rotated URF

5.3 Consequences arising from the POMME - RPC investigation

The comparison of the RPCMAG data with the POMME data revealed , that the data quality can be improved if the sensor coordinate systems are rotated by a few tenth of a degree against the original ones and shifted in time by a few seconds.
The additional rotation can be understood by remembering, how the original values have been obtained. The original sensor mounting angles have been measured on the deployed boom using an optical system at the ESTEC cleanroom facility. These measurements have of course been carried out under the influence of the Earth's gravity. So it is not really surprising that the boom is slightly differen orientated under zero-g conditions in space.

To understand the discrepancies in the time tagging of the measured data with the POMME model, additional ground tests with the spare unit have been performed at Imperial college. The result of these test revealed, that the digital filtering in deed shifts the data by a certain amount of time which is of course time independent. Details of this tests can be found in the EAICD RO-IGEP-TR0009.

According to all these results all data have been reprocessed and will be archived a slightly rotated and time shifted way. The exact correction parameters can be found in the EAICD and in the Label files.

6 Comparison of the MAG with WIND data

This section show the result of a comparison between the RPCMAG OB data and the magnetic field data measured by the WIND satellite (positioned near the Lagrange Point L_1). The comparison has been executed for March 6, 2005. On this day the Wind Satellite was about 237 $R_E = 1514768$ km away from the Earth. Assuming a reasonable solar wind speed of 537 km/s there should be a time lag of 47 min between WIND data and RPCMAG data. Exactly this time delay has to be taken into account to obtain the best coincidence between both time series. The related correlation coefficient is 0.89.
The plot shows a good accordance in the first 14 hours of the day. At later times, however, the conformity decreases. This is caused by temperature effects of the RPCMAG sensor. According to the assessment of the data quality using our temperature divergence indicator (refer to section 4) the "bad" area has been forecasted and marked red.

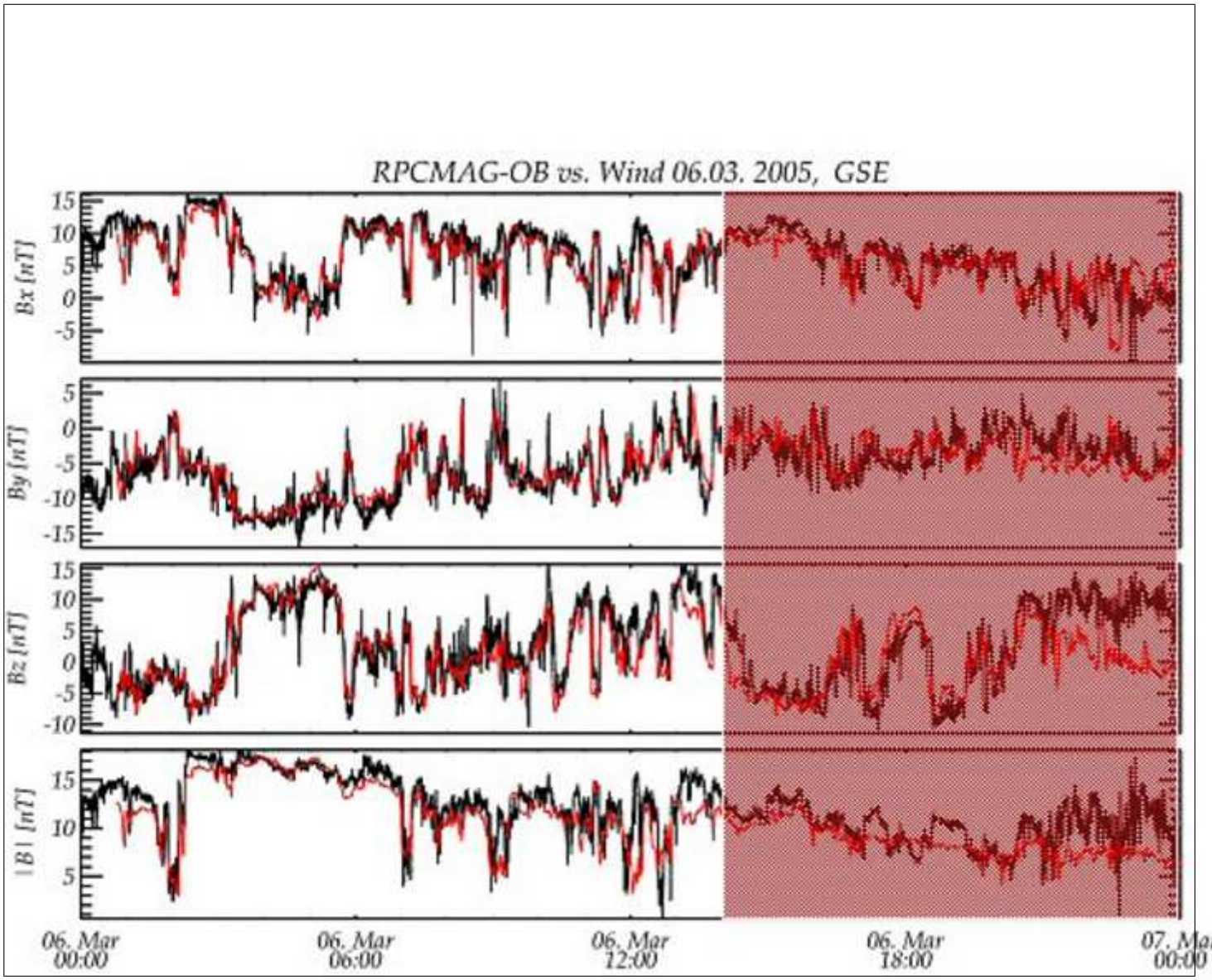

Figure 87: ROMAP OB versus WIND data

7 Dynamic Spectra of the Swing by

This section shows the dynamic spectra of the OB sensor in LEVEL_C = ECLIPJ2000 coordinates. As the sensor was operated as primary sensor in NORMAL mode, SID2, the maximum resolvable frequency is 0.5 Hz. The spectra show significant structures from afternoon of March 1 until the morning of March 5. These horizontal lines are harmonics of a base frequency of 1/30 Hz which is caused by pulsed heaters on the LANDER (refer to section 9)

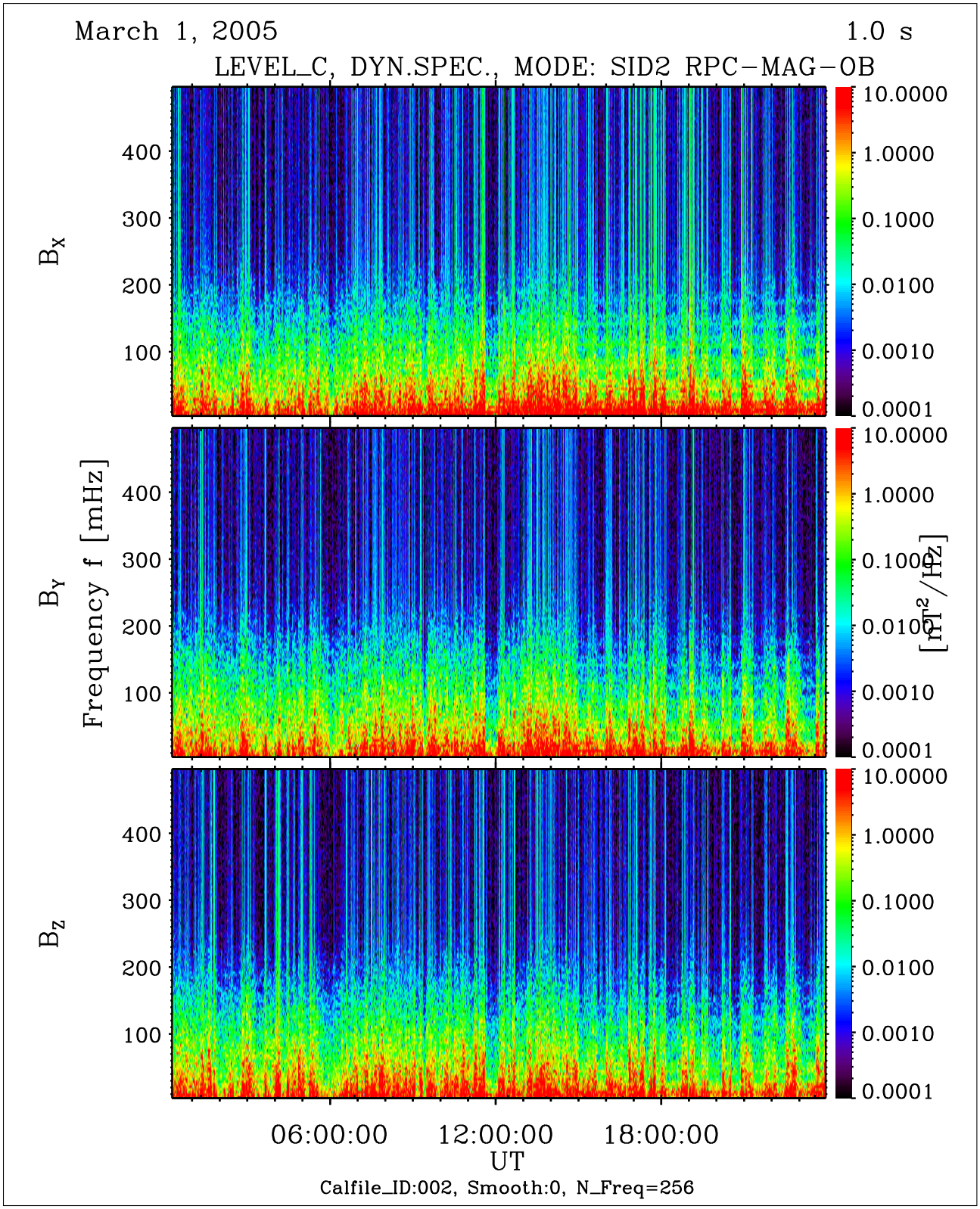

Figure 88: File: RPCMAG050301T0014_CLC_OB_M2_DS0_500_002

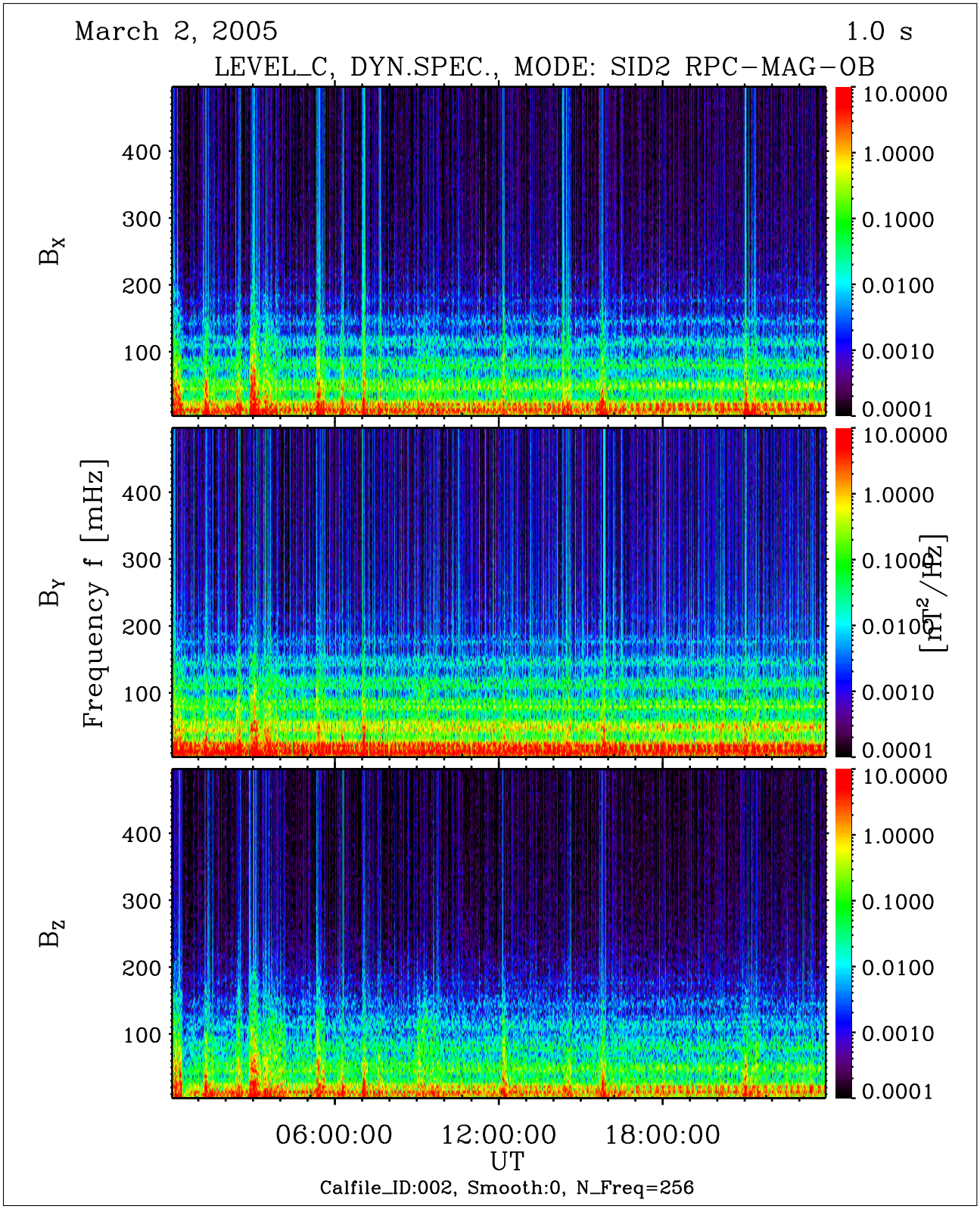

Figure 89: File: RPCMAG050302T0000_CLC_OB_M2_DS0_500_002

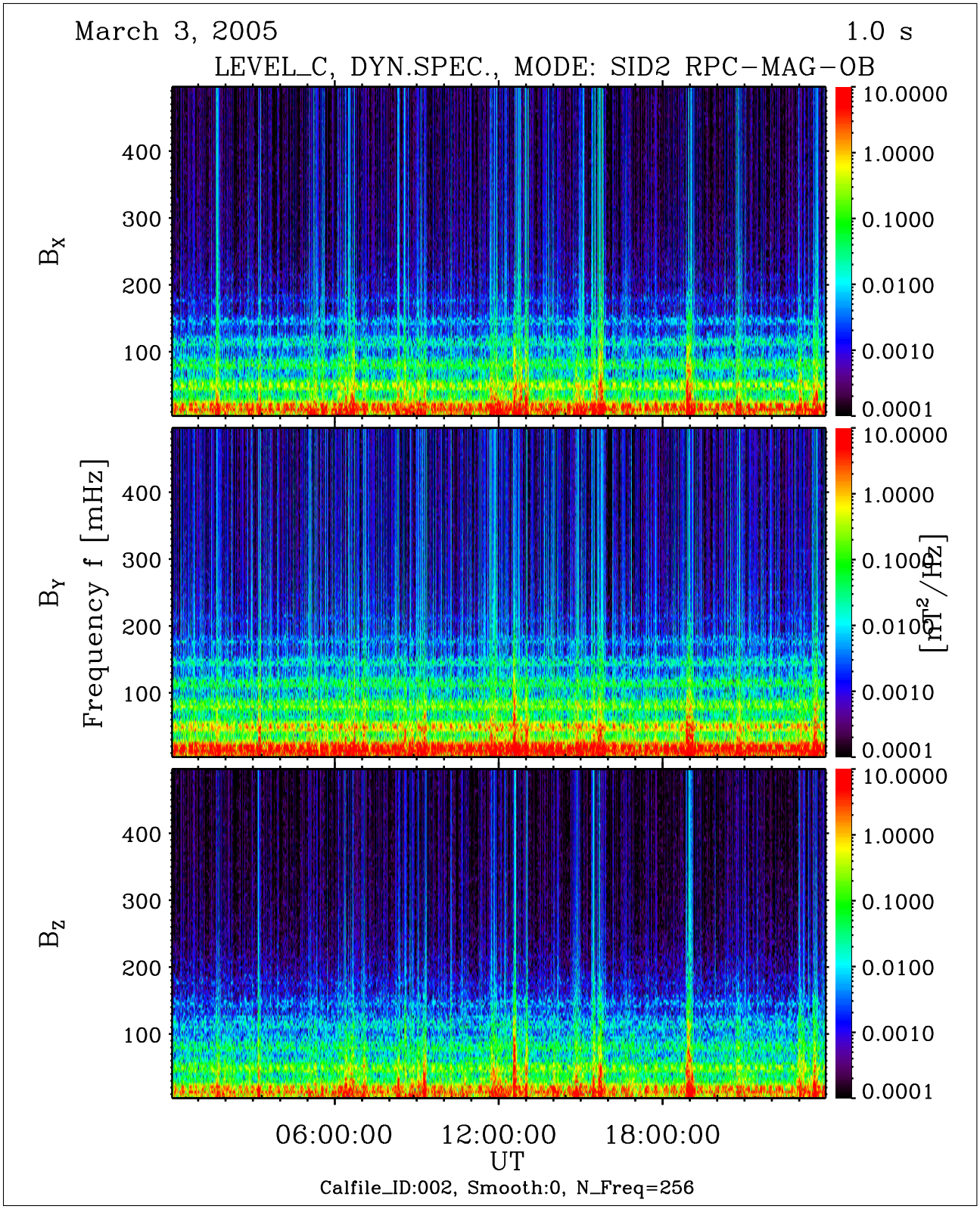

Figure 90: File: RPCMAG050303T0000_CLC_OB_M2_DS0_500_002

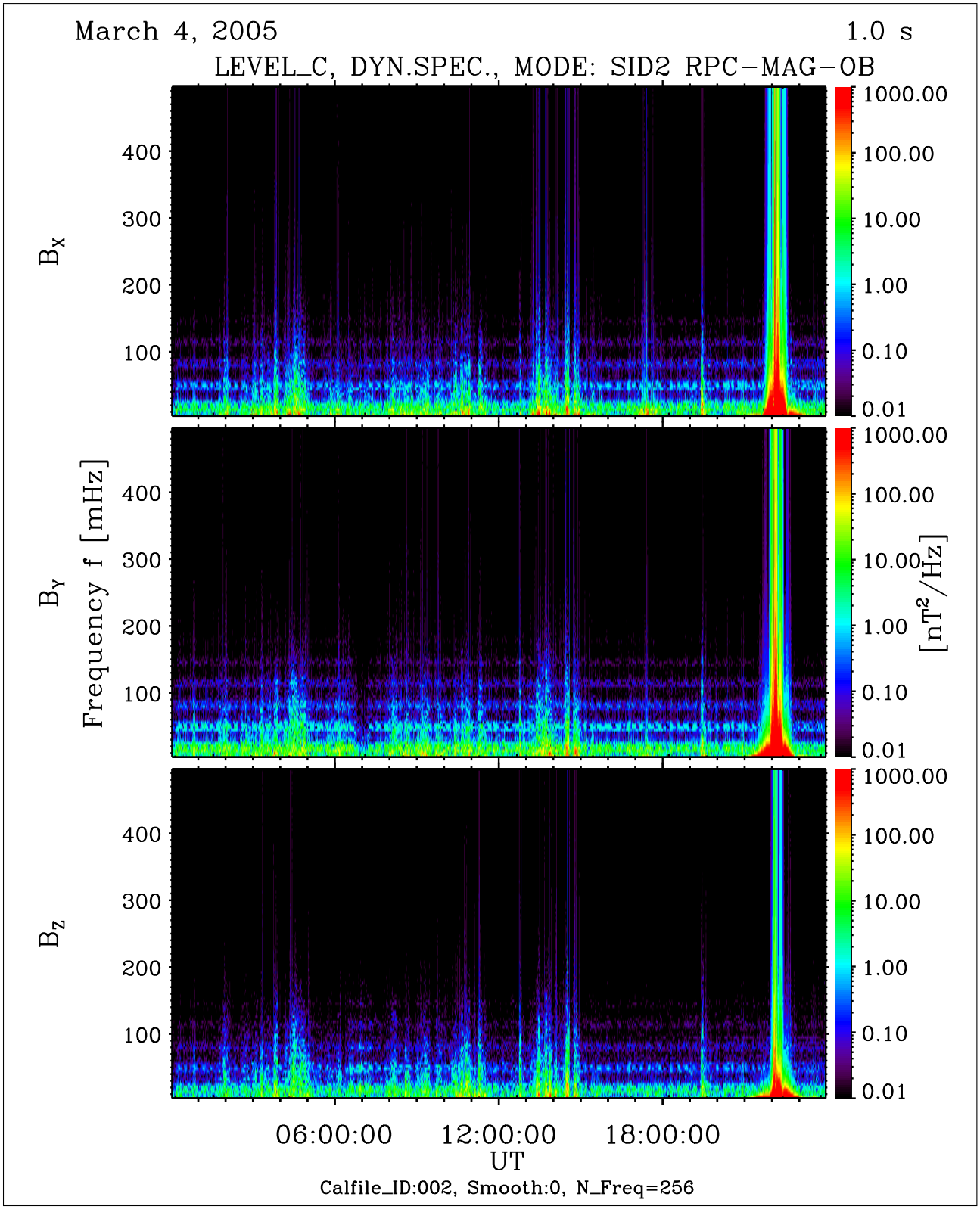

Figure 91: File: RPCMAG050304T0000_CLC_OB_M2_DS0_500_002

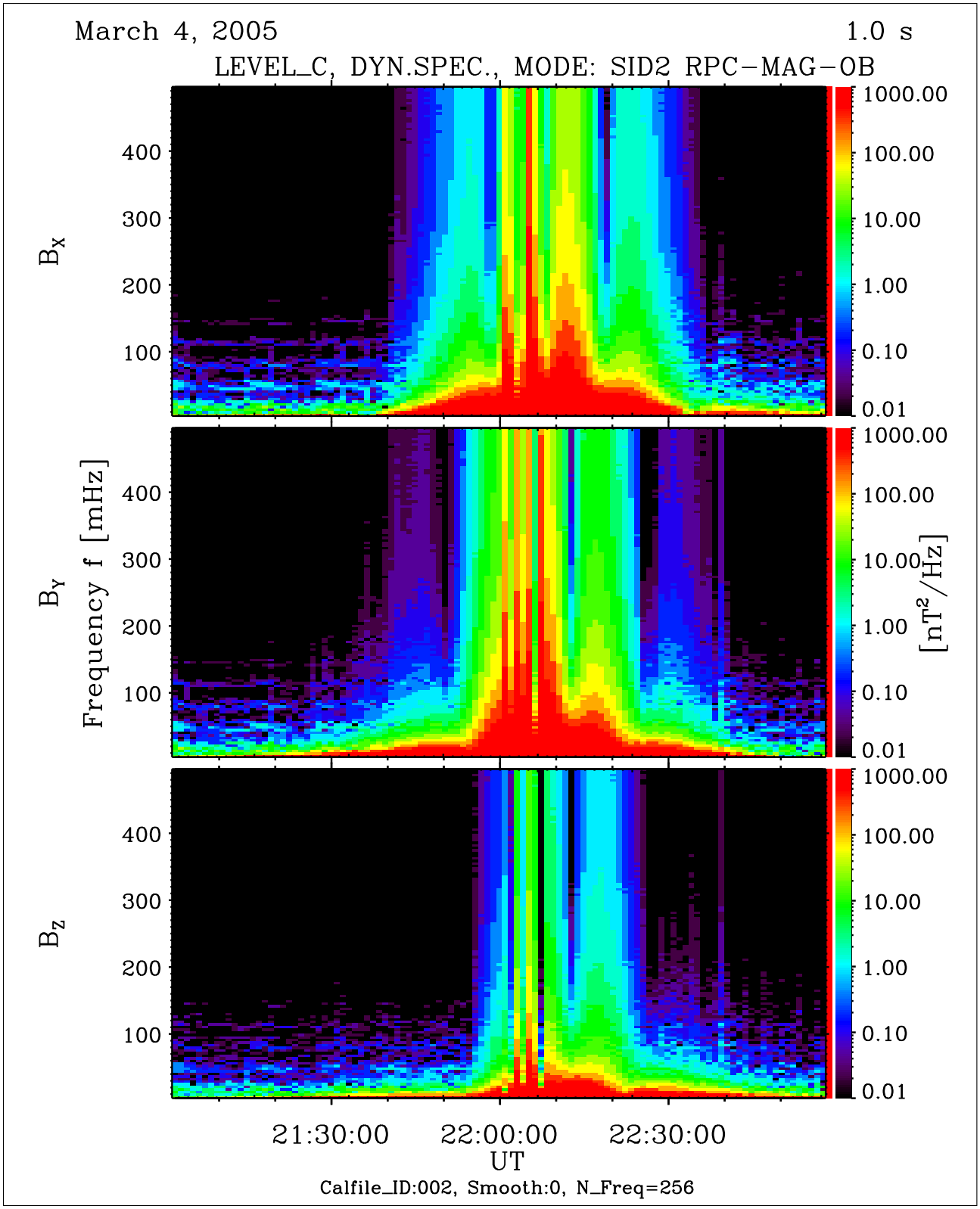

Figure 92: File: RPCMAG050304T0000_CLC_OB_M2_DS0_499_002-zoomed

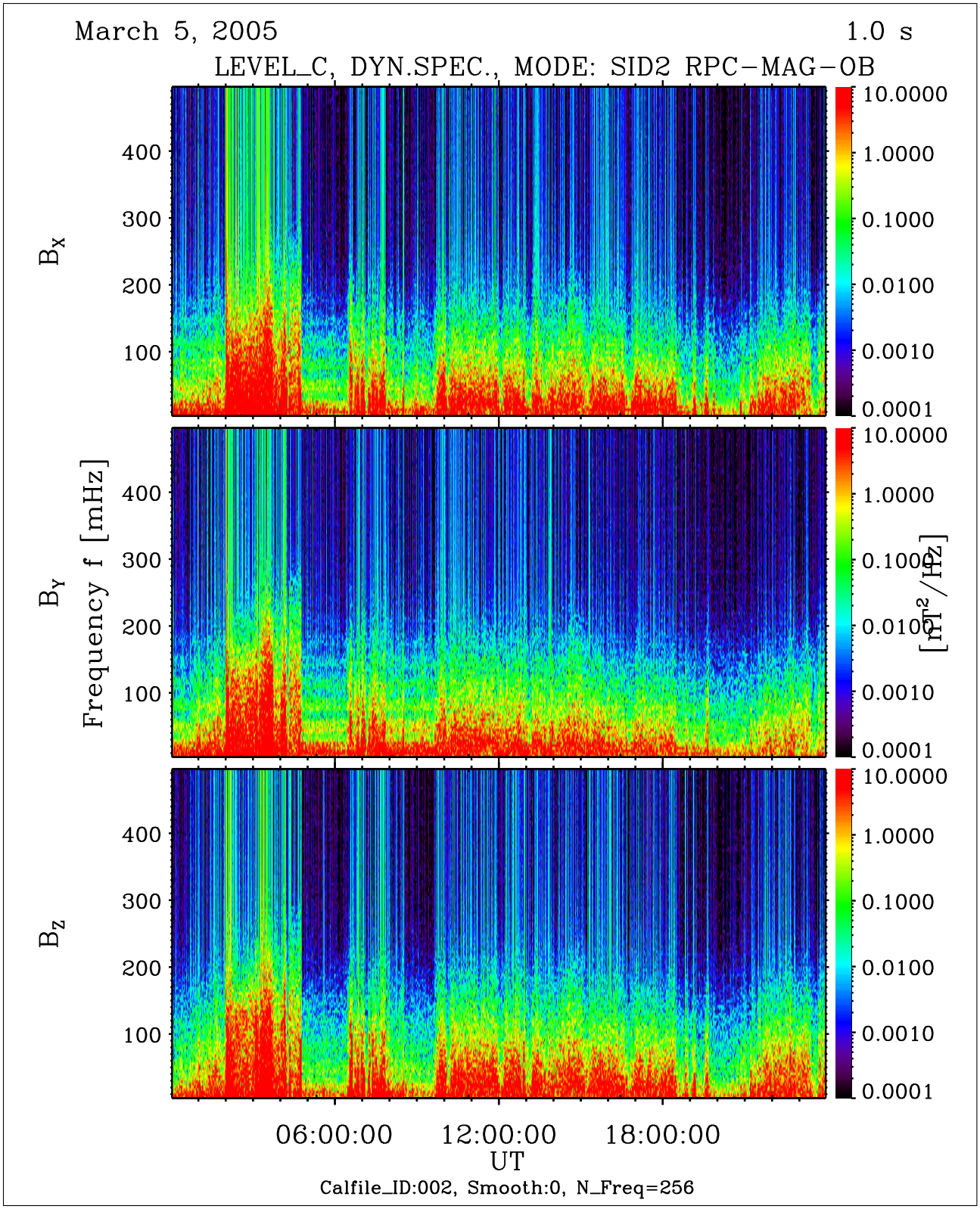

Figure 93: File: RPCMAG050305T0000_CLC_OB_M2_DS0_500_002

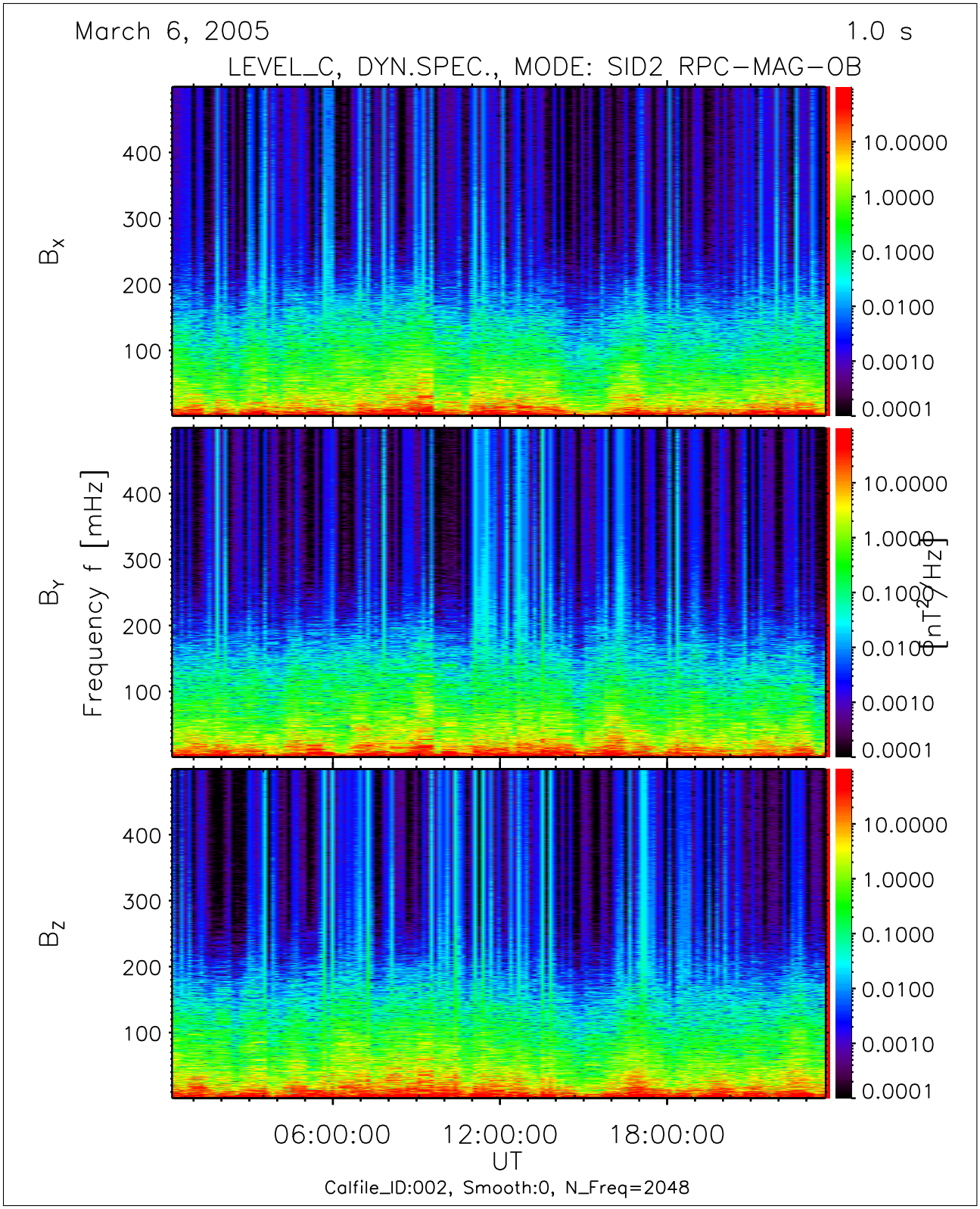

Figure 94: File: RPCMAG050306T0000_CLC_OB_M2_DS0_500_002

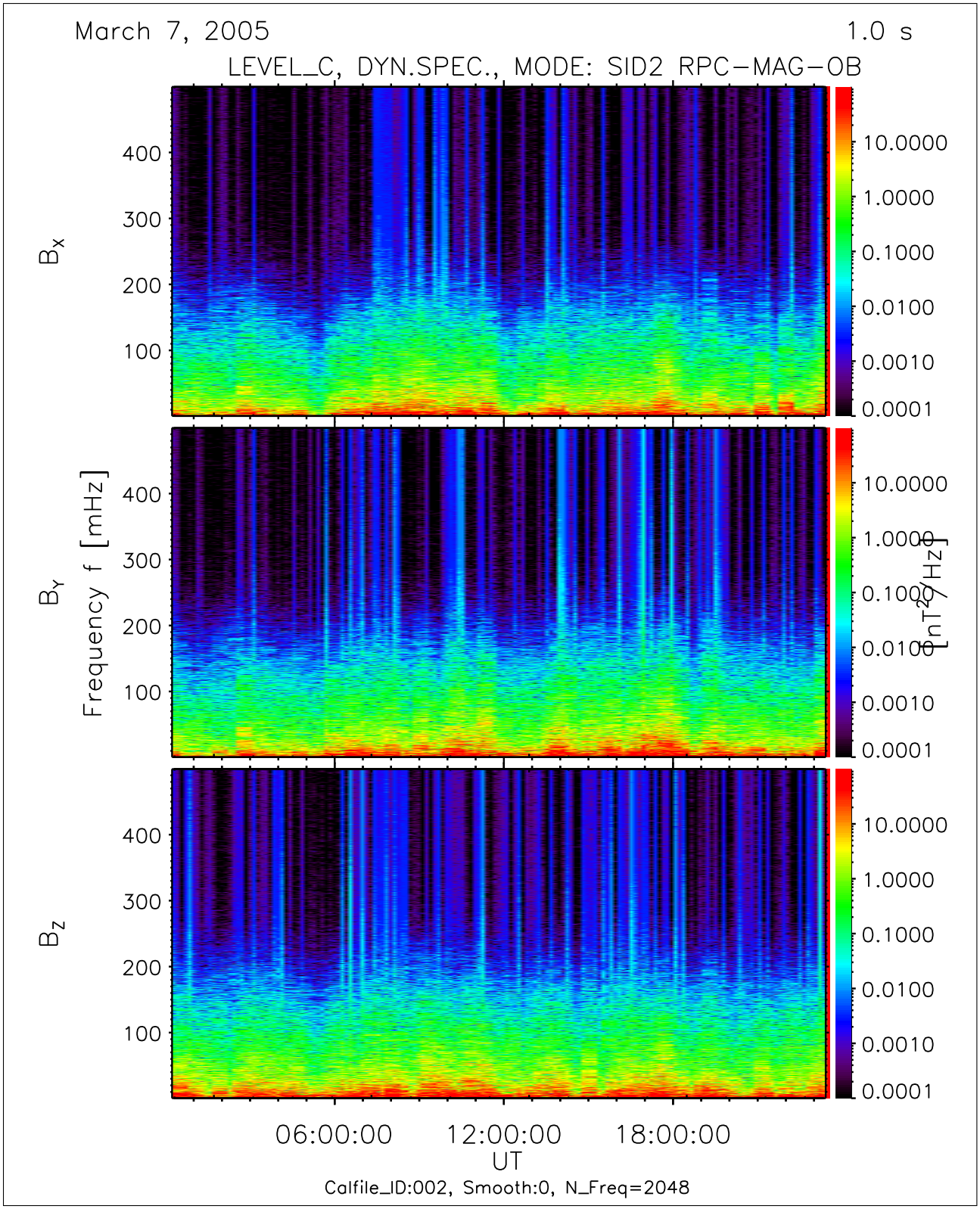

Figure 95: File: RPCMAG050307T0000_CLC_OB_M2_DS0_500_002

8 Dynamic Spectra of ROSETTAs REACTION WHEELS

This section shows the spectra of ROSETTAs Reaction Wheels (RW). There are 4 different wheels rotating with different frequencies. The plots do not show the original rotation frequencies but the signatures that would be expected using an data acquisition system operating at 1 Hz sampling frequency without any aliasing filter.
These signatures are expected to be seen on the OB sensor operated in NORMAL modes, SID2 due to our experiences from the commissioning phase.

However, a view to the spectra of the measured magnetic field (refer to section 7) shows , that there is actually no influence of the RWs. The magnetic field spectra are clean.

The MAG team is happy about this, although there is no explanation for the disappearance of the RW impact.

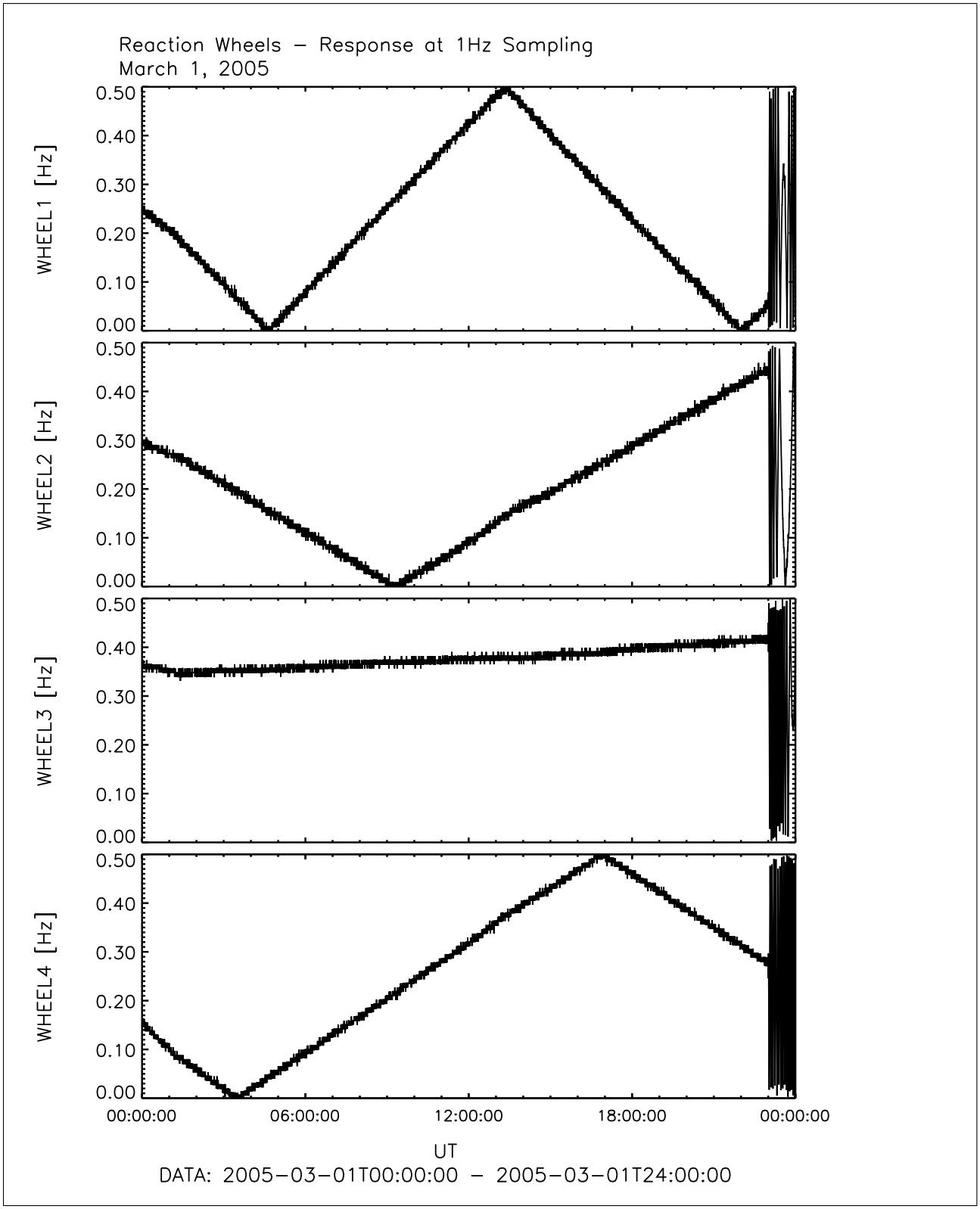

Figure 96: File: wheels_1Hz_Sampling2005-03-01T00-00

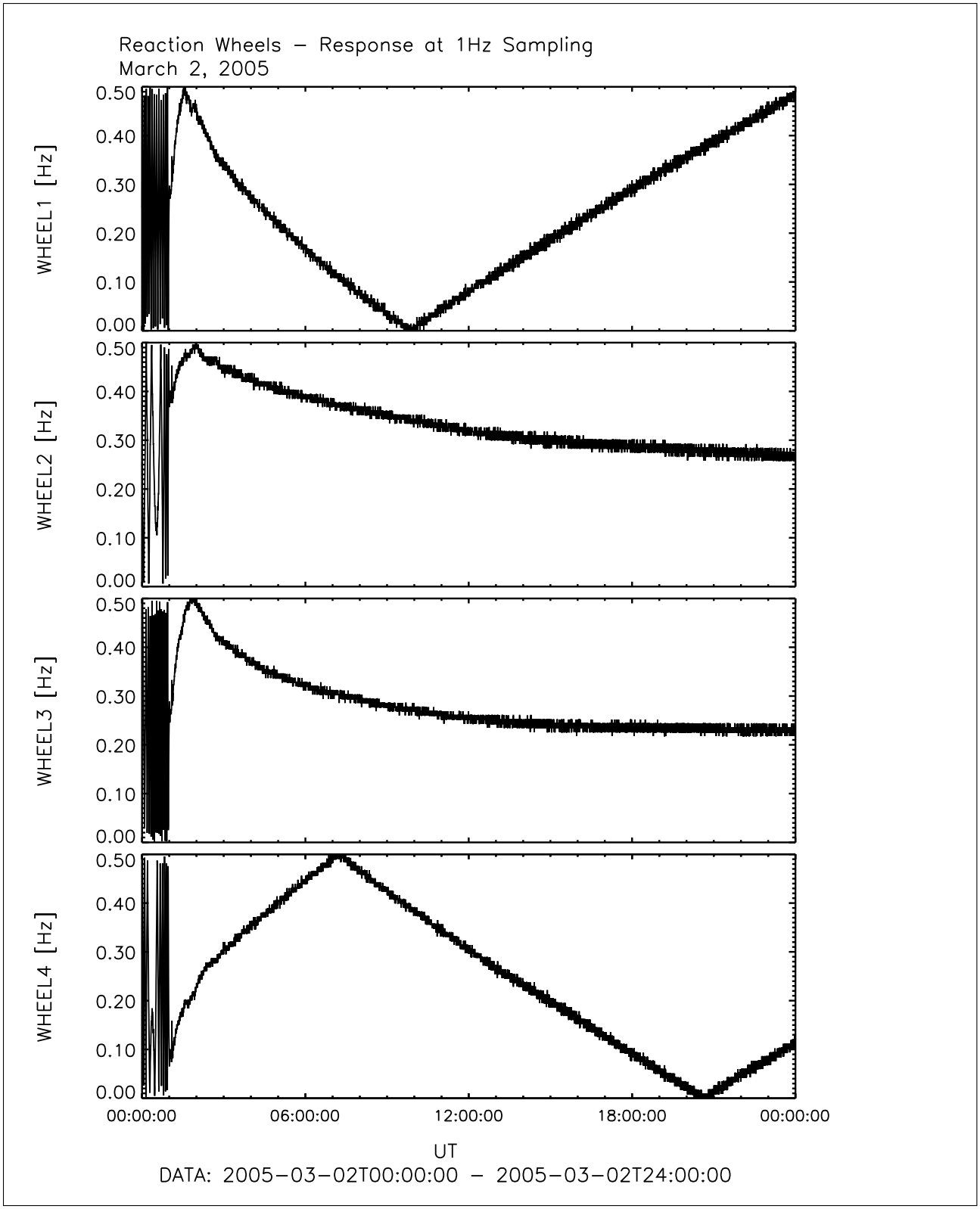

Figure 97: File: wheels_1Hz_Sampling2005-03-02T00-00

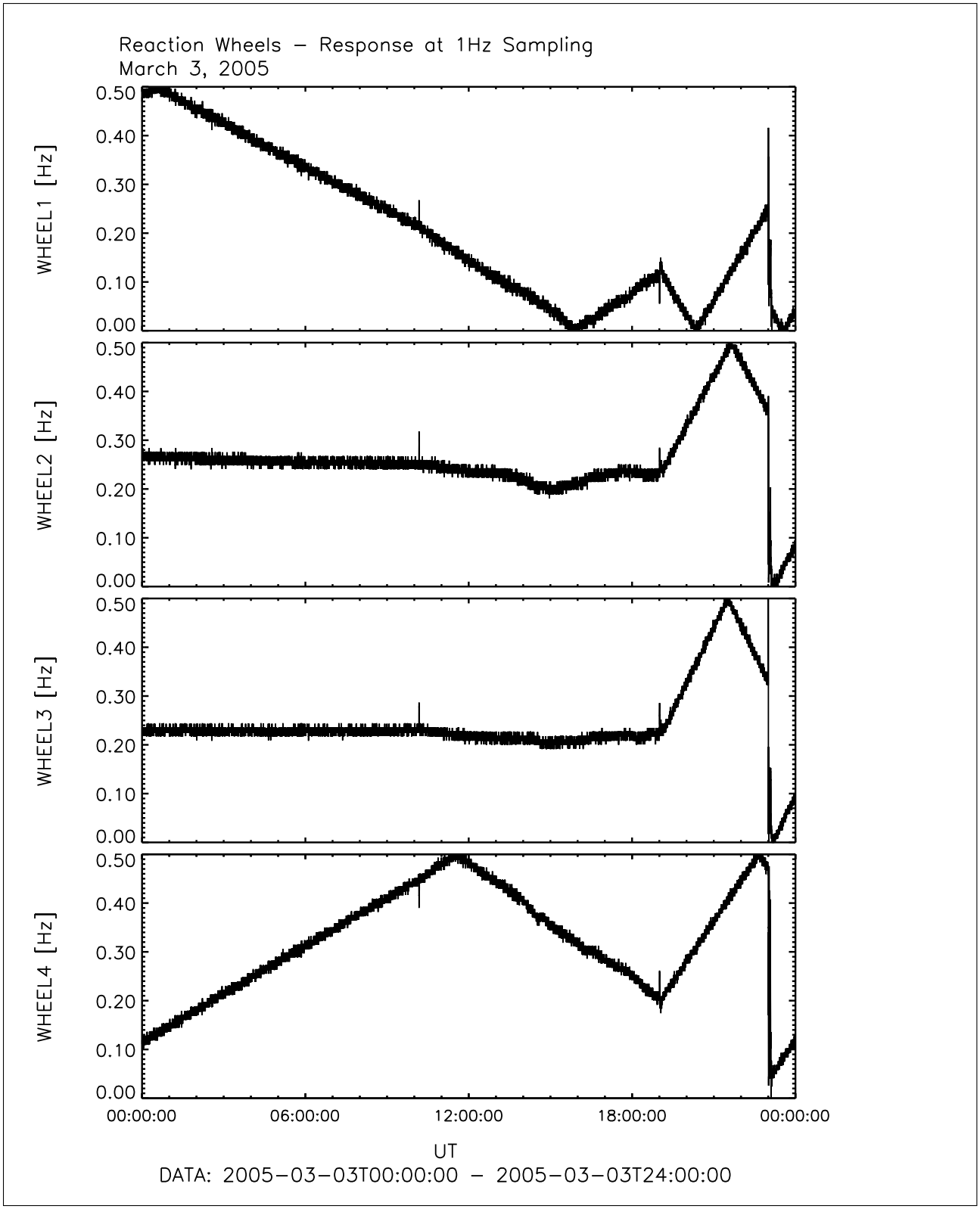

Figure 98: File: wheels_1Hz_Sampling2005-03-03T00-00

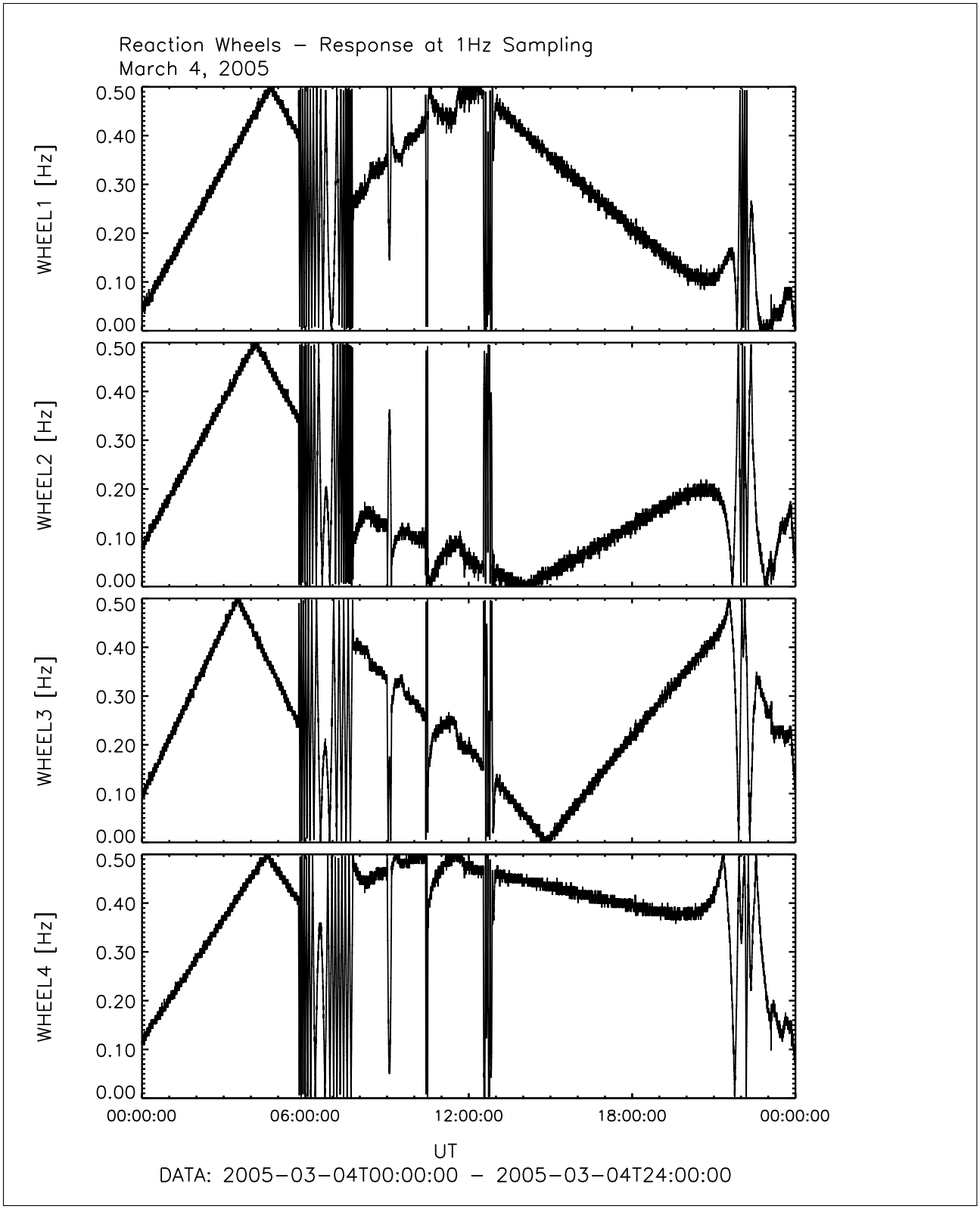

Figure 99: File: wheels_1Hz_Sampling2005-03-04T00-00

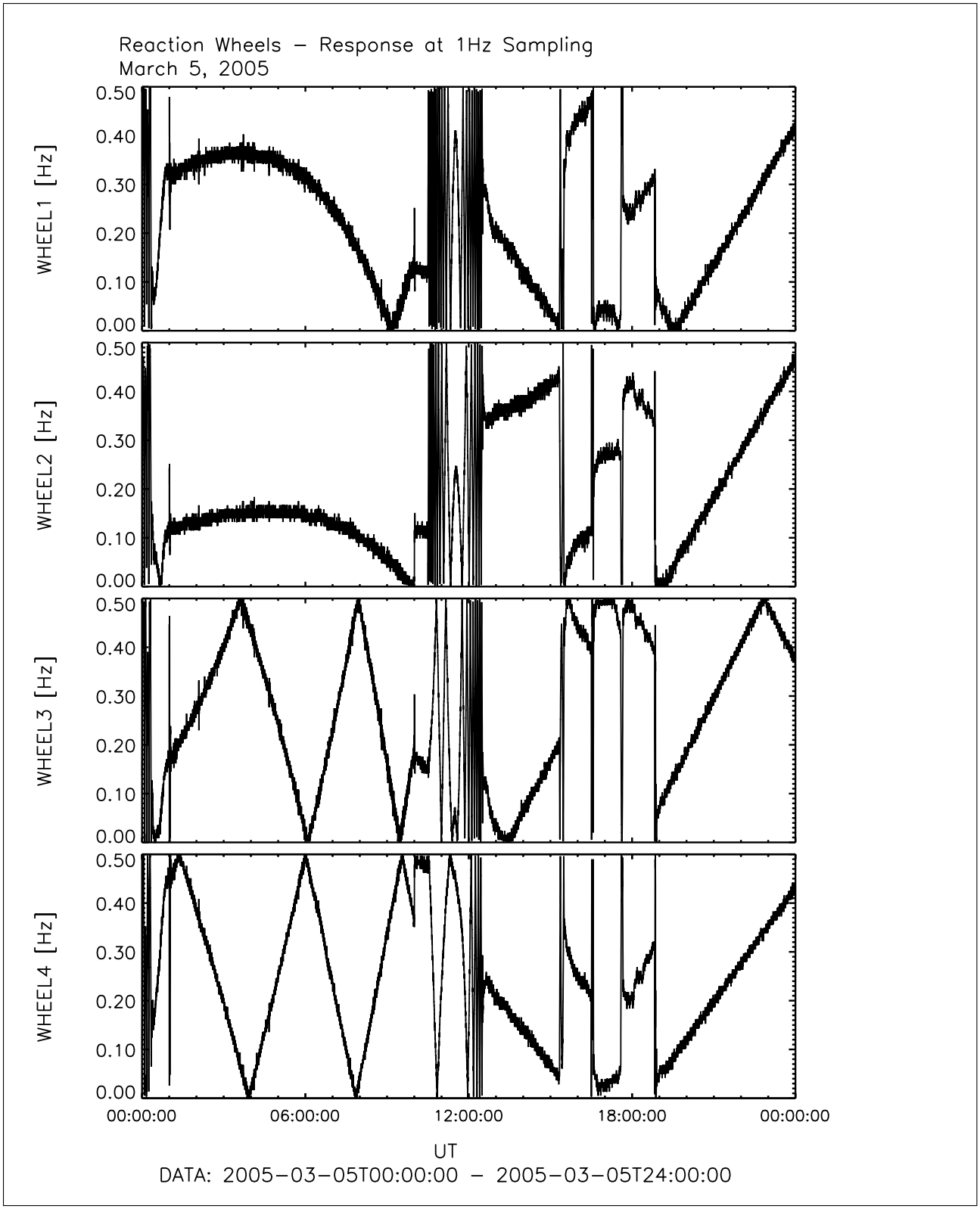

Figure 100: File: wheels_1Hz_Sampling2005-03-05T00-00

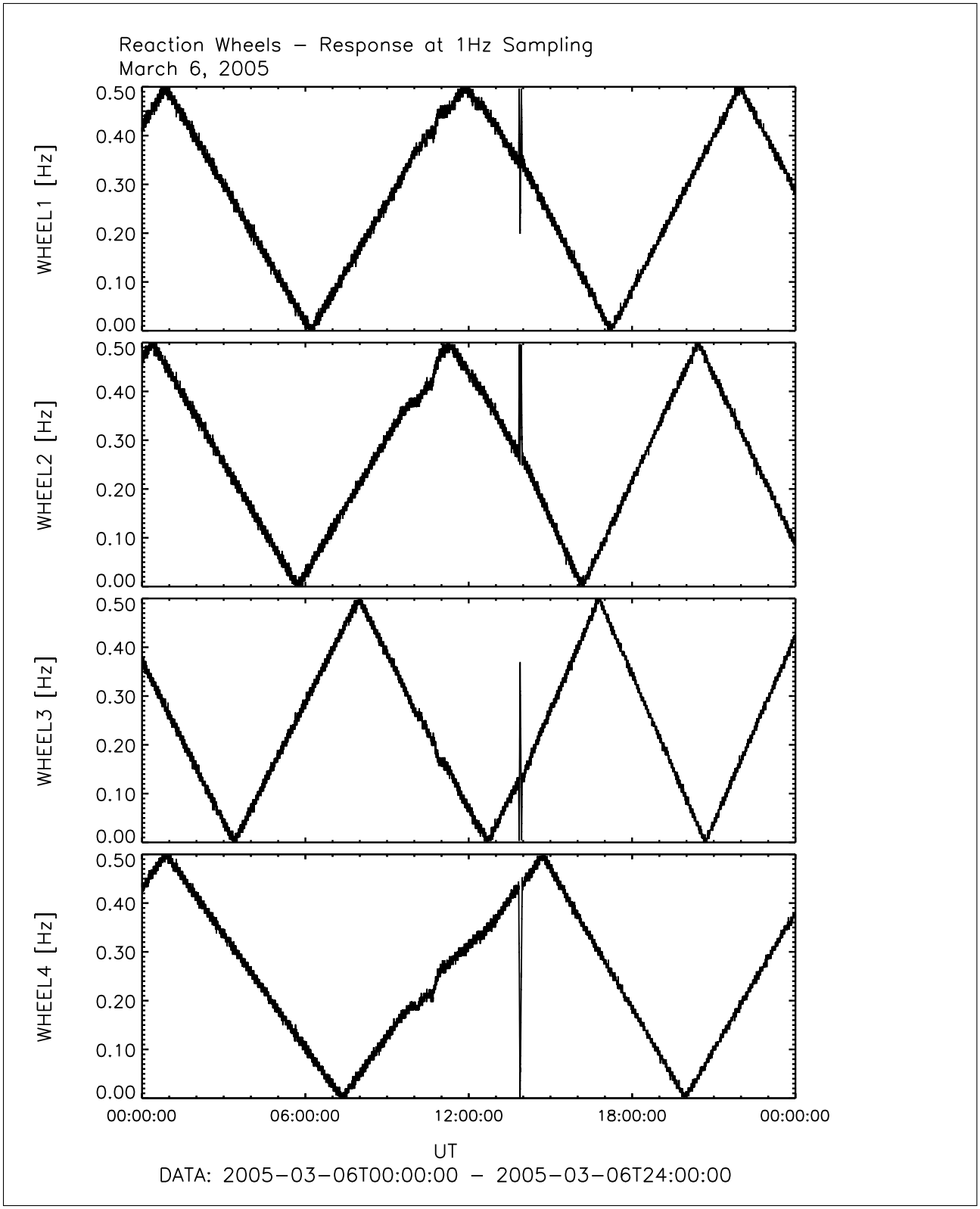

Figure 101: File: wheels_1Hz_Sampling2005-03-06T00-00

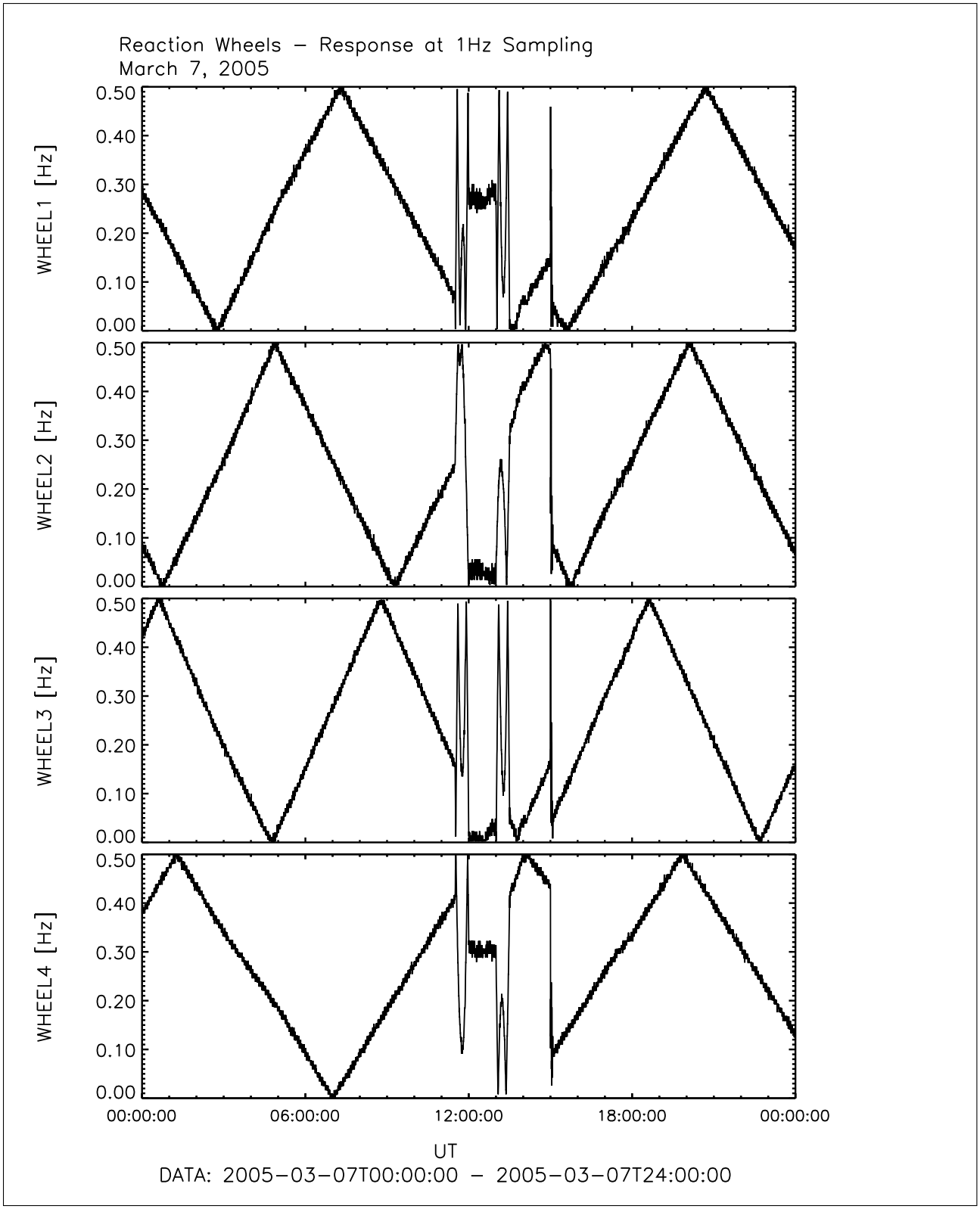

Figure 102: File: wheels_1Hz_Sampling2005-03-07T00-00

9 The impact and elimination of the LANDER heaters

During EAR1 RPCMAG had the worthy chance to perform parallel measurements with the Lander magnetometer ROMAP. ROMAP was switched on from 2005-03-01T01:00 until 2005-03-07T03:30. As, however, already mentioned, the Lander heaters were tested as well in the time from afternoon of March 1 until the morning of March 5. These heaters cause disturbances in the order of 1000—2000 nT at the ROMAP sensors and disturbances in the order of 0.5 — 1.5 nT at the RPCMAG OB sensor.

This section will show the impact of the heaters to the MAG OB sensor and the method to eliminate these disturbances.

Figure 103 shows a randomly chosen interval (March 3, 00:00 — 24:00) of RPCMAG OB data. On the first view these data look like proper magnetic field data. If we, however, zoom into the data, as done for randomly chosen interval of 30 minutes, we can clearly identify a disturbing signal in shape of a square wave with a period of T=30 s. The amplitude is not constant, but appearing with 4 different levels. This is related to three different kind of heaters (respective different currents) located on the Lander.

This disturbed signal in B_x, B_y, B_z components (ECLIPJ2000–coordinates) is redisplayed in Figure 104. As it is easier to perform a convenient signal processing on one component with a clearly disturbed signal rather than on three slightly disturbed ones, the idea arose to turn the measured magnetic field signal into a minimum variance system. The result of this preprocessing transformation can be impressively seen in Figure 105. The complete disturbance is now superimposed on the B_x signal whereas the B_y and B_z components in the MINVAR system completely purged.

The real processing is visualized in Figure 106. The most upper panels shows the preprocessed data rotated into the B_x component of the minimum variance system (which is actually the component with the maximum variance.)
The second panel shows the detection of the jumps. This is done using a moving variance indicator. A short time variance of just a few samples is evaluated and shifted step by step over the whole times series (dark blue curve). As a result strong positive peaks occur at the times of the jumps, and a nearly flat signal dominates the other times. In a second step a threshold (light blue line) has to be defined to separate between jumps and "normal" data. Everything below this threshold belongs to right data, everything above this threshold is interpreted as jump caused by the heaters.
The third panels shows the separated step in the B_x time series. The times of the jumps and intermediate values are cut out.

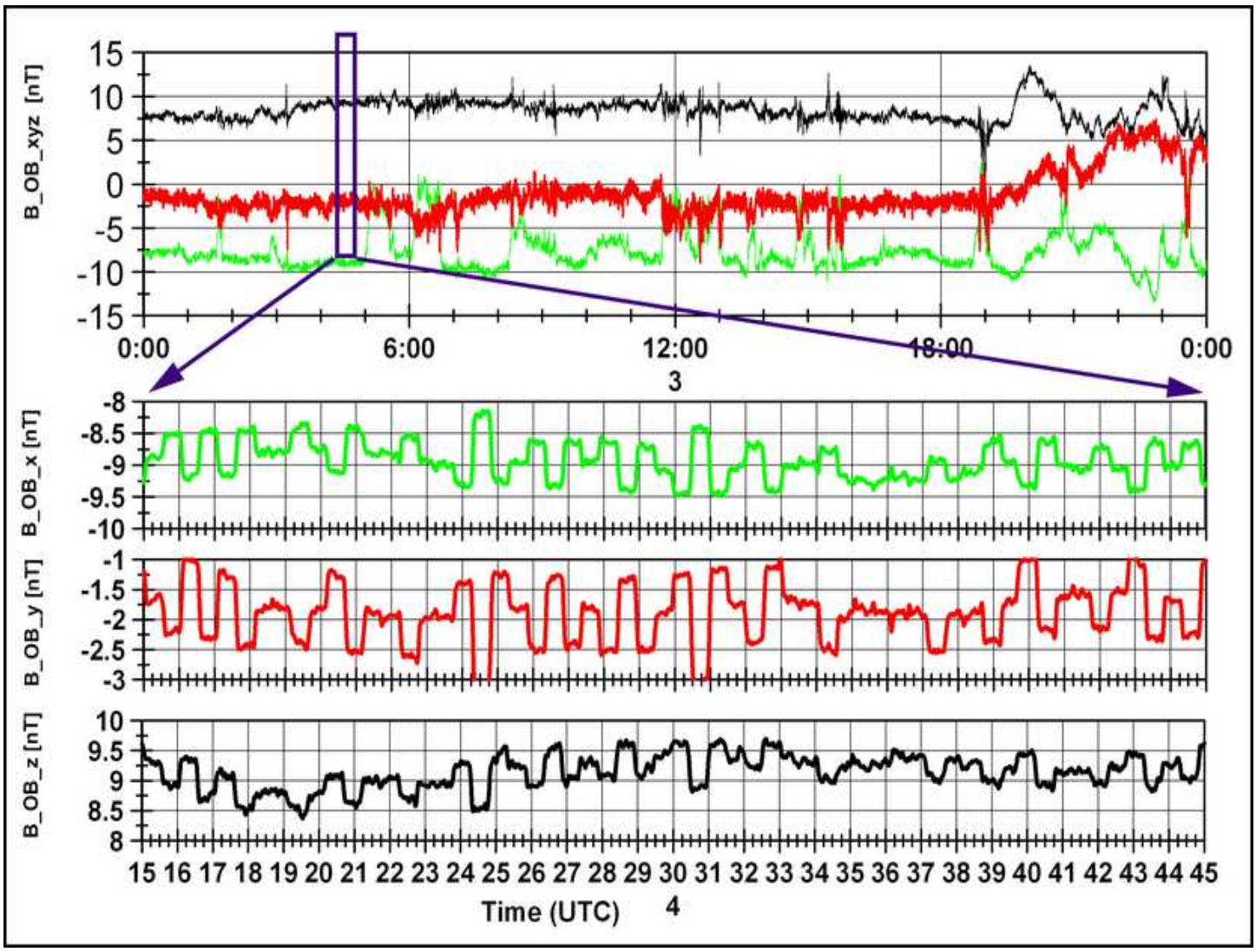

Figure 103: Original and zoomed Signal of March 3 (ECLIPJ2000).

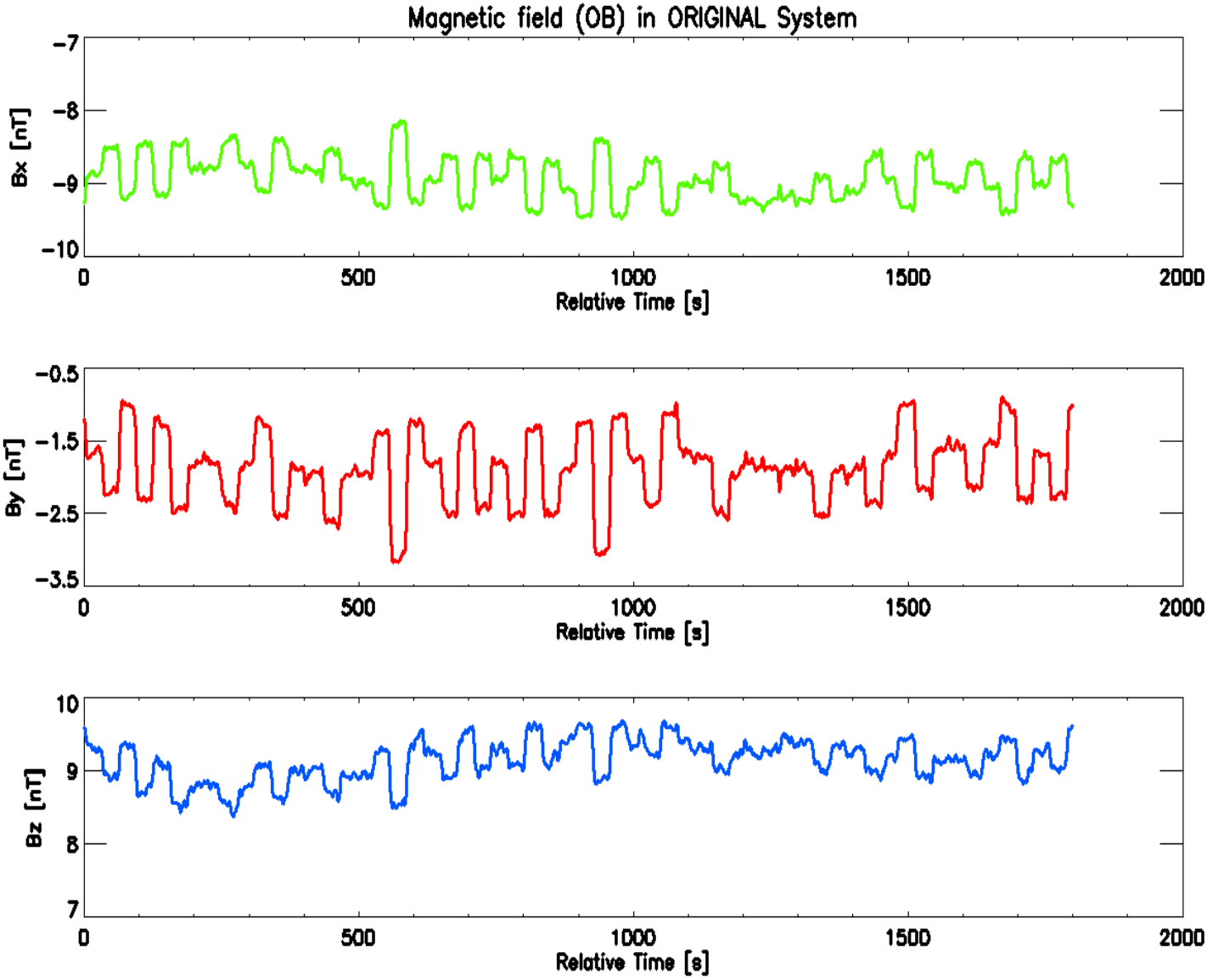

Figure 104: Original Signal disturbed by the LANDER heaters

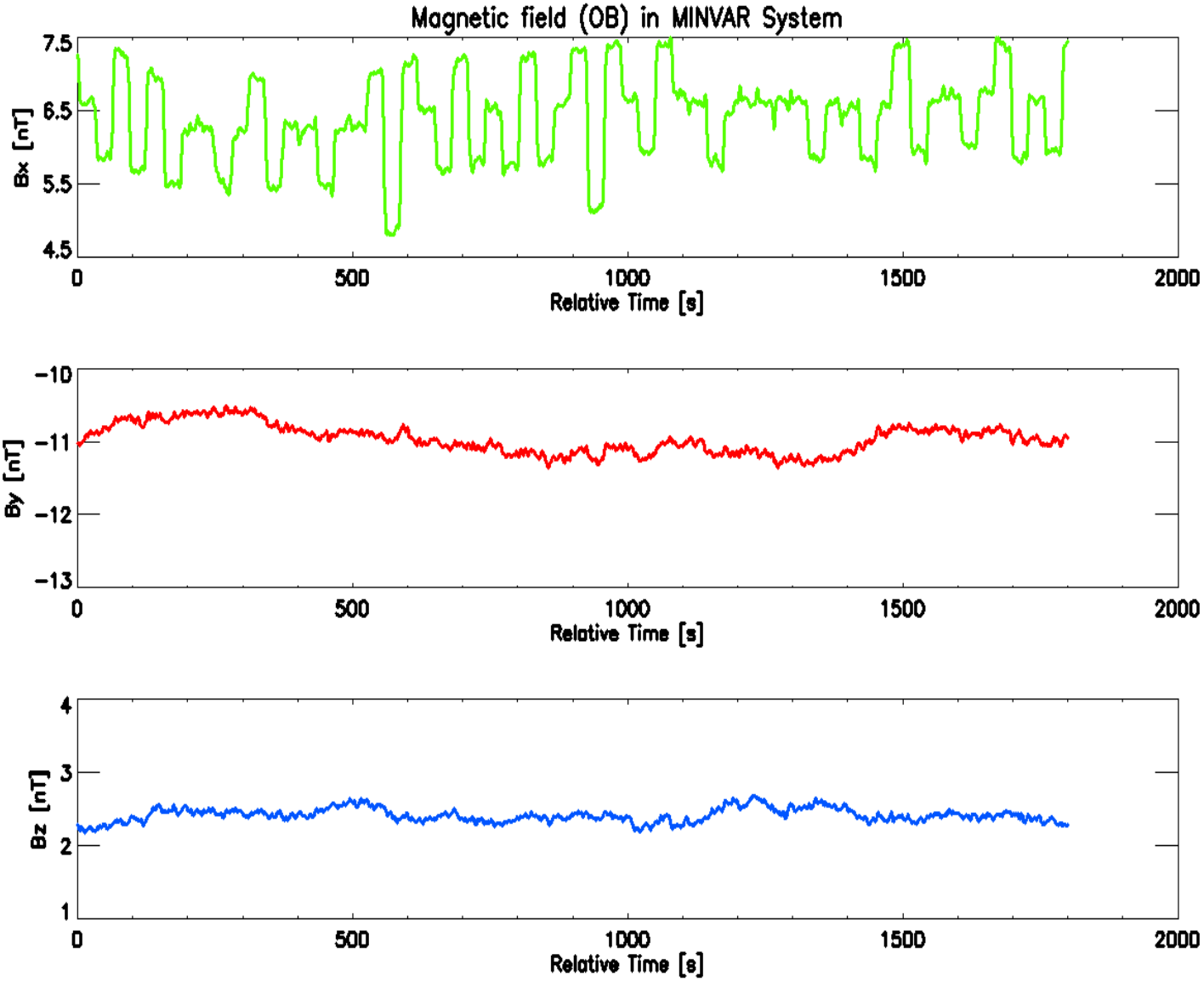

Figure 105: Disturbed signal rotated the Minimum Variance System

In the fourth panel the desired real time series is reconstructed. To do this the height of the jumps has to be computed individually for each jump. This height (level difference) is evaluated using short time averages of the last values of the level just before the jump and the average of the values just after the jump. With these data available it is possible to proceed step by step through the time series and to "flatten" all the infected levels. As the result the interrupted black–red time series is obtained.

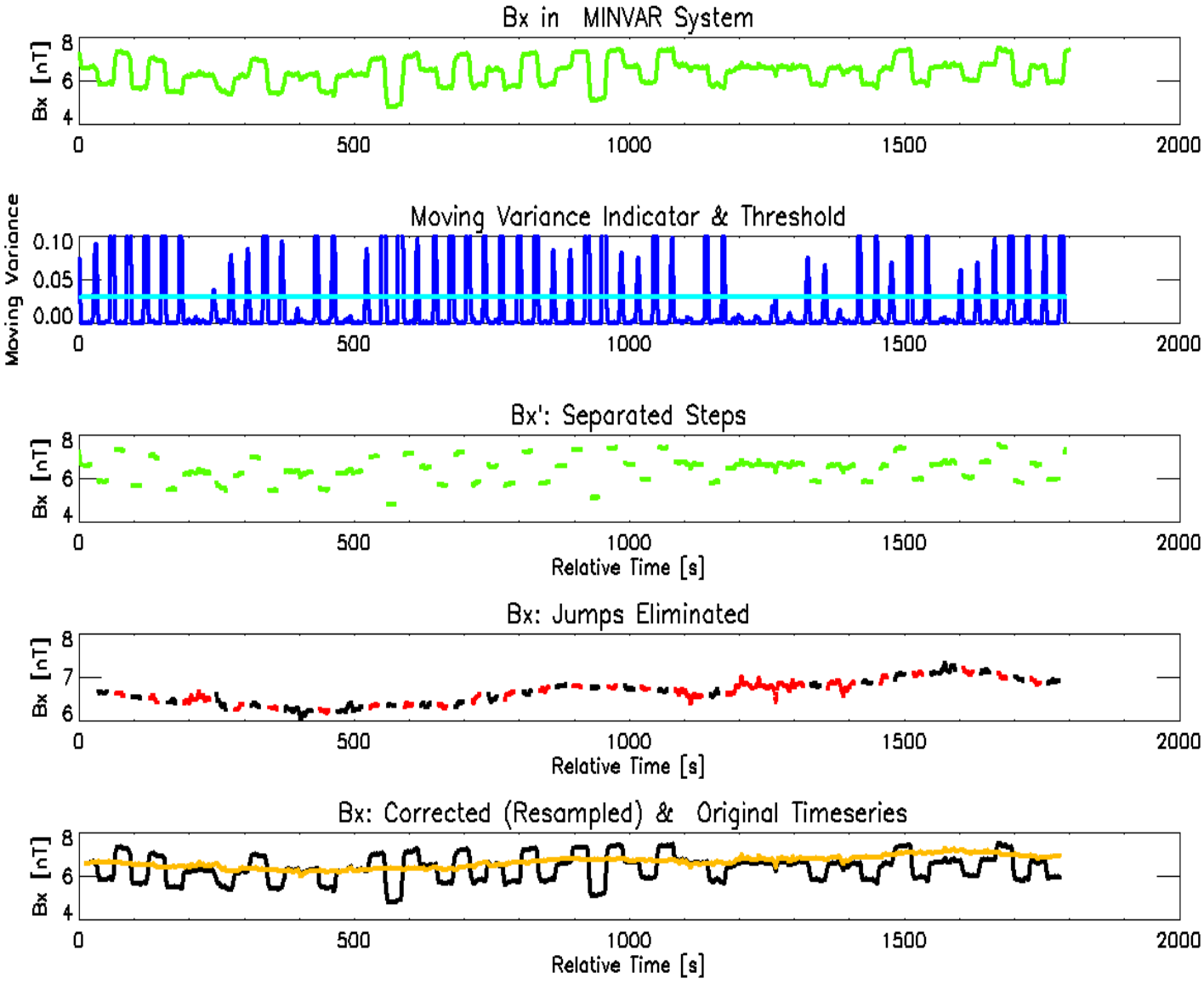

Figure 106: Processing of the heater disturbed Signal

The last step of the jump elimination can be seen in the bottom panels. The time gaps have been closed by resampling and interpolating the signal at the times of a jump. For a better comparison the original disturbed time series (black) and the improved signal (orange) are displayed.
At the very last processing step the corrected signal has to be rotated back from the minvar system to the original s/c frame. The result is shown in Figure 107.
The complete process can run quasi automatically to generate corrected PDS data.

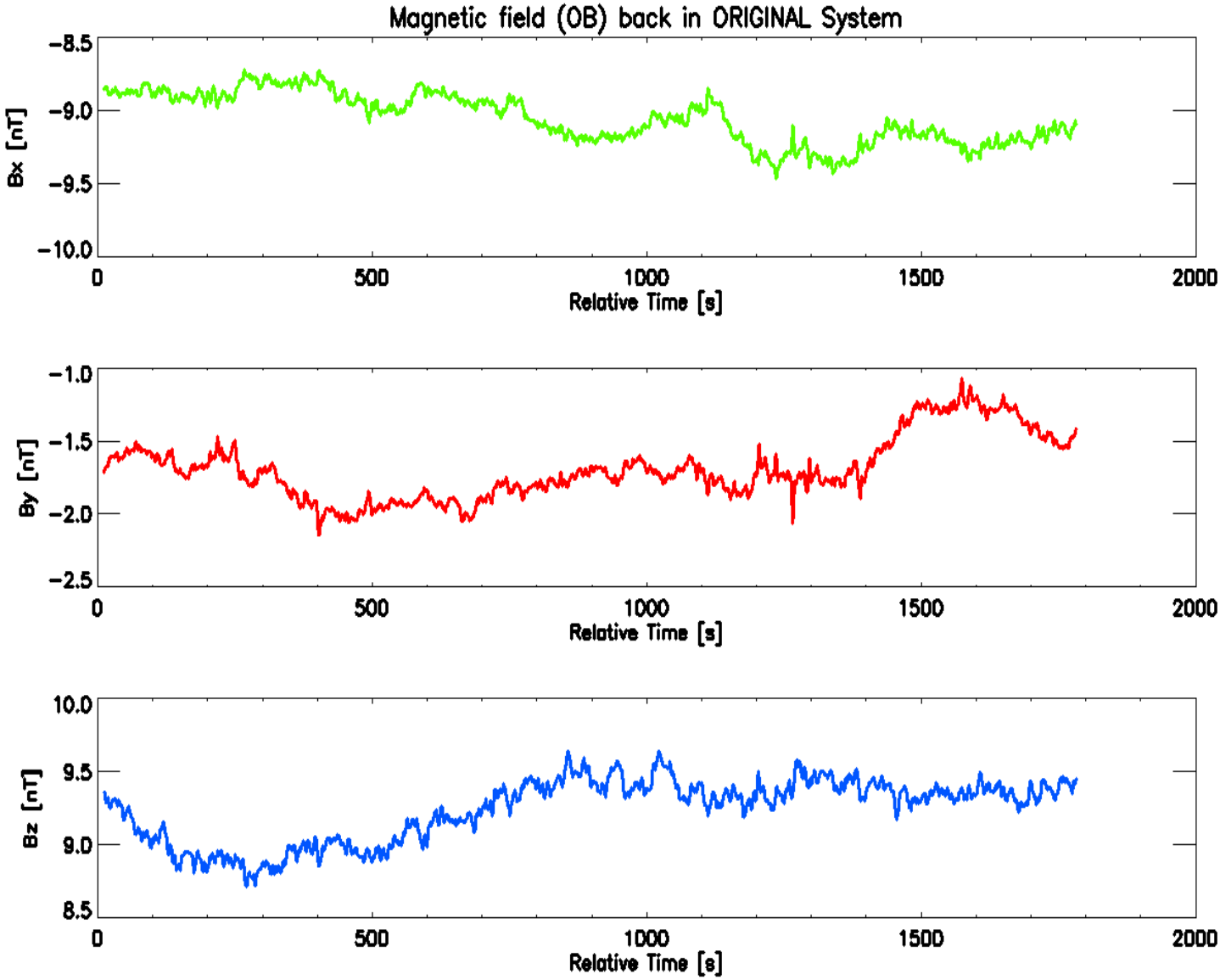

Figure 107: Processed Signal rotated back to s/c coordinate System

10 Temperature profile during EAR1

The following figure shows the measured temperatures of the OB and IB sensor during EAR1. The lower panels of the graph show the angles between x–, y–, and z–axis of the s/c frame and the sun direction.

The analysis of these plots shows that - as expected - most of the temperature changes are related to attitude changes. However, the steep increase of the temperatures at about 20:00 on March 3 can not be explained by a rotation.

A detailed model of ROSETTA using accurate SPICE kernels will hopefully reveal all shadowing effect of the earth, the moon, and the relevant units mounted onboard ROSETTA. Studies of this kind are planned for the near future.

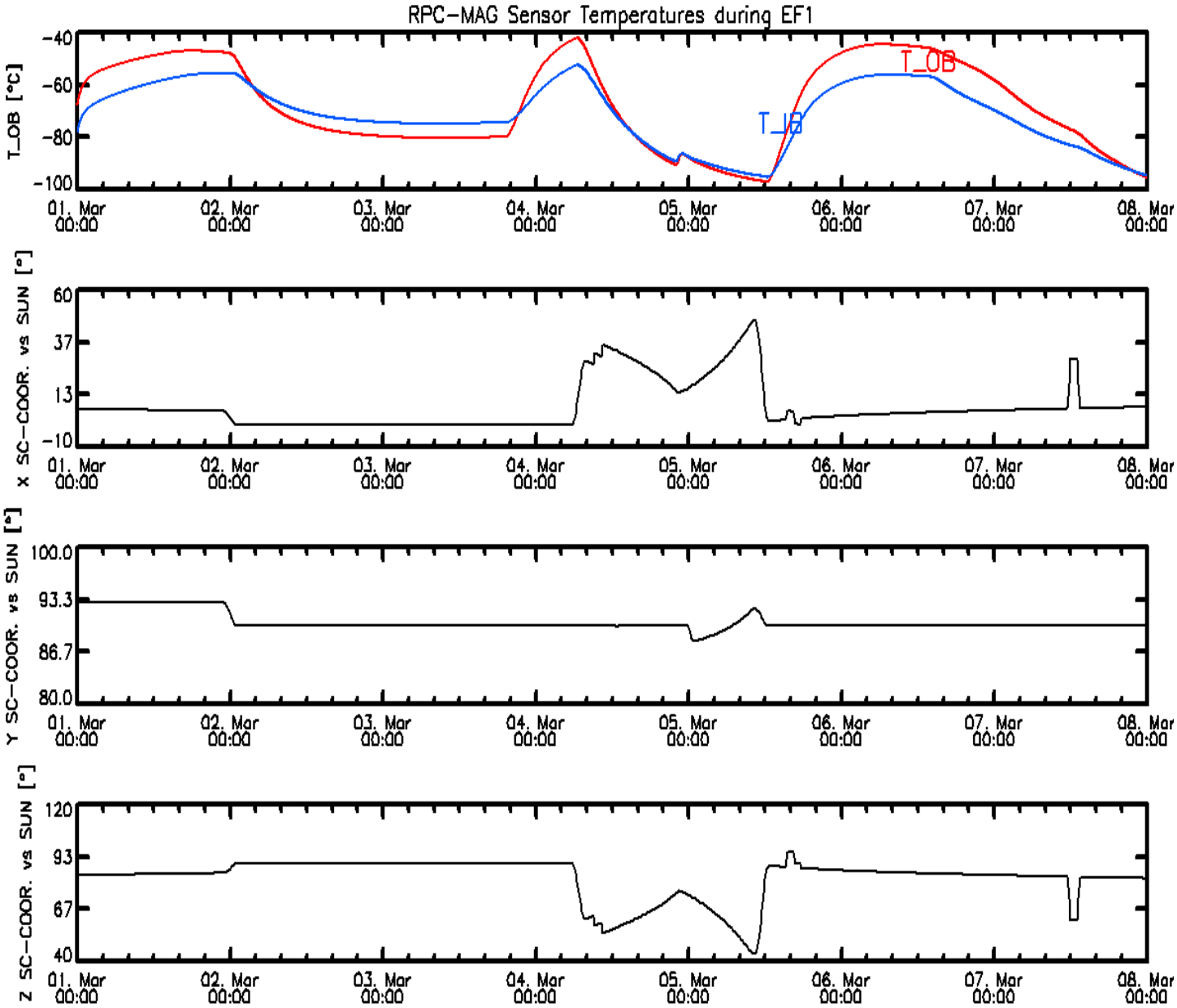

Figure 108: Measured Sensor Temperatures and attitudes during EAR1

11 Comparison of RPCMAG data with the ROMAP data

As an example for a comparison between RPCMAG and ROMAP the data of the OB (red) and the ROMAP sensor (black) of March 6, are plotted in Figures 109 (components) and 110 (differences). Here the heaters were off.

The higher frequent structures can be seen on both sensors in the same way. For the low frequencies the behavior is different, because the ROMAP sensor is not temperature calibrated at all . He shows a drift related to the temperature. After a proper temperature calibration, which is in the responsibility of the ROMAP PI, the data will probably match quite nice.

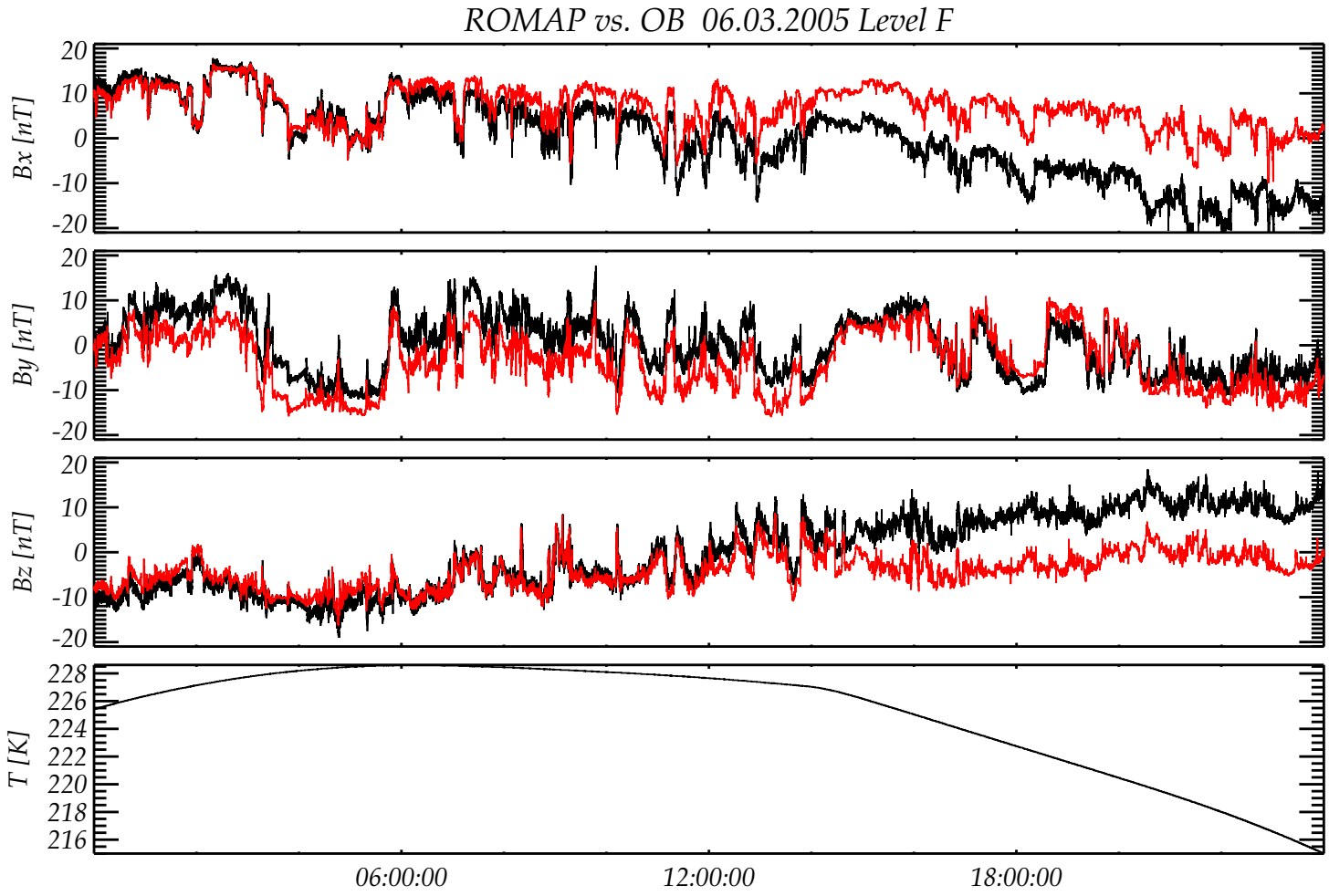

Figure 109: ROMAP versus OB: Data of March 6, 2005

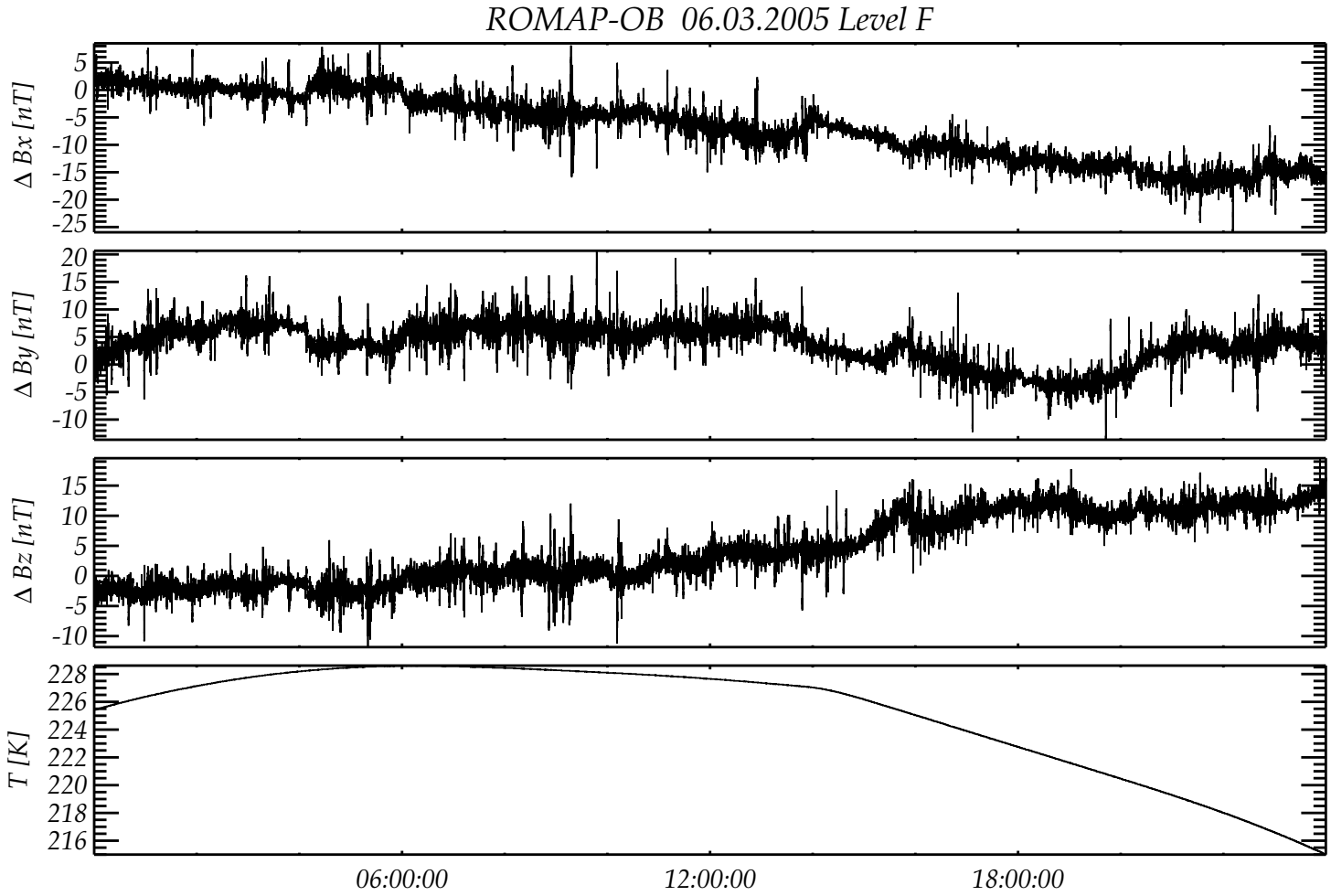

Figure 110: ROMAP versus OB: Data of March 6, 2005,Differences

12 Conclusions

- RPCMAG has performed amazing measurements during the Earth Swing by EAR1.
- A comparison of the MAG data with the forecast of a theoretical model (POMME) of the Earth's magnetic field shows only small differences in the order of less than 20 nT even in the components. This result was obtained by shifting the data in time (a few seconds [1]) and a slight rotation of the MAG URF in the order of less than 0.4 degrees.
  Thus, EAR 1 was a perfect opportunity to calibrate the actual sensor assembly matrices onboard the spacecraft.
- Disturbing heater signatures originated in the LANDER could be successfully eliminated.
- The spectra do not show any impact of ROSETTAs reaction wheels anymore.
- The comparison between IB and OB data showed that the measurements are very sensitive to specific temperature changes at the single sensors. The behavior can be used to build a data quality indicator.
- RPCMAG and ROMAP data will be in good agreement, when the temperature drifts and the heater effects are eliminated.

[1] an investigation of the onboard filter S/W has been done after EAR1 and all data have been reprocessed. Refer to the EAICD